



NBS TECHNICAL NOTE 969

U.S. DEPARTMENT OF COMMERCE / National Bureau of Standards

NBS Reactor: Summary of Activities July 1976 to June 1977



53
969
8
2

NATIONAL BUREAU OF STANDARDS

The National Bureau of Standards¹ was established by an act of Congress March 3, 1901. The Bureau's overall goal is to strengthen and advance the Nation's science and technology and facilitate their effective application for public benefit. To this end, the Bureau conducts research and provides: (1) a basis for the Nation's physical measurement system, (2) scientific and technological services for industry and government, (3) a technical basis for equity in trade, and (4) technical services to promote public safety. The Bureau consists of the Institute for Basic Standards, the Institute for Materials Research, the Institute for Applied Technology, the Institute for Computer Sciences and Technology, the Office for Information Programs, and the Office of Experimental Technology Incentives Program.

THE INSTITUTE FOR BASIC STANDARDS provides the central basis within the United States of a complete and consistent system of physical measurement; coordinates that system with measurement systems of other nations; and furnishes essential services leading to accurate and uniform physical measurements throughout the Nation's scientific community, industry, and commerce. The Institute consists of the Office of Measurement Services, and the following center and divisions:

Applied Mathematics — Electricity — Mechanics — Heat — Optical Physics — Center for Radiation Research — Laboratory Astrophysics² — Cryogenics² — Electromagnetics² — Time and Frequency².

THE INSTITUTE FOR MATERIALS RESEARCH conducts materials research leading to improved methods of measurement, standards, and data on the properties of well-characterized materials needed by industry, commerce, educational institutions, and Government; provides advisory and research services to other Government agencies; and develops, produces, and distributes standard reference materials. The Institute consists of the Office of Standard Reference Materials, the Office of Air and Water Measurement, and the following divisions:

Analytical Chemistry — Polymers — Metallurgy — Inorganic Materials — Reactor Radiation — Physical Chemistry.

THE INSTITUTE FOR APPLIED TECHNOLOGY provides technical services developing and promoting the use of available technology; cooperates with public and private organizations in developing technological standards, codes, and test methods; and provides technical advice services, and information to Government agencies and the public. The Institute consists of the following divisions and centers:

Standards Application and Analysis — Electronic Technology — Center for Consumer Product Technology: Product Systems Analysis; Product Engineering — Center for Building Technology: Structures, Materials, and Safety; Building Environment; Technical Evaluation and Application — Center for Fire Research: Fire Science; Fire Safety Engineering.

THE INSTITUTE FOR COMPUTER SCIENCES AND TECHNOLOGY conducts research and provides technical services designed to aid Government agencies in improving cost effectiveness in the conduct of their programs through the selection, acquisition, and effective utilization of automatic data processing equipment; and serves as the principal focus within the executive branch for the development of Federal standards for automatic data processing equipment, techniques, and computer languages. The Institute consist of the following divisions:

Computer Services — Systems and Software — Computer Systems Engineering — Information Technology.

THE OFFICE OF EXPERIMENTAL TECHNOLOGY INCENTIVES PROGRAM seeks to affect public policy and process to facilitate technological change in the private sector by examining and experimenting with Government policies and practices in order to identify and remove Government-related barriers and to correct inherent market imperfections that impede the innovation process.

THE OFFICE FOR INFORMATION PROGRAMS promotes optimum dissemination and accessibility of scientific information generated within NBS; promotes the development of the National Standard Reference Data System and a system of information analysis centers dealing with the broader aspects of the National Measurement System; provides appropriate services to ensure that the NBS staff has optimum accessibility to the scientific information of the world. The Office consists of the following organizational units:

Office of Standard Reference Data — Office of Information Activities — Office of Technical Publications — Library — Office of International Standards — Office of International Relations.

¹ Headquarters and Laboratories at Gaithersburg, Maryland, unless otherwise noted; mailing address Washington, D.C. 20234.

² Located at Boulder, Colorado 80302.

APR 26 1978

rot acc

NBS Reactor: Summary of Activities July 1976 to June 1977

no. 969

Frederick J. Shorten, Editor

Reactor Radiation Division
Institute for Materials Research
National Bureau of Standards
Washington, D.C. 20234



U.S. DEPARTMENT OF COMMERCE, Juanita M. Kreps, Secretary

Dr. Sidney Harman, Under Secretary

Jordan J. Baruch, Assistant Secretary for Science and Technology

U. S. NATIONAL BUREAU OF STANDARDS, Ernest Ambler, Director

Issued April 1978

National Bureau of Standards Technical Note 969

Nat. Bur. Stand. (U.S.), Tech. Note 969 188 pages (Apr. 1978)

CODEN: NBTNAE

U.S. GOVERNMENT PRINTING OFFICE
WASHINGTON: 1978

For sale by the Superintendent of Documents, U.S. Government Printing Office, Washington, D.C. 20434
Stock No. 003-003-01907-1 Price \$3.50
(Add 25 percent additional for other than U.S. mailing).

FOREWORD

The National Bureau of Standards Reactor was built not only to serve the needs of the NBS but also those of other government agencies and the greater Washington Scientific Community. The Reactor Radiation Division was established to operate the reactor and to foster its scientific and technological use. Toward this end, the Division has a small nucleus of scientists experienced in the use of reactors for a wide range of scientific and technical problems. In addition to pursuing their own research and developing sophisticated experimental facilities, they actively seek out and encourage collaboration with other scientists, engaged in challenging programs, whose work can benefit from use of the reactor, but who as yet do not have the reactor experience necessary to take full advantage of the facilities available. The Division also provides irradiation services to a wide variety of users as well as engineering and other technical services.

The reactor operates at 10 MW and is designed to provide more than 25 experimental facilities ranging from intense neutron beams to extensive irradiation facilities, making it one of the most versatile high flux research reactors in the country. Thus it is able to serve a large number of scientists and engineers in a broad range of activities both within and outside the NBS.

This report attempts to summarize all the work done which is dependent on the reactor including a large number of programs outside the Division. The first section summarizes those programs based primarily on Reactor Radiation Division (RRD) initiatives whereas the second and third sections summarize collaborative programs between RRD scientists and other NBS or non-NBS scientists respectively. The fourth section summarizes NBS work originating entirely outside the RRD which requires no collaboration with RRD scientists. The section entitled, "Service Programs" covers those programs originating outside NBS but for which RRD provides irradiation services. The remaining sections are self-explanatory.

FOREWORD

Appreciation is extended to F. J. Shorten of the Reactor Radiation Division for his extensive contributions to the editing, organization and preparation of this report, and L. Sprecher, C. O'Connor, D. Davitt and P. Lewis for efforts in typing manuscripts.

R. S. Carter

R. S. Carter
Chief, Reactor Radiation Division
National Bureau of Standards

ABSTRACT

This report summarizes all those programs which depend on the NBS reactor. It covers the period from July 1976 through June 1977. The programs range from the use of neutron beams to study the structure and dynamics of materials through nuclear physics and neutron standards to sample irradiations for activation analysis, isotope production, radiation effects studies, neutron radiography and nondestructive evaluations.

Key words: Activation analysis; crystal structure; diffraction; isotopes; molecular dynamics; neutron; neutron radiography; nondestructive evaluation; nuclear reactor; radiation.

TABLE OF CONTENTS

FOREWORD		iii
ABSTRACT		v
A.	REACTOR RADIATION DIVISION PROGRAMS	1
	The Lattice Dynamics of β -PdD _x	1
	The Lattice Vibrations of CeD _{2.12}	2
	Measurement of the Crystal Field Splitting in Cerium Dihydride	5
	Crystal Dynamics, Phase Transitions and Orientational Disorder in Ionic Crystals	8
	Neutron Diffraction Determination of the Crystal Structure of TiCuD	11
	Application of Robust/Resistant Techniques to Crystal Structure Refinement	13
	Isotope Shifts of Phonons	14
	Construction of a Neutron Flat-Cone Diffractometer.	16
	Development of a Triple-Axis Polarized Beam Spectrometer	18
	Cold Neutron Source	19
	Neutrino Scattering	19
	Neutron Radiography	23
B.	RRD COLLABORATIVE PROGRAMS	39
	Studies of the Effects of Hydrogen in Titanium	39
	Studies on the Structure of "Defect" Apatites	39
	The Structure of Guanidinium Tetramolybdimethyl Arsenate Monohydrate	42
	Crystal Structure of Triaminogaunidinium Nitrate by Neutron Diffraction	45
	The Structure of NH ₄ N ₃	48
	Study of the Crystalline Components of Portland Cements	50
	Battery Electrode Structure	51
	A Study of the Phase Transformation in Trinitrotoluene	55

Phonon Dispersion Curves of KN_3 at 1 bar and 6.6 k bar	55
Ammonium-ion Dynamics in NH_4ClO_4	56
A Search for the Central Mode in Lithium Tantalate	59
Deformation of Uniform Polybutadiene Rubber Network	61
Small Angle Magnetic Scattering From Amorphous Rare-Earth Iron Alloys	63
Magnetic Scattering in Dilute Pd(Fe) Alloys	64
Crystal Field Effects in the Superconductor ($\text{Ce}_{.73}\text{Ho}_{.27}$) Ru_2	65
Excited State Spin Waves in ErFe_2	68
Magnetism in $\text{ErFe}_2\text{-H}$	72
Application of Neutron Diffraction to Non-Destructive Testing Problems	73
C. NON-RRD NBS PROGRAMS	77
Activation Analysis: Summary of 1977 Activities	77
The Intermediate-Energy Standard Neutron Field (ISNF).	120
Fission Rate Intercomparisons with the Reactor Physics Group at Argonne National Laboratory.	123
U-235 Cavity Fission Irradiation Facility	125
Absolute Measurement of the DT Thick Target Yield at 191.3 KeV Using a Thermal Neutron Beam	126
Filtered Beam Facility	127
Precision Measurement of the Wavelength of Nuclear Gamma Lines and the Compton Wavelength of the Electron	129
D. SUMMARY OF REACTOR OPERATIONS.	132
Summary of NBS Reactor Health Physics Activities and Services	132
E. SERVICE PROGRAMS	135
The Neutron Activation Analysis Program of the Food and Drug Administration at the NBSR.	135
Activation Analysis Program of the U. S. Geological Survey . .	149
The Use of Activation Analysis in Scientific Crime Detection by the Federal Bureau of Investigation	152

ATF's Activation Analysis Program	153
Trace Elements in the Environment and Radioactive Decay Studies	154
Neutron Transmutation Doping of Silicon	163
Positron Annihilation Studies	164
Neutron Activation Analysis of Lunar Samples and Meteorites	166
F, STAFF ROSTER	167
G, PUBLICATIONS	172

A. REACTOR RADIATION DIVISION PROGRAMS

THE LATTICE DYNAMICS OF β -PdD_x

C. J. Glinka, J. M. Rowe and J. J. Rush

Efforts are continuing to study in detail the lattice dynamics of the beta phase of palladium deuteride PdD_x ($0.6 \leq x \leq 1.0$). For $x > 0.8$, PdD_x becomes superconducting and there is currently much interest in the role of the lattice vibrations, particularly the optic modes, in the inducement of superconductivity in this system. Present efforts are aimed at comparing previous coherent scattering measurements of the phonon dispersion curves¹ and phonon lineshapes² in PdD_{.63} with similar measurements on a crystal which is a superconductor.

A single crystal of PdD_{.75} was prepared by H. Flotow, Argonne National Laboratory, by slowly admitting D₂ gas to a crystal of Pd at 350°C (to avoid the two-phase region of the phase diagram and facilitate diffusion). The sample was then cooled to room temperature over a period of days under a pressure of 70 atmospheres deuterium and transferred to a high pressure sample container for further loading and examination with neutrons. The concentration of the sample was determined by weighing before and after loading and subsequently confirmed by measurement of the lattice constant. Selected inelastic scattering measurements at this concentration showed no change in the position of the peak of the optic phonon density of states from that for PdD_{.63}. Also, the optic phonon lineshapes were severely broadened as had been observed in PdD_{.63}. The only notable difference from PdD_{.63} was an upward shift of about 5 to 10% in the frequencies of the highest energy longitudinal optic modes.

To further raise the concentration, the sample cell containing the PdD_{.75} crystal was cooled to -70°C and pressurized with D₂ to 26,000 psi. The cell was then sealed off and allowed to warm to room temperature to reach a final estimated pressure of 2.4 kbar. After allowing several days for the crystal to reach equilibrium, the lattice constant was measured at 80K to be $4.063 \pm .001$ Å which corresponds to a D/Pd ratio of 0.87 ± 0.01 . At this concentration the crystal is ex-

pected to be a superconductor with a T_c of about 5K. A thorough examination of the phonon spectrum in this crystal will begin shortly.

-
1. J. M. Rowe, J. J. Rush, H. G. Smith, M. Mostoller and H. E. Flotow *Physical Review Letters* 33, 1297 (1974).
 2. C. J. Glinka, J. M. Rowe, J. J. Rush, A. Rahman, S. K. Sinha and H. E. Flotow, to be published.

THE LATTICE VIBRATIONS OF $CeD_{2.12}$

C. J. Glinka, J. M. Rowe and J. J. Rush

The complete phonon dispersion relation including both optic and acoustic modes has been measured along the major symmetry axes of a single crystal of $CeD_{2.12}$ at 295 K by coherent neutron scattering.¹ This work has been done in collaboration with A. Maeland and G. G. Libowitz of the Allied Chemical Corporation and represents our first efforts to study in detail the dynamical properties of the cerium-hydrogen system, $CeH_{2+\delta}$ where $-0.2 < \delta < 1.0$. The hydride phase of cerium is isostructural with other rare-earth hydrides and can thus be considered a prototype for a class of materials which has been widely studied in recent years.

There have been a number of studies of the dynamics of transition metal and rare-earth hydrides by neutron incoherent scattering. The results of many of these studies have been analyzed in terms of simple central force models as first proposed by Slaggie² for ZrH_2 . However, finite resolution and the inherent limitations of the incoherent scattering technique did not permit detailed conclusions to be drawn, and single crystals have not previously been available for coherent scattering measurements to critically test the models. As a result of our measurements on $CeD_{2.12}$, which are the first coherent inelastic scattering measurements on a rare-earth hydride, we have been able to test Slaggie's

model in both its original (four parameter) and more general (eight parameter) form.

The results of our measurements of acoustic phonons in $\text{CeD}_{2.12}$ are shown in figure 1 where the phonon energies are plotted versus one cartesian component of the phonon wave vector, expressed in units of $2\pi/a$. The dashed dispersion curves in the figure were calculated from Slaggie's simplified central force model in which the so-called bond-bending force constants are neglected and only four near neighbor bond-stretching force constants are treated as parameters. The dashed curves are seen to fail to fit the transverse branches. The solid curves in figure 1 were calculated by including bond-bending forces in the model and give an adequate fit to the measured dispersion curves except for the $[111]$ LA branch near the zone boundary.

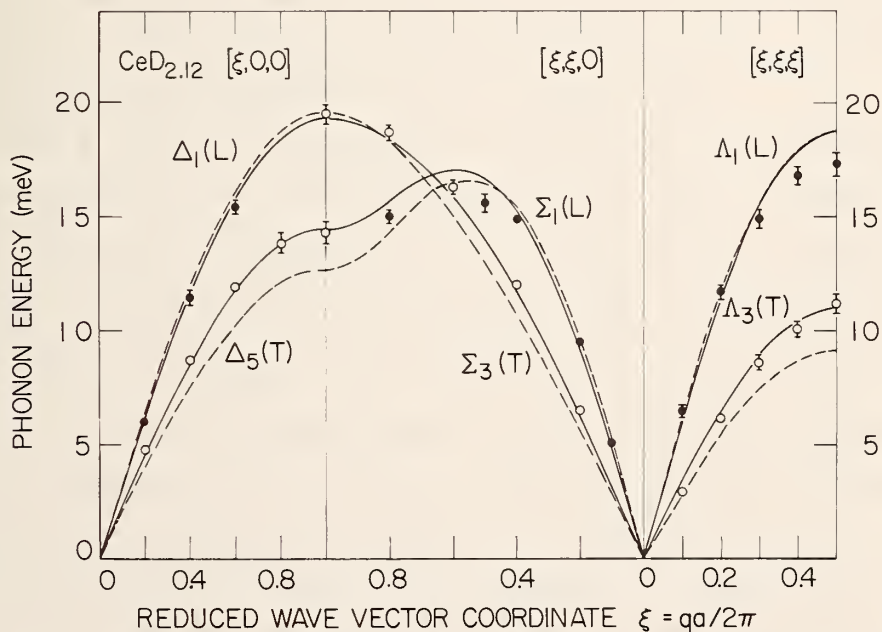


Figure 1. Acoustic phonon energies measured in $\text{CeD}_{2.12}$ at 295K along the $[100]$, $[110]$ and $[111]$ directions. The dispersion curves in the figure were calculated from the four parameter (dashed lines) and eight parameter (solid lines) central force model due to Slaggie (Ref. 2).

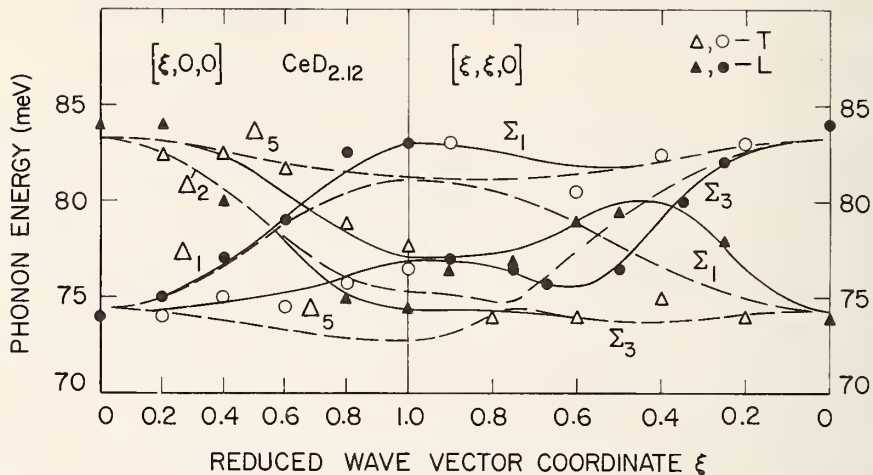


Figure 2. Optic phonon dispersion curves in $\text{CeD}_{2.12}$ along the [100] and [110] directions. The solid lines are guides to the eye where the data deviate from the dispersion curves (dashed lines) calculated from the Slaggie central force model.

Although satisfactory to describe the acoustic modes, a second near neighbor central force model fails almost entirely for the optic modes. Optic mode energies along the [100] and [110] directions are shown in figure 2 together with dispersion curves (dashed lines) calculated with the Slaggie central force model, including bond-bending forces. The model results reproduce the splitting between the two optic mode frequencies at the zone center (Γ), but progressively deviate from the measured frequencies (solid curves) as one proceeds across the zone. The data in figure 2 point out most clearly the need for a more sophisticated model for the lattice dynamics than has previously been supposed. Calculations based on a screened shell model are currently in progress.

Further inelastic scattering experiments are planned on samples with deuterium concentrations near the metal to semiconductor transition which occurs near $\text{CeD}_{2.75}$. It is hoped that changes in the lattice dynamics may be correlated with the striking changes in the electronic properties which take place as a function of absorbed hydrogen.

1. C. J. Glinka, J. M. Rowe, J. J. Rush, A. Maeland and G. G. Libowitz, *Solid St. Commun.* 22, 541 (1977).
2. E. L. Slaggie, *J. Phys. Chem. Solids* 29, 923 (1968).

MEASUREMENT OF THE CRYSTAL FIELD SPLITTING IN CERIUM DIHYDRIDE

C. J. Glinka, J. M. Rowe and J. J. Rush

In cerium dihydride, the ground state multiplet of the Ce^{3+} ion, $^2F_{5/2}$ due to a single 4f electron, is split into sublevels by the electrostatic field of the crystal. This crystal field splitting may be measured directly by inelastic neutron scattering whereby information regarding the effects of hydriding on the 4f electron, as well as the symmetry and strength of the electric field at the site of the Ce^{3+} ion, may be inferred. Thus as part of our program to study this prototype rare-earth hydride system in detail, we undertook an investigation of the crystal field splitting in the same single crystal of $\text{CeD}_{2.12}$ used to study the lattice dynamics (previous section). An additional motivation for a careful measurement on this system arose from the conflicting results for the crystal field splitting obtained recently by two groups^{1,2} from measurements on polycrystalline $\text{CeD}_{2.01}$ and $\text{CeH}_{1.98}$.

Constant-Q scans made with a triple-axis spectrometer over energy transfers (neutron energy loss) from zero to over 100 meV revealed only a single peak at $\hbar\omega = 20$ meV which could not be ascribed to a vibrational mode of the crystal. This single resonance, which showed no dispersion, was positively identified as a crystal field transition from both its temperature and Q-dependence, which are shown in figures 1 and 2. In figure 1, the intensity of the peak is seen to decrease with increasing temperature as expected for a crystal field transition and contrary to the behavior of a phonon excitation. Figure 2 shows that the scattered intensity (measured at reciprocal lattice points to avoid interference from coherent phonon scattering) decreases with Q although not as sharply as suggested by a calculation³ of the Ce^{3+} free ion magnetic form factor (solid curve in figure 2).

The observation of a crystal field transition demonstrates that the 4f electron remains localized on the Ce ion and is thus little affected by hydriding. The single transition observed corresponds to a crystal

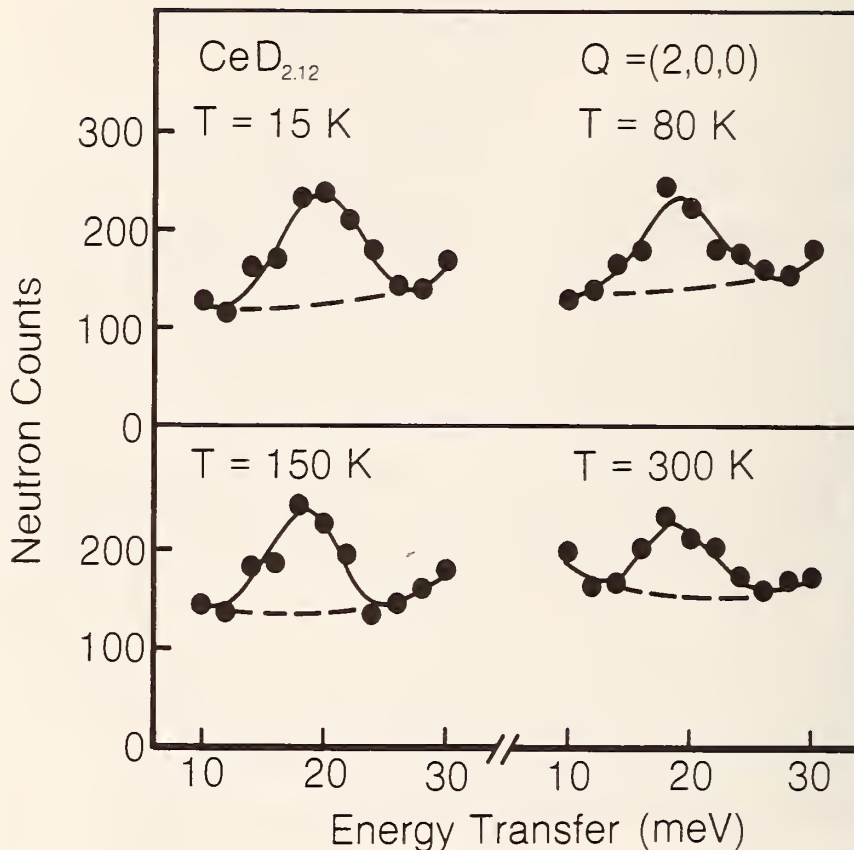


Figure 1. Neutron groups observed in constant-Q scans in the vicinity of $\hbar\omega = 20$ meV in $\text{CeD}_{2.12}$ at various temperatures. The peak intensity decreases with increasing temperature as expected for a crystal field transition.

field of cubic symmetry which splits the ${}^2F_{5/2}$ level into a quartet (Γ_8) and a doublet (Γ_7). A transition energy of 20 meV, however, contradicts the suggestion¹ that a nearest neighbor point charge model, in which the hydrogens have the charge $-1e$, is adequate to explain the crystal field splitting. In this model a transition energy of 20 meV would correspond to a charge of $-0.6e$. Our results suggest that screening effects are important and must be considered in any realistic calculation of the crystal field.

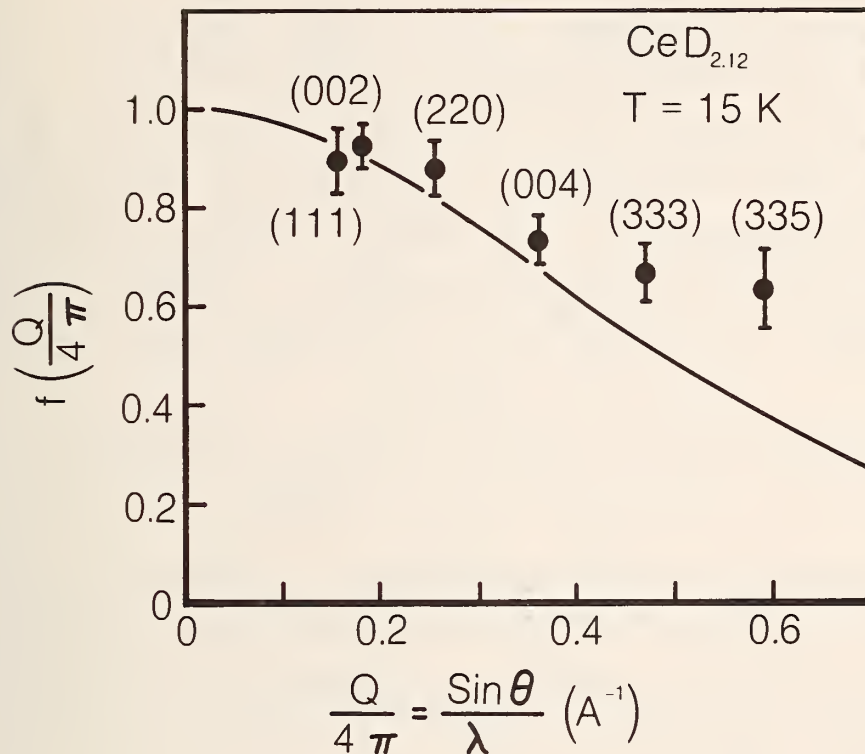


Figure 2. Data points are proportional to the square root of the integrated intensity of the crystal field peak (figure 1) in $\text{CeD}_{2.12}$ measured at several reciprocal lattice points at 15K. Data are plotted relative to a calculation (solid curve) of the Ce^{3+} free ion magnetic form factor.

1. D. G. Hunt and D. K. Ross, *J. Less-Common Met.* 45, 229 (1976).
2. P. Vorderwisch, S. Hautecler, J. B. Suck and H. Dachs, "Crystal Field Effects in Metals and Alloys," A. Furrer ed., *Plenum Press*, p. 47 (1977).
3. M. Blume A. J. Freeman and R. E. Watson, *J. Chem. Phys.* 37, 1245 (1962).

CRYSTAL DYNAMICS, PHASE TRANSITIONS AND
ORIENTATIONAL DISORDER IN IONIC CRYSTALS

During this past year, we have achieved a breakthrough in our understanding of the high temperature phase transition in KCN, which is a widely studied prototype of a large number of inorganic solids of formula M^+XY^- which exhibit similar transitions. In addition, we have begun measurements on the $(KCN)_x(KBr)_{1-x}$ alloy system with $x = 0.25$.

1. The 168K Phase Transition in KCN J. M. Rowe, N. J. Chesser, J. J. Rush, and K. H. Michel, J. Naudts, (University of Saarland, W. Germany.)

We have completed detailed high-resolution studies of the [100] TA mode in KCN as a function of temperatures. There is no "central" peak for this soft mode system. However, we have been able to fit out data to a model which treats the interactions of the non-spherical $(CN)^-$ ions with the elastic strains in the system. This model was first proposed by Naudts and Michel to successfully explain the temperature dependence of the elastic constant C_{44} observed by ultrasonic techniques.

In figures 1 - 3 we show the fit of this new model to our data for KCN at various temperatures and wavevectors. As can be seen, the agreement is good - the remaining discrepancies are likely due to an over-simplified resolution correction applied to the theory. With these latest results and the new model, we can now describe the 168K phase transition in a manner consistent with all of the data.

This is a first order phase transition from a disordered NaCl structure to a partially ordered orthorhombic structure. However, in a limited sense, the phase transition can be thought of as almost second order and the strain associated with the elastic constant C_{44} is the order parameter in the high temperature phase. Although this phase transition has been described as ferroelastic, our earlier diffraction studies clearly preclude such a model since there is very little change in preferred orientation of (CN) ions and no occupation of the low

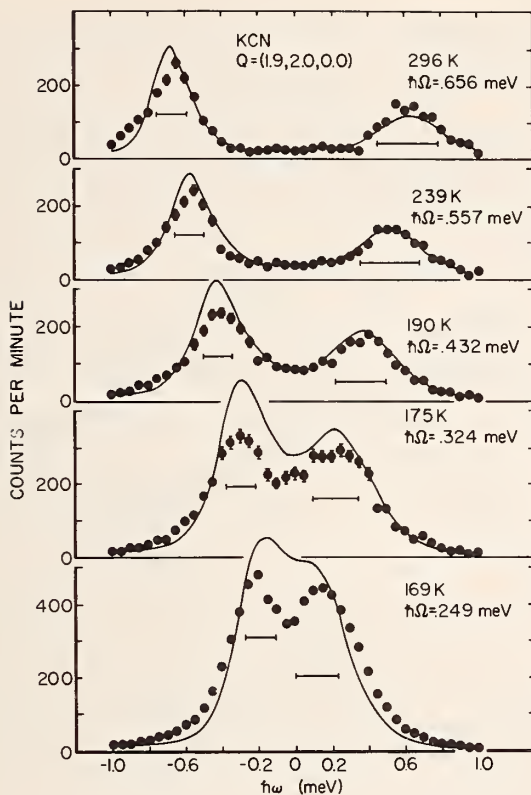


Figure 1. Neutron scattering lineshapes for KCN fitted to model of nickel (note no central peak).

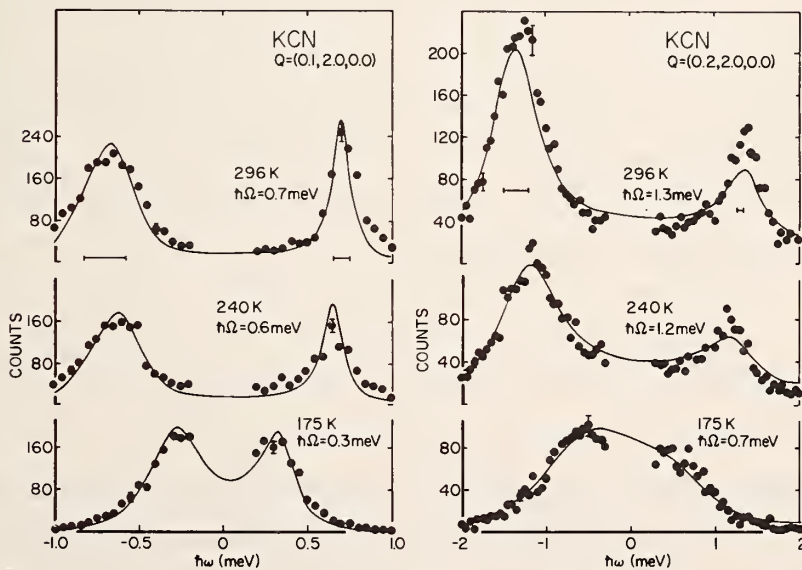


Figure 2. Neutron scattering lineshapes for KCN at different wavevectors and reciprocal lattice points.

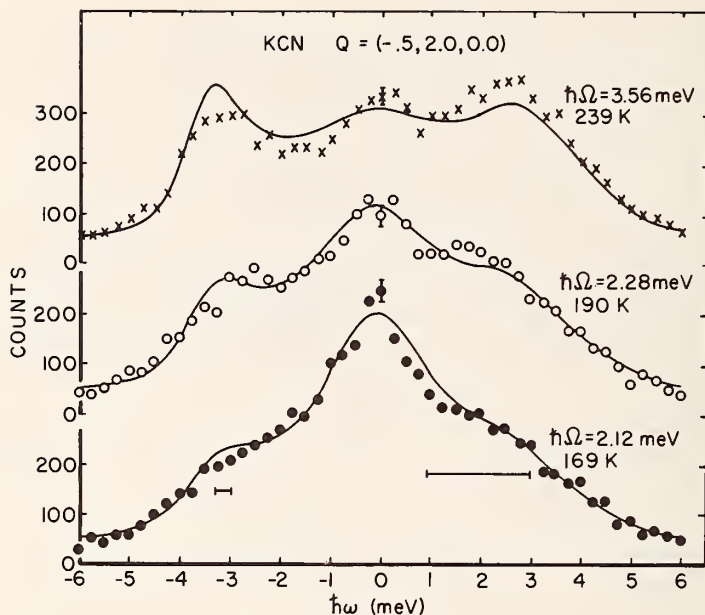


Figure 3. Neutron scattering lineshapes for KCN for wavevectors of $1/2$ the distance to the Brillouin zone edge. Note that softening point persists.

temperature orientation as one approaches the transition temperature. In the present model, which agrees with the neutron, ultrasonic and Brillouin data, the elastic constant C_{44} is driven soft by fluctuations in the local $(CN)^-$ ion orientations. There is no critical scattering. Thus, a more correct analogy is to a Jahn-Teller system, rather than a ferromagnetic system. A final paper on KCN is being prepared in which all available data will be presented.

2. $(KCN)_{0.25}(KBr)_{0.75}$ J. M. Rowe, J. J. Rush, N. J. Chesser, Argonne National Laboratory.

As a first step in a program to study mixed cyanide-bromide crystals, we have begun to study the lattice dynamics of $(KCN)_{0.25}(KBr)_{0.75}$. Preliminary results of these studies indicate that where the widths and centroid frequencies of the neutron groups observed

in this crystal are presented for three temperatures as a function of momentum transfer for the [100] TA mode. (This branch is soft in pure KCN as one approaches 168K). Since there is no phase transition in this mixed crystal we can cool the sample down to 10K. The neutron groups increase in width as T is decreased to 100K and the centroid frequency decreases, in analogy with KCN, showing an interaction between the (CN) ions and the C_{44} elastic constant. However, at 100K and 10K the widths do not change but the frequencies increase. Although we cannot yet explain these results in detail, we do believe that the model used above for KCN can be adopted to these mixed crystals and work is proceeding along these lines.

NEUTRON DIFFRACTION DETERMINATION OF THE CRYSTAL STRUCTURE OF TiCuD

A. Santoro and J. J. Rush

and

A. Maeland

(Allied Chemical Research Center, Morristown, NJ)

As a part of a research effort involving compounds potentially useful for hydrogen storage, the crystal structure of the compound TiCuD has been determined and refined with neutron diffraction powder techniques using the total profile analysis proposed by Rietveld.¹

The experimental conditions used to take the neutron powder pattern are:

Monochromatic Beam: reflection 220 of a Cu monochromator

Take-off angle and mean neutron wavelength: 42.5° and 0.925 \AA

Horizontal divergences of collimators (in min arc) 20,23,24

Mosaic spread of monochromator ~ 10 min arc

Theoretical values of full-width at half maximum parameters

$$U = 1200, V = -4650, W = 2420 \times 10^{-4} \text{ deg}^2$$

Sample container: Vanadium can of ~ 1 cm diameter

The results of refinement are indicated below:

$$\text{TiCuD}_{0.9}, P4/nmm; a = 3.0324(7), c = 6.847(2) \text{ \AA}$$

$$2\theta_{\text{initial}} = 5.0^\circ, 2\theta_{\text{final}} = 90.0^\circ, \text{step} = 0.1$$

No. of ind. reflections = 102, no. of observation above background = 584

$$R = [(\Sigma |I_{\text{obs}} - I_{\text{cal}}|) / \Sigma I_{\text{obs}}] = 0.092$$

$$R_p = [(\Sigma |y_{\text{obs}} - y_{\text{cal}}|) / \Sigma y_{\text{obs}}] = 0.13$$

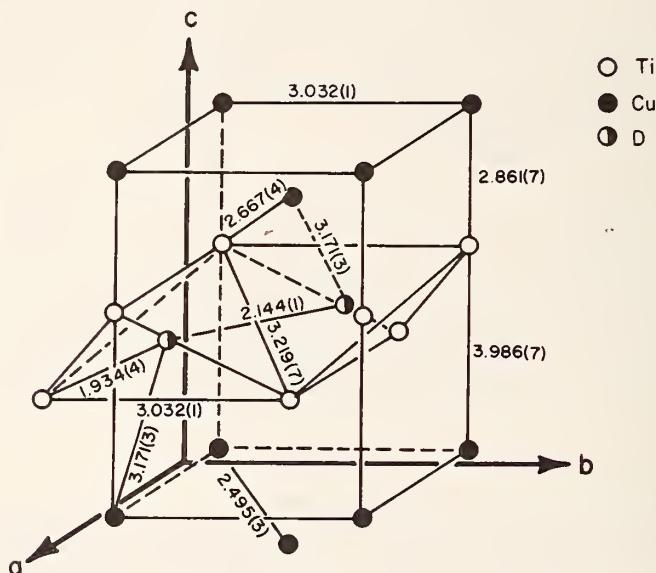


Figure 1. The crystal structure of $\text{TiCuD}_{0.9}$. The Ti-D distance of $1.934(4) \text{ \AA}$ compares well with the structure of $1.923(3) \text{ \AA}$ found in $\text{TiD}_{1.97}$ by Sidhu, Heaton and Zaubers (Acta Cryst. 9, 612, 1956).

Atom	x	y	z	N(occupancy factor)
Ti	1/4	1/4	0.6753(9)	1.0
Cu	1/4	1/4	0.0932(5)	1.0
D	3/4	1/4	1/2	0.89(1)

Overall temperature factor = $0.64(2) \text{ \AA}^2$

The D atoms are located at the center of slightly distorted tetrahedra of Ti atoms.

1. Rietveld, *J. Appl. Cryst.* 2, pp. 65-71 (1969).

APPLICATION OF ROBUST/RESISTANT TECHNIQUES TO
CRYSTAL STRUCTURE REFINEMENT

W. L. Nicholson

(Battelle Pacific Northwest Laboratories, Richland, WA)

and

E. Prince

The philosophy of robust/resistant statistical estimation and its application to crystal structure refinement was described in NBS Technical Note 939 (1977). The program of refinement outlined there has been completed on 12 data sets of the single-crystal intensity project of the International Union of Crystallography. Specifically, each data set consisting of measured structure factors on 1) (4) tartaric acid has been analyzed four times with various options of RFIN4:

1) attempt to "recreate" the literature results of Hamilton and Abrahams;²

2) add secondary extinction to the classical weighted least squares refinement; incorporate the biweight w-function and do robust/resistant refinements with outliers cutoff 3) at estimated six sigma; and 4) at estimated four sigma.

The results of Hamilton and Abrahams are not reproduced exactly partially because of a difference in convergence criteria and inclusion or not of several extreme outliers in each data set. For a selected subset of six good data sets the recreation has more consistent parameter estimates. Over all experiments the recreation has a tendency to give larger diagonal thermal coefficients possibly because of small differences in the treatment of atomic scattering factors.

Inclusion of the Zachariasen model for secondary extinction significantly improved the seven refinements which had discrepant strong reflections. Again there was a reduction of variability across parameter estimates for the six good experiments (four of these were among the seven with strong extinction).

Inclusion of biweight with estimated six sigma cutoff did not

change the results significantly. Inclusion of biweight with estimated four sigma cutoff increased the variability of parameter estimates across the six good experiments.

Further data analysis is in progress on the calculation of parameter estimate precision and agreement measures for the biweight approach to refinement. The most obvious advantage of the biweight procedure is associated with resistance. In the classical refinement with secondary extinction subjective decisions were required to eliminate extreme outlier reflections, whereas biweight performs the same function automatically and objectively. The affect of the robust aspect of the procedure, dealing with error distributions with tails that are thicker than three of a gaussian distribution, is subtler, and more difficult to document in real experimental data sets, although studies of synthetic data sets³ have shown that there are advantages here also.

Hamilton and Abrahams noted strong biases in parameter estimates for several data sets. These biases were not removed by inclusion of either secondary extinction or biweight. Thus biweight compensates for lack of careful screening of the data base, and for non-gaussian error distributions, but not for bias in the experimental data.

-
1. E. Prince and W. L. Nicholson, *NBS Tech. Note* 939 (1977).
 2. W. C. Hamilton and S. C. Abrahams, *Acta Cryst.* A26, 18 (1970).

ISOTOPE SHIFTS OF PHONONS

R. C. Casella

Recently H. Prask and G. Rosasco have studied isotopic shifts between the Raman spectra of hydrogenous and deuterated ammonium perchlorate at NBS. The work is part of a broader program for determining the phonon spectra of ammonium perchlorate, also involving inelastic neutron-scattering studies by H. Prask and N. Chesser. This experimental work has motivated a theoretical study of the general isotopic shift problem in crystals for the case when more than one atomic species is involved with

a given symmetry type, i.e. irreducible representation of the little group at wavevector \vec{q} . We also consider the case where the rigid molecule approximation applies (e.g., to the ammonium and perchlorate complexes) and where nonvanishing components exist for both translational and librational motions (involving several molecular species) in association with a given observed eigenmode. When only one molecular type is involved and the motion is either purely translational or purely librational, then the well known relations, $\tilde{\omega} = (M/\tilde{M})^{1/2} \omega$ and $\tilde{\omega} = (I/\tilde{I})^{1/2} \omega$ apply to the translational and librational frequencies respectively. Here, ω and $\tilde{\omega}$ denote the frequencies associated with the molecular masses M and \tilde{M} involved in the substitutions; I and \tilde{I} are the corresponding moments of inertia (assumed isotropic). For the general case mentioned earlier, the product rule of molecular systems is extended to translationally invariant crystalline solids at arbitrary wavevector \vec{q} , making use of properties of the projected symmetry states elucidated by Rao and Trevino.¹ We find that the frequencies $\tilde{\omega}(\vec{q}r\gamma)$ and $\omega(\vec{q}r\gamma)$ associated with irreducible representation r at \vec{q} are related by the following expression:

$$\prod_{\gamma=1}^{N_r} \tilde{\omega}(\vec{q}r\gamma) = x_A^{P_A} \left(\prod_{\lambda} y_{A\lambda}^{Q_{A\lambda}} \right) x_B^{P_B} \left(\prod_{\lambda} y_{B\lambda}^{Q_{B\lambda}} \right) \dots \prod_{\gamma=1}^{N_r} \omega(\vec{q}r\gamma). \quad (1)$$

The quantities $x_A, x_B, \dots, y_{A\lambda}, y_{B\lambda}, \dots$ appearing in Eq.(1) refer to the mass and principal moment ratios associated with the isotopically substituted molecular species, A, B, \dots . That is,

$$x_A = (M_A/\tilde{M}_A)^{1/2} \quad (2)$$

$$y_{A\lambda} = (I_{A\lambda}/\tilde{I}_{A\lambda})^{1/2}, \quad (3)$$

where, in Eq.(1), λ runs over inequivalent principal moment axes. $P_A, P_B, \dots, Q_{A\lambda}, Q_{B\lambda}, \dots$ denote the number of symmetry states (belonging to a given row of the r th irreducible representation at \vec{q}) associated

with translations and rotations of molecular species A, B, N_r is the dimension of the symmetry reduced block diagonalized dynamical matrix associated with the representation, r .² Work continues in this area.

1. K. K. Rao and S. F. Trevino, *J. Chem. Phys.* 53, 4624 (1970) and S. F. Trevino, private communication.
2. R. C. Casella, *Phys. Rev.* B11, 4795 (1975).

CONSTRUCTION OF A NEUTRON FLAT-CONE DIFFRACTOMETER

A. Wlodawer, E. Prince and A. Santoro

The principles of construction of a flat-cone diffractometer utilizing a position-sensitive detector have been presented two years ago.¹ Such an instrument has now been constructed. It was designed as a modification of an existing four-circle diffractometer, in which a

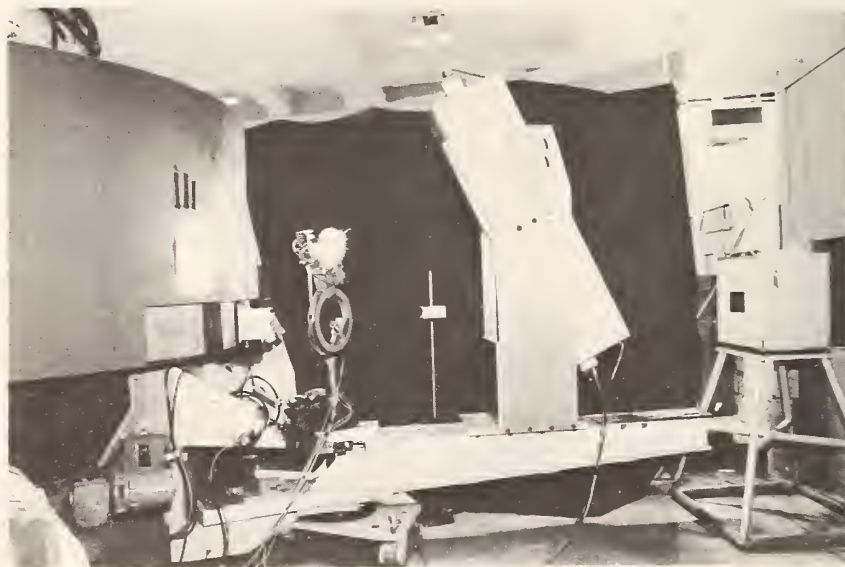


Figure 1. Flat-cone diffractometer. The position sensitive detector is housed in a vertical shield, visible on the right. All other components are those of a standard four-circle diffractometer.

counter was replaced with a 1 m long position-sensitive detector placed in the vertical plane as shown in figure 1. The flat-cone diffractometer is capable of counting several diffracted beams simultaneously. The software for on-line control by the PDP-11/40 computer has been written. The system was tested by collecting preliminary diffraction data using a Ta_2O_5 single crystal, which with one long unit cell axis (40.4Å) serves as a model of macromolecular samples. An example of diffraction intensities obtained by rotating the crystal around c^* axis in 1° increments is given in figure 2. It is clear that the intensities are well resolved along the shortest reciprocal axis (b^*). We are planning to start the data collection using a protein crystal very soon.

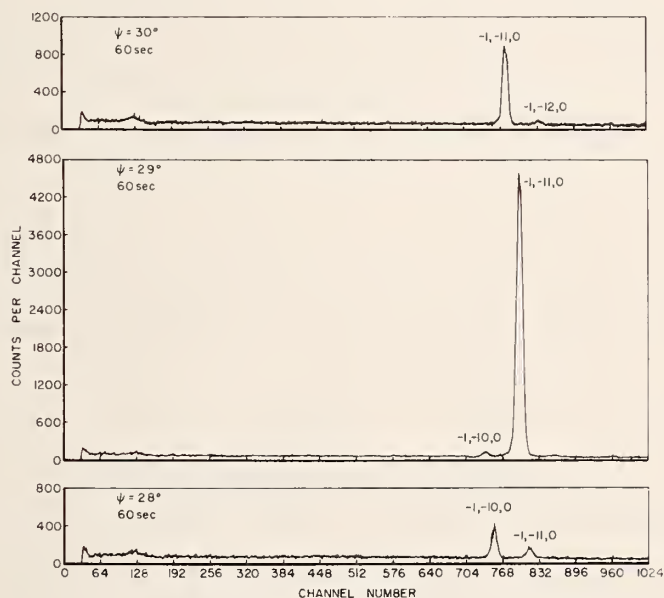


Figure 2. Output of the position sensitive detector in three orientations of the Ta_2O_5 crystal. Each frame was counted for 60 sec, $\lambda=2.4\text{\AA}$.

1. E. Prince and A. Santoro, *NBS Tech. Note* 896, 17 (1976).
A. Wlodawer and A. Santoro, "Flat-cone Diffractometer Utilizing a Linear Position Sensitive Detector," to be published.

DEVELOPMENT OF A TRIPLE-AXIS POLARIZED BEAM SPECTROMETER

C. Glinka, J. Rhyne

and

R. Williams

(Naval Surface Weapons Center, Whiteoak, MD)

A state of the art triple-axis neutron spectrometer utilizing polarization-sensitive crystals as monochromator and analyzer is under development at NBSR. With such an instrument not only the momentum and energy dependence of the neutron cross section but also its spin dependence may be determined in a scattering experiment. For many measurements, particularly on magnetic systems, this added capability can be used to discriminate against unwanted sources of scattering and thus greatly improve the precision of the measurement. Many other experiments, in which the spin dependence of the cross section is of chief interest, are possible only with polarization analysis of the scattering.

Although the methodology of polarized neutron scattering has been known for several years, use of the technique has been limited by the relatively low intensities obtained from polarizing crystals. Recently, however, we have tested single crystals of the Heusler alloy Cu_2MnAl and have found these crystals to have both good reflecting and polarizing properties. For example, the integrated reflectivities of these crystals are comparable to those of "good" copper crystals and are some three to five times greater than were measured for typical $\text{Co}(\text{Fe})$ crystals, which are the crystals most often used in polarized beam work. With the Cu_2MnAl crystals magnetized in a field of 3 kilogauss, polarization efficiencies up to 99% could be attained when care was taken to eliminate stray magnetic fields. Thus, use of these crystals should significantly improve the practicality of polarized beam experiments.

Samples to be studied will be mounted between the coils of a 60 kgauss superconducting magnet. Also incorporated in the spectrometer

is an rf neutron spin resonance flipper coil for reversing the direction of polarization. The flipper coil has been tested and a flipping efficiency of 99% is easily attainable. The spectrometer is expected to be completed and become fully operational in the near future.

COLD NEUTRON SOURCE

E. Guglielmo

The cold source facility consists of a cryostat, bismuth tip, main shield plug, cryostat shield plug, helium refrigerator, and associated transfer lines.

The major components for the facility are nearing completion. All parts of the bismuth tip have been fabricated and the final pairing of lead and bismuth should be accomplished by December, 1977.

The cryostat was damaged in testing but has since been repaired and vacuum tests have been run. Only final tests remain before assembly. The cryogenic plug needs to be filled with concrete and this will be accomplished after final tests on the cryostat. Final tests on the whole assembly with associated hook-up equipment remain to be completed.

NEUTRINO SCATTERING

R. C. Casella

The scattering of neutrinos and antineutrinos from nucleons is analyzed within the (V - A) charged-current four-quark model of Glashow, Illipoulos, and Maiani. Neutral current processes are obtained within the Weinberg-Salam picture utilizing model parameters determined from the charged-current processes. Rather pronounced scaling violations in the small x region observed in weak and electromagnetic lepton-nucleon interactions are accounted for via an energy dependent parameter

$\xi = \langle p_{\perp}^2 \rangle^{1/2}/k$, where k is the center of mass momentum and $\langle p_{\perp}^2 \rangle^{1/2} \approx 0.3$ GeV is the r.m.s. parton transverse momentum. Letting x and y be the customary scaling variables, the naive parton model is assumed to hold (in some average sense) for $x \gg \xi$, whereas for $x < \xi$ quark-antiquark ($q\bar{q}$) binding is expected to play an important role. The model leads to an increasing number of sea quarks being freed as the neutrino energy E increases and the region $x < \xi$ recedes towards zero as $E^{-1/2}$. The cross section ratio $\sigma_c^{\bar{\nu}N}/\sigma_c^{\nu N}$ (figure 1) and $\langle y \rangle_{\bar{\nu}}$ (figure 2) are found to rise with energy in the range $10 \text{ GeV} < E < 150 \text{ GeV}$, but less so than indicated by earlier experiments,¹ maintaining values closer to the recent CIT and CERN data.² The ratios of neutral to charged current cross sections vary even less (figure 3). The weak angle θ_W is found to assume its canonical value, $\sin^2 \theta_W = 0.3$. Nevertheless, the $d\sigma_c^{\bar{\nu}}/dy$ model distributions exhibit an increase near $y = 1$ as E increases. Within the

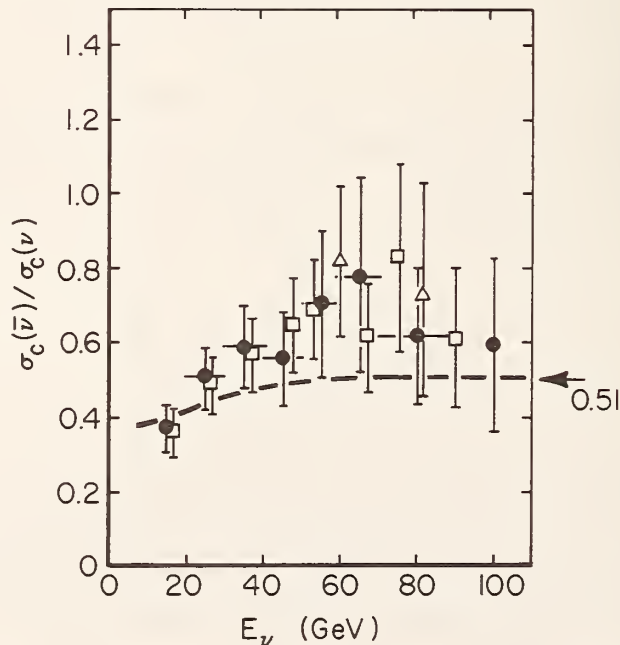


Figure 1. Ratio of antineutrino ($\bar{\nu}$) to neutrino (ν) charged-current nucleon cross sections vs. energy E . Data from HPWF (Ref. 1). At 150 GeV we obtain 0.51 for this ratio with an upperbound, 0.55. Recent CERN and CIT determinations lie in the range 0.4 to 0.5 (Ref. 2).

model, analysis of dimuon experiments implies semimuonic branching ratios for the decay of charm in the range 5% to 10%, assuming an SU(3) invariant sea (figure 4).³ The calculated mean number of strange particles per neutrino induced dilepton event is 1.4 for the broad-band sources employed at Fermilab in these experiments. The amount of $q\bar{q}$ sea in the model increases from $\approx 10\%$ at 10 GeV to $\approx 30\%$ at 150 GeV. A paper is in preparation.

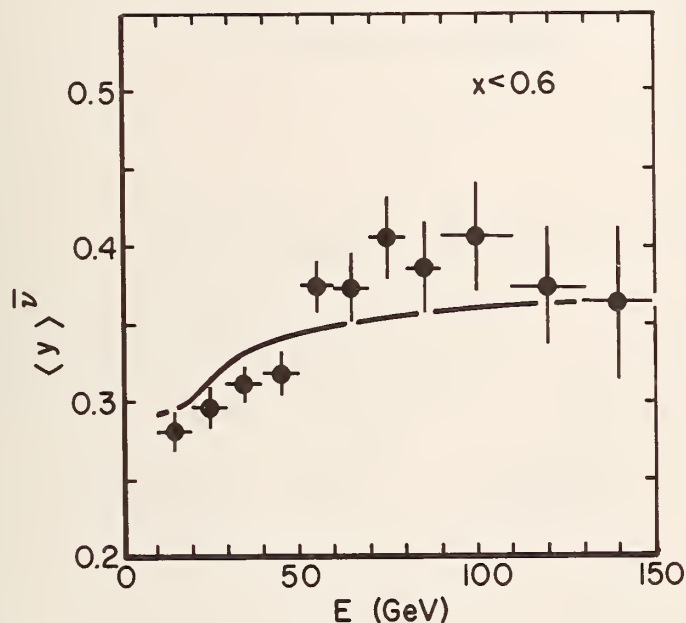


Figure 2. Average energy loss $\langle y \rangle_{\bar{\nu}}$ of the lepton in $\bar{\nu}$ -nucleon scattering vs. energy E. Earlier HPWF data (Ref. 1) are shown. Recent CERN and CIT results lie between 0.3 and 0.35 (Ref. 2).

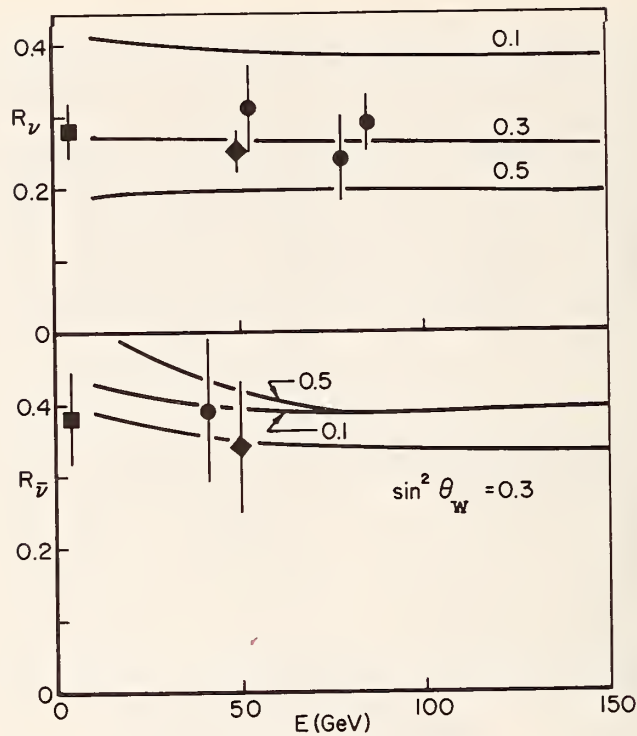


Figure 3. Ratios of charged to neutral current cross sections, R_ν and $R_{\bar{\nu}}$. Agreement occurs when the weak angle θ_W satisfies $\sin^2 \theta_W = 0.3$. Data from HPWF (Ref.1), CIT (Ref.2), and Gargamelle (low E).

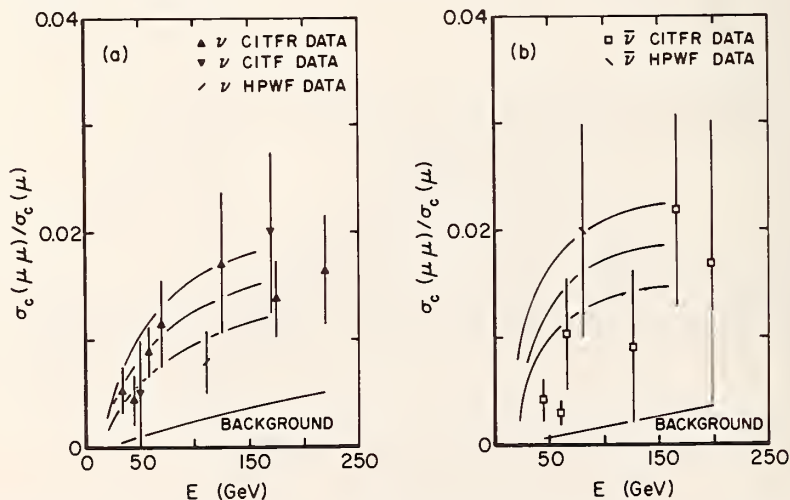


Figure 4. Model predictions for the ratio of dimuon to single muon production for values of the semimuonic branching ratio B (treated as an unknown parameter) equal to 5%, 7%, and 9%. CIT and HPWF data are shown (Ref. 3). Employing the (recent) CERN data (Ref. 3), the model leads to $B \approx 10\%$, in satisfactory agreement with the value obtained from the e^+e^- DORIS colliding ring experiments ($B \approx 10\% - 15\%$).

1. A. Benvenuti *et al.*, *Phys. Rev. Lett.* 37, 189 (1976); 36, 1478 (1976); 37, 1039 (1976).
2. J. Steinberger and C. Cundy, in papers presented at the Conference on Particle Physics, Budapest (July 1977); F. Scullli, M. Shaevitz, private communications.
3. B. C. Barish *et al.*, CIT preprint (1977); M. Holder *et al.*, CERN preprint (1977).

NEUTRON RADIOGRAPHY

D. A. Garrett

and

W. L. Parker

(Reed College, Portland, OR)

1. Technique and Facility Development

a. Thermal Neutron Xeroradiography

Xeroradiography was developed to take advantage of an edge enhancement inherent in the method which emphasizes small discontinuous changes in object density with resulting improved contrast and accuracy of interpretation. The "image" is produced on the surface of a layer of selenium which is non-conducting and has been given a uniform surface charge. Spatially-modulated ionizing radiation renders the selenium conducting so that the charge leaks off to the grounded backing plate in an amount proportional to the exposure, provided that saturation does not occur. The image is developed by spraying on graphite particles which adhere to the selenium and are then transferred to a special paper producing an opaque radiograph. It can operate in either the positive or negative mode. At a discontinuity in the surface charge density the electric field has a tangential component which produces lateral motion of the particles with a resulting "starvation" at the discontinuity. This is the edge effect.

Since neutrons by themselves are non-ionizing, it is necessary to employ a converter which emits ionizing radiation following neutron capture. The converter cannot be in contact with the selenium surface or the charge pattern will be destroyed. Good results have been obtained using a standard gadolinium oxysulfide screen separated from the selenium by about 0.5 mm. There is considerable evidence that the image is produced primarily by the 70 keV electrons resulting from thermal neutron capture by the Gd nuclei. In the positive mode the optimum exposure (10^8 n-cm^{-2}) is comparable to AA film used with a 25.4 μm Gd foil. The resolution is also comparable. In the negative mode the resolution is markedly poorer. At this point this behavioral characteristic is unexplained.

The resulting radiographs definitely show edge enhancement which could prove very valuable in certain applications such as the detection of corrosion. Other advantages are the absence of a darkroom and the ability to have the final radiograph within two minutes after exposure.

b. Background Subtraction

The gamma ray contamination in collimated neutron beams used in neutron radiography often results in a gamma radiograph being superimposed on the regular neutron radiograph. The result is a reduction in radiographic contrast due to this gamma background. Although in general, the energetic gamma rays generated from radiative capture of thermal neutron have little or no effect on the film, the softer gamma components can result in a gamma image on the film. Indeed these soft gamma rays can be filtered with polycrystalline bismuth or lead, however at the expense of some neutron flux. This loss can be an important factor especially in the case of transportable neutron radiography systems.

Although the technique of background subtraction has been employed for a number of years for medical application in the subtraction of x-ray images, no use has been made in the field of industrial radiography.

The technique has been successfully applied to the subtraction of

the gamma fogging from neutron radiographs. Basically the principle of background subtraction is as follows. Referring to figure 1, a positive neutron radiograph utilizing on metal foil converters is produced having gamma background fog. This is denoted by $n + g$. The converter is then removed from the cassette, a positive gamma radiograph, denoted by g , is produced of the object under inspection. Subtraction film having a film

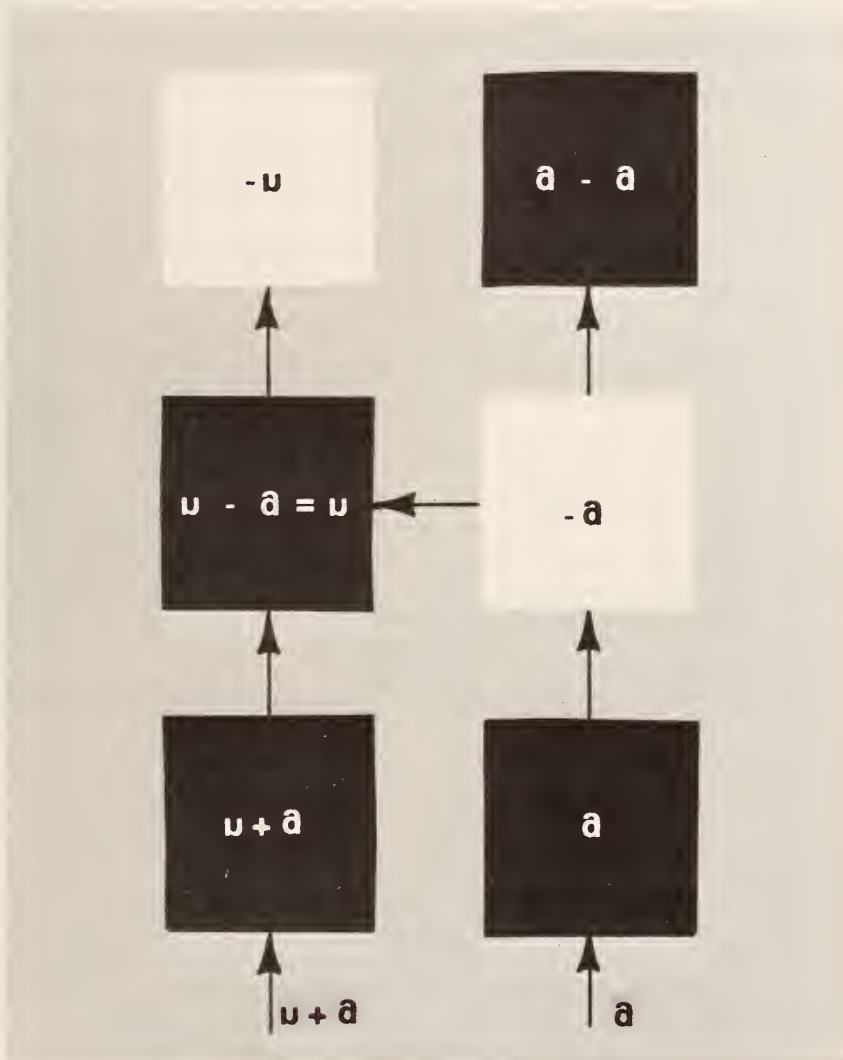


Figure 1. Block diagram illustrating the principles of background subtraction.

gamma of 1, i.e. the D-log E curve has a slope of 1 over a range of radiographic densities, is employed to produce a negative image -g of film g. Film -g is superimposed on film n + g to produce $n + g - g = n$. A negative film -n is then produced to furnish the finished neutron radiograph with the gamma ray effect eliminated.

The method will have a significant impact in the area of field neutron radiography since it is unfeasible to employ lead or bismuth filters to eliminate the gamma ray background at a sacrifice in neutron beam intensity. The technique is rapid, inexpensive and simple requiring no computerized subtraction techniques. For the purposes of field neutron radiography film registration can be sufficiently well produced to satisfy the needs at hand for field applications.

c. Corrosion Detection In Aluminum Airframe Components

The primary objective of these investigations was to determine the feasibility of detecting corrosion in aluminum Naval aircraft components with neutron radiographic interrogation and the use of standard corrosion penetrameters. Secondary objectives included the determination of object thickness on corrosion image quality, the defining of minimum levels of detectability and a preliminary investigation of a means whereby the degree of corrosion could be quantified with neutron radiographic data.

The nondestructive detection and visualization of environment-induced corrosion in aircraft presents an important maintenance problem and economic impact in both the civilian and military sectors. Since there is no reliable instrumental method by which corrosion can be detected in inaccessible areas of aircraft structures, visual and destructive inspection methods must presently be employed.

Corrosion in aircraft generally is induced by the presence of moisture and oxygen. The corrosion products so generated oftentimes, but not always, contain hydrogen in the forms of hydrated oxides or

hydroxides. In the case of salt water induced corrosion, chlorine may also be present. Because of the high attenuation of thermal neutron by hydrogen and chlorine, it should be possible to visualize corrosion areas using neutron radiographic interrogation.

The basic procedures governing the neutron radiographic inspection methods employed in these studies are outlined in this section. In addition, the results of preliminary experiments at the NBS to establish minimum levels of corrosion detectability and proposed methods to quantify the degree of corrosion were investigated.

All radiographic data generated in these investigations was obtained using direct neutron imaging methods with various converter screens. Manual film development was performed throughout with standard industrial radiography chemistry. A 7 in.-thick section cut from an uncorroded C-2 aircraft vertical fin was used as a standard object to be radiographed. The fin, which was obtained from the NAVAIR Rework Facility at North Island, San Diego, California.

All radiographic data generated in these investigations was obtained using direct neutron imaging methods. Manual film development was performed throughout with Eastman Kodak standard industrial radiography chemistry. A 7 in.-thick section cut from an uncorroded C-2 aircraft vertical fin was used as a standard object to be radiographed. The fin was obtained from the NAVAIR Rework Facility at North Island, San Diego, California.

Standard corrosion penetrameters were fabricated from aircraft-grade aluminum which had been corroded under controlled environments for predetermined periods of time. The penetrameter samples were obtained from the Naval Air Development Center, Warminster, Pennsylvania. Two types of penetrameters were employed in these investigations.

The first was fabricated from aircraft-grade aluminum which had been subjected to a super-saturated saltwater spray for 6.5 hrs. Nominal step thicknesses were 0.125 in. and 0.87 in.

The second set of four penetrameters was fabricated from 0.062 in.-thick aircraft-grade aluminum plates which had been subjected to a salt water spray/SO₂ gas environment for zero, four, eight and fifteen days.

Using a 0.0005 in.-thick vapor deposited Gd converter, we were able to form the following conclusions.

(1) Salt water induced corrosion signatures in aircraft-grade aluminum can be visualized with neutron radiography using a 200:1 L/D ratio. The effect of the 7 in.-thick fin thickness is to degrade the image quality. However, the signature can still be discerned.

(2) The time required for the exposure was 50 min. for a L/D ratio of 200:1.

(3) With the penetrameter on either side of the fin, analog edge enhancement aids in identifying the corrosion signature.

(4) When the L/D ratio is reduced to that of a field system, e.g., 43:1, the corrosion signature can only be visualized when the penetrameter was placed on the cassette side of the fin, making it necessary to inspect each side of an airfoil of 7 in. thickness individually.

(5) The time required for the exposure was 90 sec. for a L/D ratio of 43:1.

(6) With a L/D ratio of 43:1, image edge enhancement aids in visualizing the corrosion penetrameter when placed on the source side of the film, however, paint could possibly produce a similar signature.

To compare the results of another conventional direct imaging method utilizing a gadolinium oxysulfide converter, the following results were obtained.

(1) Corrosion signatures can be visualized using Gd₂O₂S converters with the penetrameter placed on either side of the 7 in.-thick fin, using an L/D ratio of 200:1. The apparent contrast was not as high as that obtained with Gd foil.

(2) The exposure time required using a Gd_2O_2S converter was 15 min. for a L/D ratio of 200:1.

(3) Image edge enhancement aided in identifying the corrosion signature on either side of the fin with a L/D ratio of 200:1.

(4) When the L/D ratio was reduced to 43:1 using a Gd_2O_2S converter, the corrosion signature could only be visualized with the penetrometer placed between the cassette and the fin. All image detail was eliminated due to geometrical unsharpness when the corrosion penetrometer was placed on the source side of the fin.

(5) The exposure required 45 sec. to complete.

(6) Edge enhancement did aid in the visualization of the penetrometer when it was placed between the fin and cassette, however, played little role in the detection of the corrosion signature when the penetrometer was placed on the source side of the cassette.

A third direct imaging technique was employed utilizing a light-emitting $^6LiF/ZnS$ converter in conjunction with a light sensitive x-ray film. This was the fastest imaging technique tested, however, the experimental results left much to be desired where image quality was concerned.

(1) Using a $^6LiF/ZnS$ light-emitting converter in conjunction with photographic film and a L/D ratio of 200:1, it was possible to visualize the corrosion signature when the penetrometer was placed between the vertical fin and cassette. The image quality was so poor however, that it could easily be confused with the scintillator mottling.

(2) The exposure time required was 5 sec.

(3) When the corrosion penetrometer was placed on the source side of the fin section, it was impossible to differentiate accurately between the corrosion signature and the background mottling.

(4) Edge image enhancement provided no useful purpose in the visualization of the corrosion signature with the penetrometer on either side of the film.

(5) When the L/D ratio was reduced to 43:1, it was impossible to accurately distinguish between the corrosion signature and the background mottling with the penetrometer on either side of the vertical fin.

(6) The exposure time required for this radiograph was approximately 0.2 sec.

A fourth set of investigations was conducted employing a 0.0001 in. thick Gd converter foil in an effort to define the lower limit of corrosion detectability in aircraft-grade aluminum utilizing reactor-based neutron radiographic procedures. A set of four calibrated corrosion penetrameters were fabricated from 0.062 in.-thick aluminum plates which had been subjected to a salt water spray/SO₂ gas environment for 0, 4, 8 and 15 days. Thermal neutron radiographs were made of the seven in.-thick C-2 vertical fin with calibrated penetrameters placed on the cassette side of the C-2 vertical fin. As a result of these investigations we concluded that:

(1) In the corrosion radiographs taken of the 0 and 4 day corrosion penetrameters, the corrosion cannot be distinguished from the background noise as observed in the edge enhanced inspection. It is likely that the mottled background noise is due to the neutron response to the fin paint.

(2) Environment induced corrosion can be observed without image enhancement in the 8 and 15 day corrosion samples. Image enhancement serves to render the corrosion images more observable.

Based on the experience gained in these preliminary investigations, empirical quantification of corrosion appears to be a possibility, either by isodensity scanning of neutron radiographs and comparison of scans of the corrosion areas with sound aluminum, or by digital image enhancement techniques. This conclusion is based on the fact that differences in corrosion density in the penetrometer could be visualized and that a minimum level of detectability could be established with the plague penetrameters.

The significant results of these investigations at the NBS may be summarized conclusively in the following statements.

(1) Environment-induced corrosion in aircraft-grade aluminum can be detected with a high degree of sensitivity with thermal neutron radiographic interrogation.

(2) The fluence (integrated neutron flux) at the image plane required to visualize corrosion with conventional imaging methods e.g., gadolinium converter in conjunction with a medium contrast industrial x-ray film at density of 2.5, is approximately $4 \times 10^8 \text{ n-cm}^{-2}$. Assuming that a transportable neutron radiography system were capable of producing $1.5 \times 10^4 \text{ n-cm}^{-2}\text{-sec}^{-1}$ at a L/D ratio of 40:1, an exposure of 7.2 hrs. would be required.

(3) At a L/D ratio of 40:1, the corrosion signature of both surfaces of a thick object, e.g., a wing or airfoil, must be interrogated individually. This is due to the fact that geometrical unsharpness tends to obliterate signature detail on the surface opposite the cassette.

(4) The possibility of corrosion quantification does exist, based on investigation with standard corrosion plaque penetrameters.

(5) Although the use of $^6\text{LiF/ZnS}$ light emitting converters is the most efficient method by which thermal neutron beams can be imaged, the results are inadequate for unambiguous corrosion signature analysis.

In light of these investigations we propose that the following ongoing programs in corrosion detection be initiated, i.e., converter development, real-time imaging methods evaluation for corrosion detection and corrosion quantification and standard penetrameter development.

The most efficient light-emitting neutron imaging system in so far as speed is concerned consists of a physical mixture of ^6LiF and ZnS powders. The components are held in suspension with a binder and settled on a thin aluminum substrate. The nuclear reaction which takes place is $^6\text{Li}(n,T)\alpha$, the tritons and alpha particles producing light in the ZnS scintillator.

The neutron radiographic images produced when this type of imaging screen is placed in intimate contact with light-sensitive film is quite grainy, exhibiting poor resolution. This is due, in fact, to several factors which include:

(1) The fact that the matrix is composed of powders having a finite grain size. If this grain is too coarse, a granular image will result.

(2) The ${}^6\text{LiF/ZnS}$ is partially transparent to light generated within the matrix, making it possible for light generated at one point to be scattered and emitted at a neighboring site.

(4) Light sensitive films generally tend to exhibit greater grain than industrial x-ray films.

We propose that a funded R & D program be initiated at NBS to develop a neutron sensitive scintillating converter which will overcome the aforementioned problems of the presently available continuous ${}^6\text{LiF/ZnS}$ thermal neutron imaging screens. Specifically, (1) we propose to size the ${}^6\text{LiF/ZnS}$ components so that only the finest grains available are employed to mix the final matrix using a fluorocarbon binder and (2) to break the initial continuous screen into a myriad of discrete information centers, or cells in order to eliminate the cross-talk generated as a result of the light transmission within the scintillator screen matrix. We have in mind to deposit the converter matrix in individual cells using chemically milled meshes having cells of approximately 0.0001 in. on a side separated by 0.005 in. walls to minimize cross-talk.

Pending the outcome of the screen development work, we propose that an evaluation of state-of-the-art real-time imaging systems be conducted for corrosion detection under field conditions. It would be most cost effective to evaluate the available real-time imaging systems on a lease basis.

This method has the advantage of speed and high sensitivity, based on the assumption that a suitable fast imaging screen can be developed which would provide the required resolution.

The quantification of detectable corrosion could produce an economic impact on military aircraft maintenance costs. By being able to quantify the corrosion, it should be possible to predict the time at which a defective area of skin or component should be replaced, rather than replacement on a preventative maintenance basis.

We propose that several avenues of investigations towards this end be pursued, e.g.

(1) Automated radiographic image analysis based on the isodensity pattern comparison with standard corrosion penetrameters or edge enhanced shadow analysis.

(2) Microchemistry of actual aircraft corrosion samples to aid in the fabrication of standard corrosion penetrameters.

(3) Subtraction of x-ray data from neutron data to eliminate the radiographic interferences caused by structural airframe members.

d. Facility Design and Fabrication

The thermal neutron radiography facility design was frozen in February 1977 and fabrication begun in March 1977. The pneumatically operated dual shutter mechanism has been completed, however problems have been experienced in stripper threads on the pneumatic pistons caused by severe momentum transfer when the 100 lb. shutters are stopped. The shutter design has been modified so that double acting oil-filled shock absorbers can be added to the system.

The cart employed to support the exposure cave has been completed. The exposure cave itself is approximately 80 percent complete.

2. Applications

a. NASA Langley Research Center - Neutron Interrogation of Resin-Impregnated Graphite Fiber Reinforced Polyimide Composites

Several samples of of resin-impregnated polyimide panels were submitted by the NASA Langley Research Center for neturon radiographic interrogation. This material is a high-strength graphite reinforced composite material that is capable of withstanding temperatures of approximately 600°F and will be employed for the aft body flap of the orbited space shuttle.

The purposes of these investigations were (1) to detect resin depletion in the samples and (b) to determine the graphite reinforcing fiber distribution in the composite matrix. Using microdensitometer scanning of neutron radiographs, it was possible to both detect resin depletion and in spite of the fact that the base matrix was a long N-O-CH₂ chain, it was possible to discern the carbon fiber distribution.

b. Smithsonian Institution - Thermal Neutron Radiography of Ancient Lead on Artifacts

The Chinese Yu shown here is a ceremonial vessel made of lead dating from the Western Chou period, approximately 1,000 B.C. It is part of the collection of the Hermatage Foundation Museum, Norfolk, Va. and is now on loan to the Freer Gallery of the Smithsonian Institution in Washington, DC.

Members of the Smithsonian brough the Yu to NBS, where Bureau researchers used it to test their new nondestructive evaluation technique--neutron xeroradiography. The result (original in color) can be compared with the photograph and the x-ray.

Unlike x-rays, neutrons can penetrate lead. Thus, the radiograph shows the mottled areas between the cap and the vessel where corrosion has sealed the urn. Note too the corroded area near the base. Also



Figure 1. The Chinese Yu shown here is a ceremonial vessel made of lead dating from the Western Chou period, approximately 1000 B.C.



Figure 2. The Yu was brought to NBS where researchers used it to test their new nondestructive evaluation technique - neutron xeroradiography. The result can be compared with an x-ray shown on the right.

visible in the radiograph on the left side is the outline of some material--paper or perhaps fabric--that may have been used in repairing the vessel. Other repair work can be distinguished without the aid of neutrons: Near the center, a triangular portion has been patched, possibly with bronze.

The exact purpose the vessel served and how it was damaged are, of course, matters of speculation. One theory is that this Yu was made for a burial service as one of the items to be included in the grave. The damage could have been done by early excavators, possibly grave robbers, who searched by poking the ground with sharp objects until they struck metal.

Evidence of corrosion product formation which holds the urn lid shut can be visualized in the neutron radiograph.

c. Smithsonian Institution - Thermal Neutron Radiography of Wooden 18th Century Harpsichord Lid

A 18th century harpsichord lid was radiographed both with thermal neutrons and x-rays ranging in energy from 40 pkv to 160 pkv. The purpose of these investigations was to visualize paint layers and internal details of the method employed to fasten individual boards together. The results of these experiments may be summarized as follows:

(1) X-radiography could discern paint layers on the harpsichord with good clarity.

(2) X-radiography permitted visualization of details of the nails employed to fasten individual boards of the lid together.

(3) The adhesive applied between the individual boards was radioopaque.

(4) The nails were also discernable using neutron radiography, however appeared to differ in detail from that obtained with x-radiography

(5) Details of artifacts in the wood matrix could be visualized with neutrons which could not be with x-rays.

(6) The adhesive employed to glue the individual boards of the lid was also neutron opaque.

(7) The migration of corrosion products formed on the nail surface into the wooden matrix could be visualized with neutron radiography.

Subtraction of x- and neutron radiographs also lead to new image information. However because of stringent demands on available personnel, it was not feasible to pursue this work further.

d. Smithsonian Institution - Neutron Radiography of a 3,000 Year-Old Bronze Chisel

A bronze chisel was subjected to neutron radiography in an attempt to visualize laminations of the bronze employed in the original fabrication. Extensive corrosion product formation on the chisel surface, however was thermal neutron opaque making visualization of the chisel matrix internals impossible.

It was determined using gamma-ray spectroscopy on the slightly radioactive chisel that the base bronze matrix was fabricated from a copper arsenic alloy instead of a copper-tin alloy as one might have expected.

3. Observations

a. Beam Gamma Contamination and Pair Production

The effect of the high-energy gamma ray contamination in the thermal column neutron radiography beam was discovered accidentally when an image of a high pressure nitrogen valve was observed in spite of the fact that no thermal neutrons were present in the beam. It was found that the intensity of the image varied markedly with cassette entrance window thickness.

Preliminary experiments were conducted with and without thermal neutrons in an attempt to determine the nature of this phenomenon. A number of exposures were made with samples of high atomic number materials. In all cases, film darkening was observed on those cases in which a light area should have been.

A gamma ray spectral examination of the beam was made using lithium carbonate to filter the neutrons from the beam with a 3" x 3" NaI(Tl) crystal spectrometer. Well-defined gamma ray photopeaks were observed to energies as great as 10 MeV, although no attempt was made to correct the data for detector efficiency. The gamma intensity (under normal operating conditions) at an L/D ratio was approximately $2R\text{-hr}^{-1}$.

All indications point to the fact that the observed effects are due to pair production generated in the object under inspection by gamma rays having energies in excess of 1.02 MeV. Final conclusions concerning the observed phenomenon have not been reached pending spectral analysis of the observed decay products.

STUDIES OF THE EFFECTS OF HYDROGEN IN TITANIUM

H. Alperin
(Naval Surface Weapons Center, White Oak, MD)

and

H. Flotow
(Argonne National Laboratory, IL)

and

J. J. Rush

Quasielastic incoherent scattering by hydrogen in titanium metal can be used to determine the true internal hydrogen diffusion rate. Neutron time-of-flight measurements on α -Ti and on the same sample loaded with $\sim 7\%$ hydrogen at temperatures from room temperature to 540°C have been performed. At each temperature, separate runs were also made to measure the inelastic scattering. Preliminary analysis of the results indicates that the diffusion of hydrogen in the α -phase is very low.

Experiments have also begun to develop a method to measure residual stress in bulk samples by neutron scattering. It has been shown possible to focus on a volume of interest as much as 3 cm below the surface of a specimen. Measurement of strains with a relative sensitivity of $\sim 2 \times 10^{-5}$ has been achieved.

STUDIES ON THE STRUCTURE OF "DEFECT" APATITES

A. Santoro

and

L. W. Schroeder
(Polymers Division)

The interpretation of the results previously obtained on "defect" hydroxyapatite requires comparison with a well characterized "standard" apatite. Fluoroapatite (FAP) was chosen because it has been studied several times by single crystal methods and because a well crystallized

powder (particle size 3-20 μm) of high phase purity was available.

Powder diffraction data was collected under conditions of high resolution; neutron wavelength = 1.518(1) \AA , Cu monochronator TOA = 74° . Horizontal divergences; in-pile collimator - $10'$, beam collimator - $23'$ and diffracted beam collimator - $10'$. Peak FWHM appeared to be about $15'$. The region from $2\theta = 5^\circ$ to 100° was scanned in 0.1° steps. Background points were available up to $2\theta = 90^\circ$. A plot of the background intensity against 2θ values indicated a minimum around 45° and then a slight rise although the variation was barely significant in terms of counting statistics. Some support for this observation comes from the fact that refinements utilizing the well known parameters of the apatite structure and this background did not require an overall temperature factor.

At convergence the agreement factor was 10% compared to an expected value of 7%. All constants agreed within 0.001 \AA of values obtained from single crystals of FAP. All positional parameters agree within 2σ ($\sigma = .0005$) of those obtained previously by x-ray diffraction studies. Table 1 gives values of the isotropic temperature factors obtained in this study. For comparison temperature factors obtained by neutron diffraction on a single crystal of hydroxapatite (HA) and by x-ray diffraction on a crystal of FAP are also given. Table 1 shows, with the possible exception of B(P), that temperature factors obtained by the neutron powder profile method are comparable to those obtained by single crystal methods. The trends in temperature factor, i.e. B(P) is smallest, B(0) largest, are reasonable for the apatite structure.

As a test of the sensitivity of the method to composition a reasonable temperature factor for fluoride was used and the occupancy allowed to vary. The refined value is 0.176(3); the theoretical 0.166 and the difference is barely significant. This would give 2.1 fluoride ions per unit cell instead of the stoichiometric 2.0.

In conclusion, these results indicate the neutron powder profile method is well-suited for the crystal chemical study of apatite powders provided the sample is well crystallized. It may be applied to non-

stoichiometric samples and may be expected to give results good to 5%.

Table 1. Isotropic temperature factors for apatites as obtained by powder profile and single crystal methods. Estimated standard errors for all methods are 0.01-0.02.

ATOM	B(FAP)	B(FAP)*	B(HA)**
Ca1	0.55	0.73	0.66
Ca2	0.56	0.63	0.33
P	0.04	0.34	0.19
01	0.77	0.85	0.30
02	0.65	0.78	0.50
03	0.77	0.99	0.63
F(or OH)***	0.61	1.2	0.87

(*) From x-ray diffraction studies of single crystals of fluoroapatite (Mackie and Young, *J. Appl. Cryst.* 6, 26, 1973).

(**) From a neutron diffraction study of a crystal of hydroxyapatite (Kay, Young and Posner, *Nature*, 204 1050, 1964).

(***) The isotropic thermal factor is a poor approximation of the motion of the F^- or OH^- ion in apatites and this probably accounts for some of the variation among the three studies.

At present, the technique is being used to study a sample of manganese containing fluoroapatite in order to test the capability of the method for determining cation distributions.

-
- Schroeder, L. W. and Prince, E., "Hydrogen Bonded Dimers in Tin (II) Hydrogen Phosphate," *Acta Cryst.*, B32, 3309 (1976).

THE STRUCTURE OF GUANIDINIUM TETRAMOLYBODIMETHYL
ARSENATE MONOHYDRATE

K. M. Barkigia and C. O. Quicksall
(Chemistry Department, Georgetown University)

and

E. Prince

The title compound, $(\text{CN}_3\text{H}_6)_2[(\text{CH}_3)_2\text{AsMo}_4\text{O}_{14}(\text{OH})]\cdot\text{H}_2\text{O}$, is one of a new class of heteropoly complexes in which organic groups are linked to a heteroatom through stable covalent bonds.^{1,2} As part of the continuing program at Georgetown University to develop and understand these complexes, an x-ray crystal structure of the compound was undertaken.^{3,4} The results of the x-ray investigation show that the anion is a remarkably compact and symmetrical structure which consists of a ring of four alternately face and edge-shared MoO_6 octahedra capped by the $(\text{CH}_3)_2\text{AsO}_2$ tetrahedron. This compound is one of the smallest heteropoly compounds yet reported and is only the second heteropoly in which face-sharing of octahedra has been found to exist.⁵

A unique feature of the title compound is the tightly bound, crystallographically ordered proton. Its presence was indicated by stoichiometry and confirmed by IR and NMR spectroscopy.⁴ Although the x-ray data did not directly reveal its position, the presence of a water of hydration 2.8\AA from the unique basal oxygen suggested that the proton was bound to this site. In light of the unusual features of this anion, a single crystal neutron diffraction study was undertaken with the particular aim of verifying the location of the unique proton.

A total of 4297 reflections were measured to $2\theta_{\text{max}} = 106^\circ$ with a neutron wavelength of 1.22\AA . Of these, 3216 unique reflections for which $I \geq 2\sigma(I)$ were used in the solution and refinement of the structure. The initial parameters for the heavy atoms were taken as the final coordinates from the x-ray analysis. The protons were easily found in the first difference map and after exhaustive least squares refinement, the final values of R and R_w were 0.047 and 0.037 respectively. The final positional and thermal parameters along with their corresponding

RRD COLLABORATIVE PROGRAMS

Table 1. Final positional and thermal parameters for $(\text{CN}_3\text{H}_6)_2[(\text{CH}_3)_2\text{AsMo}_4\text{O}_{14}(\text{OH})]\cdot\text{H}_2\text{O}$

Atom	x	y	z	β_{11}	β_{22}	β_{33}	β_{12}	β_{13}	β_{23}
Mo1	.1718(2)	.1156(2)	.44591(6)	59(3)	59(3)	5.6(2)	-14(2)	29.5(6)	-1.4(6)
Mo2	.3705(2)	.1076(2)	.35501(6)	51(3)	65(3)	6.1(2)	-14(2)	4.0(6)	-1.2(6)
Mo3	.1900(2)	-.1993(2)	.32033(6)	55(3)	60(2)	6.7(2)	7(2)	4.1(6)	-5.0(6)
Mo4	-.0036(2)	-.1943(2)	.41143(6)	53(3)	56(2)	6.0(2)	10(2)	2.0(6)	.1(6)
As	-.0367(2)	.1377(2)	.34125(6)	45(3)	60(2)	6.2(2)	10(2)	1.3(6)	1.9(6)
O1	.3467(3)	.0938(3)	.47816(8)	85(4)	149(5)	8.7(3)	-28(4)	-6.8(9)	3.3(10)
O2	.0770(3)	.2637(3)	.47003(8)	135(5)	73(3)	8.6(3)	-9(3)	12.3(10)	7.0(8)
O3	.0721(3)	-.0735(3)	.46224(7)	74(3)	74(3)	5.5(2)	-14(3)	3.8(8)	1.0(7)
O4	-.0302(3)	.0655(3)	.39415(7)	52(3)	66(3)	5.9(2)	3(3)	3.4(7)	.7(7)
O5	.2540(3)	.2193(2)	.39603(8)	74(4)	56(3)	6.8(3)	-11(3)	5.5(8)	-2.5(7)
O6	.2440(3)	-.0956(2)	.39266(7)	48(3)	67(3)	6.7(3)	0(3)	2.3(8)	.6(8)
O7	.5414(3)	.0766(3)	.38839(9)	59(4)	145(4)	9.4(3)	-5(4)	-1.1(9)	-4.8(10)
O8	.4124(3)	.2535(3)	.31929(9)	117(5)	90(3)	9.8(3)	-27(4)	13.6(10)	3.4(9)
O9	.3775(8)	-.0760(3)	.31717(8)	58(3)	77(3)	7.6(3)	-4(3)	8.4(8)	-3.8(8)
O10	.1262(3)	.0684(2)	.31913(7)	50(3)	66(3)	5.6(2)	2(3)	3.2(7)	-.1(7)
O11	.1166(3)	.2178(3)	.26587(8)	119(5)	139(4)	7.1(3)	-24(4)	4.8(10)	-11.7(9)
O12	.2747(3)	-.3754(3)	.33469(10)	90(4)	74(4)	15.3(4)	11(3)	11.2(11)	-3.4(10)
O13	-.0050(3)	-.2133(3)	.34739(7)	47(3)	78(3)	5.9(3)	-12(3)	1.7(7)	-1.5(7)
O14	.0798(3)	-.3687(3)	.42773(9)	126(5)	66(3)	9.5(3)	3(3)	-8.1(10)	3.1(8)
O15	-.2018(3)	-.2193(3)	.41540(9)	68(4)	134(4)	9.7(3)	-33(4)	7.7(9)	-7.1(10)
O16	.5050(3)	.2657(3)	.05735(9)	76(4)	95(4)	9.1(4)	-5(4)	2.1(10)	-.6(10)
N1	.2411(3)	.4827(2)	.51621(8)	176(4)	117(3)	18.5(4)	-55(3)	-19.0(10)	2.5(9)
N2	.4646(2)	-.4225(2)	.56135(6)	138(3)	93(3)	13.3(3)	1(3)	-9.2(8)	-1.4(7)
N3	.3006(2)	-.2261(2)	.53206(6)	124(3)	89(3)	13.7(3)	-8(3)	-7.4(8)	.7(7)
N4	.4575(2)	.0057(2)	.23075(5)	101(3)	148(3)	7.0(2)	51(3)	3.1(6)	3.5(6)
N5	.3758(2)	.1138(2)	.16306(6)	101(3)	192(4)	7.5(2)	-6(3)	1.3(7)	11.2(7)
N6	.2291(2)	.1511(2)	.22256(6)	88(3)	117(3)	10.2(2)	35(2)	1.7(7)	.1(7)
C1	-.0346(3)	.3602(2)	.34385(9)	149(5)	55(3)	11.0(3)	29(4)	-.6(11)	3.6(8)
C2	-.2212(3)	.0614(3)	.30747(8)	60(3)	120(3)	8.4(3)	-8(3)	-2.4(8)	5.3(9)
C3	.3340(3)	-.3758(2)	.5368(7)	87(3)	91(3)	8.4(3)	-22(3)	-1.8(8)	.7(7)
C4	.3540(3)	.0903(2)	.20587(7)	68(3)	93(3)	7.5(2)	-3(3)	2.2(7)	1.1(7)
H1	.3303(5)	-.1551(5)	.4094(1)	89(7)	102(6)	8.2(5)	11(6)	2(2)	3(1)
H2	.4982(7)	-.1821(7)	.4704(2)	229(13)	210(10)	8.8(6)	41(9)	5(2)	-8(2)
H3	.5878(6)	-.1997(6)	.4312(2)	117(8)	168(9)	14.2(7)	-31(8)	7(2)	0(2)
H4	-.1281(13)	.3937(7)	.3592(3)	500(28)	144(11)	43.3(22)	60(15)	79(7)	-12(4)
H5	-.0489(12)	.4021(8)	.3119(2)	608(29)	142(10)	15.5(9)	25(12)	-2(4)	2(3)
H6	.0613(11)	.3985(7)	.3604(4)	361(21)	95(9)	55.9(25)	14(12)	-91(7)	-6(4)
H7	-.2756(8)	-.0235(9)	.3267(2)	175(11)	316(14)	19.0(9)	-108(11)	-11(3)	29(3)
H8	-.1899(8)	.0131(11)	.2780(2)	160(11)	513(22)	13.8(8)	-93(13)	1(13)	-37(4)
H9	-.2987(8)	.1528(8)	.2996(3)	159(10)	198(11)	34.4(15)	15(10)	-43(3)	8(3)
H10	.2076(6)	.1263(6)	.2533(2)	161(9)	207(9)	9.2(16)	82(8)	7(2)	0(2)
H11	.1483(6)	.2063(6)	.2020(2)	141(9)	173(9)	12.9(7)	42(8)	-6(2)	9(2)
H12	.3034(7)	.1804(7)	.1431(2)	160(10)	258(12)	10.2(6)	-1(9)	-7(2)	19(2)
H13	.4780(7)	.0894(9)	.1530(2)	168(11)	347(15)	10.6(7)	41(12)	14(2)	16(3)
H14	.4360(6)	-.0217(5)	.2621(1)	141(8)	159(8)	6.9(5)	51(7)	5(2)	4(2)
H15	.5366(7)	-.0561(7)	.2158(2)	167(10)	249(11)	9.5(6)	104(9)	6(2)	2(2)
H16	.2011(8)	.1920(6)	.5150(2)	188(12)	158(9)	18.5(9)	-4(9)	-18(3)	3(2)
H17	.3622(8)	.1499(6)	.5512(2)	212(12)	134(8)	23.9(11)	16(9)	-27(3)	-11(3)
H18	.2628(10)	-.5940(7)	.5208(3)	344(20)	142(11)	32.5(15)	76(12)	-36(4)	-3(3)
H19	.4965(7)	-.5374(6)	.5606(2)	189(11)	124(8)	16.1(8)	21(8)	-5(2)	5(2)
H20	.1565(9)	-.4531(8)	.4945(3)	268(16)	208(13)	29.1(14)	-95(12)	-45(4)	4(3)
H21	.5427(7)	-.3477(7)	.5739(2)	160(10)	170(10)	19.5(10)	-7(9)	19(3)	-4(2)

a. The form of the anisotropic thermal ellipsoid is $\exp[-(\beta_{11}h^2 + \beta_{22}k^2 + \beta_{33}l^2 + 2\beta_{12}hk + 2\beta_{13}hl + 2\beta_{23}kl)]$

Table 2. Selected bond lengths in $(\text{CN}_3\text{H}_6)_2[(\text{CH}_3)_2\text{AsMo}_4\text{O}_{14}(\text{OH})]\cdot\text{H}_2\text{O}$

Atoms	No. Averaged	Type	Range	Mean
Mo-O	8	Terminal	1.699(3)-1.719(3)	1.707
Mo-O	8	Doubly Shared by 2 Mo atoms	1.906(3)-1.941(3)	1.920
Mo-O	4	Triply Shared by 3 Mo atoms	2.252(3)-2.346(3)	2.290
Mo-O	4	Quadruply Shared by 4 Mo atoms (unique basal)	2.360(3)-2.527(3)	2.416
As-O	2		1.704(3);1.704(3)	1.704
As-C	2		1.906(3);1.899(3)	1.903
C-H	6	Methyl	.972(9)-1.060(7)	1.021
N-H	12	Guanidinium	.961(8)-1.018(6)	.989
O(6)-H(1)			.991(5)	
O(16)-H(1)			1.779(5)	
O(16)-H(2)			.945(6)	
O(16)-H(3)			.941(7)	

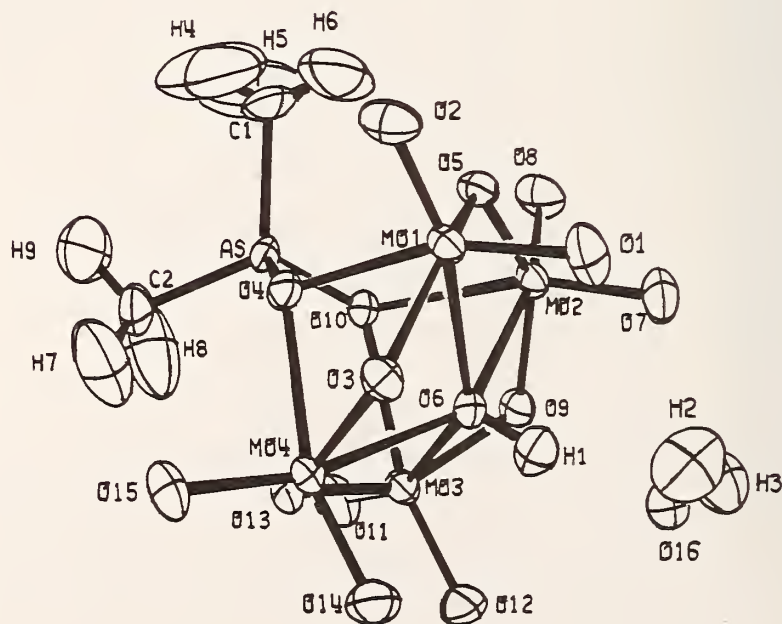


Figure 1. Tetramolybdodimethyl arsenate ion.

standard deviations are presented in table 1.

Figure 1 shows the results of the neutron study. As hypothesized, proton H(1) is indeed located on the unique basal oxygen O(6). The O(6)-H(1) bond distance is $.991(5)\text{\AA}$ and the hydrogen-bonded distance of H(1) to O(16) is $1.779(5)\text{\AA}$. Although a number of oxometallate complexes have been shown to contain protons by spectroscopic means,⁶ this study presents the first structural data for a proton in these species. A list of selected bond distances is given in table 2.

-
1. W. Kwak, L. M. Rajkovic, J. K. Stalick, M. T. Pope, and C. O. Quicksall, *Inorg. Chem.*, 15, 2778 (1976).
 2. W. Kwak, M. T. Pope, and T. F. Scully, *J. Am. Chem. Soc.*, 97, 5735 (1975).
 3. K. M. Barkigia, M. S. Thesis, Georgetown University, 1975.
 4. K. M. Barkigia, L. M. Rajkovic, M. T. Pope, and C. O. Quicksall, *J. Am. Chem. Soc.*, 97, 4146 (1975).
 5. D. D. Dexter and J. V. Silverton, *J. Am. Chem. Soc.*, 90, 3589 (1968).
 6. See, for example, M. T. Pope and G. M. Varga, Jr., *Chem. Commun.*, 653 (1966).

CRYSTAL STRUCTURE OF TRIAMINOGAUNIDINIUM NITRATE BY NEUTRON DIFFRACTION

C. S. Choi

(Energetic Materials Division, AARADCOM, Dover, NJ)

and

E. Prince

Triaminogaunidinium nitrate (hereafter called TAG-nitrate), $(\text{NH}_2\cdot\text{NH})_3\text{C}\cdot\text{NO}_3$, is a fuel, and is used as an additive for propellants. The crystal structure has recently been determined by A. J. Bracuti at ARRADCOM by using x-ray diffraction, but least squares refinement was not satisfactory, mainly because of very large amplitudes of thermal motion of the oxygen atoms. This neutron diffraction study was aimed

Table 1. Final least squares parameters of TAG-nitrate. The parameters of the nitrate group atoms* are converted from those of the rigid body refinement.

Atom	\underline{x}	\underline{y}	\underline{z}	\underline{B}_{11}	\underline{B}_{22}	\underline{B}_{33}	\underline{B}_{12}	\underline{B}_{13}	\underline{B}_{23}
C	.2803(4)	.2399(3)	1/4	2.9(1)	2.6(1)	2.9(1)	.1(1)	-	-
N1	.3332(3)	.1409(2)	1/4	3.1(1)	2.8(1)	4.9(2)	.1(1)	-	-
N2	.1253(4)	.2594(3)	1/4	2.8(1)	3.5(1)	4.7(1)	.2(1)	-	-
N3	.3837(3)	.3200(2)	1/4	3.1(1)	2.7(1)	4.7(2)	.1(1)	-	-
N4	.2219(3)	.0590(3)	1/4	3.7(1)	3.2(1)	5.7(2)	-.4(1)	-	-
N5	.0736(4)	.3644(3)	1/4	3.4(1)	4.5(2)	6.2(2)	1.0(1)	-	-
N6	.5483(4)	.2971(2)	1/4	3.0(1)	3.3(1)	5.5(2)	-.2(1)	-	-
H1	.4506(9)	.1268(7)	1/4	3.4(4)	3.9(3)	7.6(6)	-.1(3)	-	-
H2	.0487(10)	.1978(9)	1/4	4.1(4)	5.3(4)	7.8(6)	-.1(4)	-	-
H3	.3444(10)	.3939(7)	1/4	5.3(4)	2.9(3)	6.0(5)	.2(3)	-	-
H4	.2409(8)	.0143(5)	.1280(15)	6.3(3)	4.1(3)	7.5(5)	-.7(2)	-.5(3)	-.9(3)
H5	.0074(10)	.3778(6)	.1291(15)	5.9(3)	6.5(4)	8.3(5)	2.2(3)	-.5(4)	1.8(4)
H6	.5984(8)	.3287(6)	.1286(14)	4.7(3)	6.1(4)	7.7(5)	-.8(2)	1.3(3)	.2(3)
*N	-.2396	.0979	1/4	2.54	2.57	5.06	-.08	-	-
*O1	-.3575	.0468	1/4	3.60	2.80	25.93	.07	-	-
*O2	-.1832	.1224	.4030	9.31	8.20	5.47	2.91	-1.67	-1.25

at completing the structure by determining the hydrogen positions in the structure, as well as studying the thermal motions of the nitrate group.

Table 2. Hydrogen bonds in TAG-nitrate.

<u>Bond</u>	<u>N-H(A°)</u>	<u>H...O(A°)</u>	<u>N...O(A°)</u>	<u>N-H...O(°)</u>
N(1)-H(1)...O(1)	1.001(9)	1.847(10)	2.793(6)	156.4(7)
N(3)-H(3)...O(1)	0.994(10)	1.932(10)	2.864(7)	155.1(8)
N(5)-H(5)...O(2)	0.981(10)	2.104(10)	3.058(7)	163.6(8)

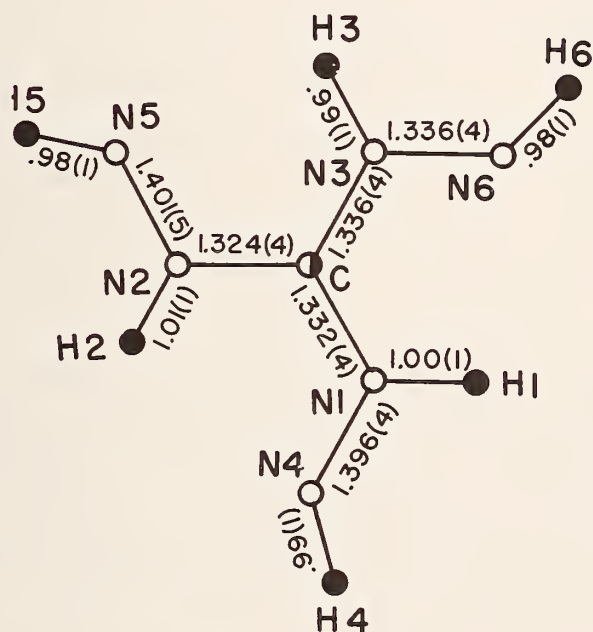


Figure 1. Interatomic distances in the TAG nitrate molecule.

TAG-nitrate crystallizes in the orthorhombic space group Pbcm, with cell constants at room temperature, $a=8.389$, $b=12.684$, and $c=6.543\text{\AA}$. There are four molecules per unit cell. A total of 875 reflections were measured within the limiting sphere defined by a maximum 2θ angle of 106° using 1.23\AA wavelength neutrons. Among these, 613 reflections had observable intensity. All hydrogen atoms were located by a Difference Fourier synthesis. An attempt to refine this structure

by means of the conventional method based on the harmonic oscillation model again failed to give a reasonable fit to the large thermal motion of the oxygen atoms. To accommodate such large, and therefore markedly curvilinear thermal motions, the nitrate group was constrained to have an ideal planar trigonal shape, and its size (N-O bond length) and the rigid body motion was refined with the use of third cumulant. This constrained rigid body refinement converged normally and reduced the R-indices to $wR=0.054$ and $R=0.058$.

The crystal structure of TAG-nitrate is composed of an infinite network of hydrogen bonds running between the planar ions. The TAG cation (except the amino hydrogens) lies in the mirror plane. The nitrogen atom and one oxygen atom of the nitrate anion also lie in the mirror, while the other two oxygen atoms are symmetrically placed on either side. Each ion is linked to four surrounding ions with opposite charge by strong N-H...O type hydrogen bonds (see table 2). The TAG cation has essentially trigonal symmetry, and the C-N bond lengths, as given in figure 1, are about 1.33Å indicating partial double bonding. This is an indication of the resonance structure of the guanidinium ion. The NO_3 ion also has similar resonating electronic structure, and hence its true (unconstrained) structure should be very close to the trigonal model. The nitrate anion undergoes an intense librational motion with amplitude of 20° for one principal axis, and about 6° for the other two axes. The orientation of the largest principal axis is not perpendicular to the plane of the group but tilted about 26° in the mirror plane.

THE STRUCTURE OF NH_4N_3

E. Prince

and

C. S. Choi

(ARRADCOM, Dover, NJ)

Ammonium azide crystallizes in the orthorhombic space group $Pnma$, with cell constants $a=8.948\text{\AA}$, $b=3.808\text{\AA}$, $c=8.659\text{\AA}$. The structure,

Table 1. Selected bond distances and angles in ammonium azide. Corrected distances and angles are determined from the rigid body model.

Atoms	Uncorrected	Corrected
N(1)-N(2)	1.168Å	1.186(4)Å
N(3)-N(4)	1.171Å	1.186(4)Å
N(5)-H(1)	1.036Å	1.073(9)Å
N(5)-H(2)	0.998Å	1.021(9)Å
N(5)-N'(2)	2.974Å	2.967(3)Å
N(5)-N(4)	2.981Å	2.974(3)Å
H(1)-N(5)-H(1) ¹	105.8°	107.2(1.2)°
H(1)-N(5)-H(2) ¹	110.3	109.6(0.0)°
H(2)-N(5)-H(2) ¹	109.9	110.2(1.1)°
N(5)-H(1)-N(2)	177.6	178.9(8)
N(5)-H(2)-N(4)	177.9	178.2(9)

determined originally by Frevel¹, consists of two crystallographically independent, symmetric azide ions bound to the ammonium ions by strong N-H...N hydrogen bonds. The central nitrogen atom of each azide ion occupies a center of symmetry, but one ion lies in a mirror plane, while the other lies along a 2-fold rotation axis perpendicular to the mirror plane.

We have refined the structure from single crystal neutron diffraction data. Of 359 independent reflections within the limiting sphere defined by a wavelength of 1.230Å and a maximum 2θ angle of $106^\circ 23'$ had observable intensities. Using the robust/resistant techniques described previously,² an unconstrained refinement gave a weighted agreement index of 5.5%, and a constrained refinement treating both azide groups and the ammonium group as rigid bodies gave a weighted agreement index of 6.0%. It may be that the assumption of rigidity in the ammonium group is not justified. Table 1 gives selected bond dis-

tances in the structure. The N-N bond length in the azide groups is 1.186(4)Å, in excellent agreement with the values found in the azides of monovalent metals. The N-N distances in hydrogen bonds, 2.974(4)Å and 2.967(3)Å, are indicative of unusually strong hydrogen bonds.

-
1. L. K. Frevel, Z. Krist. 94, 197 (1936).
 2. W. L. Nicholson and E. Prince, *NBS Tech Note* 939, p. 23 (1977).

STUDY OF THE CRYSTALLINE COMPONENTS OF PORTLAND CEMENTS

A. Santoro

and

P. Brown

(Center for Building Technology)

Studies on the crystalline components of Portland cements have continued during the past year. The first problem at hand has been to find components sufficiently pure to be used as standards in subsequent investigations.

A powder sample of β -2CaO·SiO₂ (β -C₂S) has been refined with the method of total profile analysis to a value of the R factor of 0.05. This refinement seems to be better than that carried out with x-ray single crystal techniques mainly because all the crystals used in the x-ray experiment were twinned. The analysis of this compound is still in progress.

BATTERY ELECTRODE STRUCTURE

P. D'Antonio
(Naval Research Laboratory, Washington, DC)

and

J. J. Rhyne and A. T. Santoro

The basic questions of electrochemical activity, as related to the atomic arrangement of the active constituents in the electrodes of the lead-acid battery, are being investigated. The structural information is being derived from the radial distribution function, which is the Fourier sine transform of the experimental total intensity after the atomic background scattering has been determined and removed^{1,2}, and the total profile procedure.³ We plan to systematically analyze the inter-atomic distance distribution and correlate structural changes with electrochemical activity changes as the battery is cycled and its capacity declines.

The structure of chemically prepared beta-PbO₂ has been determined by x-ray⁴ and neutron⁵ diffraction. The alpha modification has only been studied by x-ray diffraction⁶ and we are planning to verify the oxygen parameters using the profile refinement method.³

Figure 1 illustrates the advantages of a neutron diffraction experiment over an x-ray diffraction experiment when the atomic number of the atoms present is not very different.

At the top of figure 1 the spatial atomic arrangement⁵ of beta-PbO₂ is shown with the unit cell outline. The table in the middle of the figure 1 describes which atom pairs contribute to the first four peaks in the G(r) curve and lists the coordination numbers (N). For example, the first peak is a cluster of the 2.157 and 2.165A distances. The 2.157A distance arises from origin atom Pb(A) and target atoms of type O(B). There are four of these distances. In addition, two more distances at 2.157A occur between origin atom O(B) and target atoms of type Pb(A), namely, Pb(A) and Pb(D).

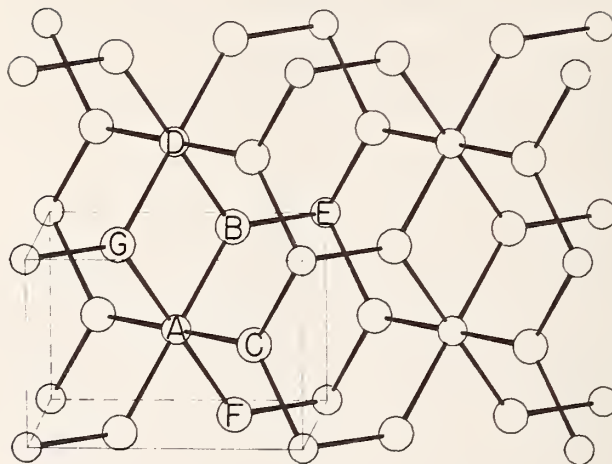


Figure 1. Beta-PbO₂
 TOP - Spatial Atomic arrangement⁵ with unit cell outline.

In the theoretical neutron diffraction (ND) $G(r)$ curve, in the lower part of figure 1, the first four resolved peaks are numbered.

As can be seen by comparing the neutron diffraction (ND) and x-ray diffraction (XD) $G(r)$ curves, $G(r)$ (XD) is missing the second and third oxygen-oxygen peaks due to the fact that the scattering factor for Pb is about 10 times that for O, for x rays, whereas only 1.6:1 for neutrons.

As a control and test of the applicability of the radial distribution procedure, chemically prepared beta-PbO₂ was examined by neutron diffraction. In figure 2 we see the calculated $G(r)$ curve for beta-PbO₂ using the atomic coordinates given by Leciejewicz.⁵ The experimental $G(r)$ curve was determined from a data reduction least-squares program^{1,2}, which determines the scale and shape parameters of the atomic background which minimize the spurious detail in the inner region of the radial

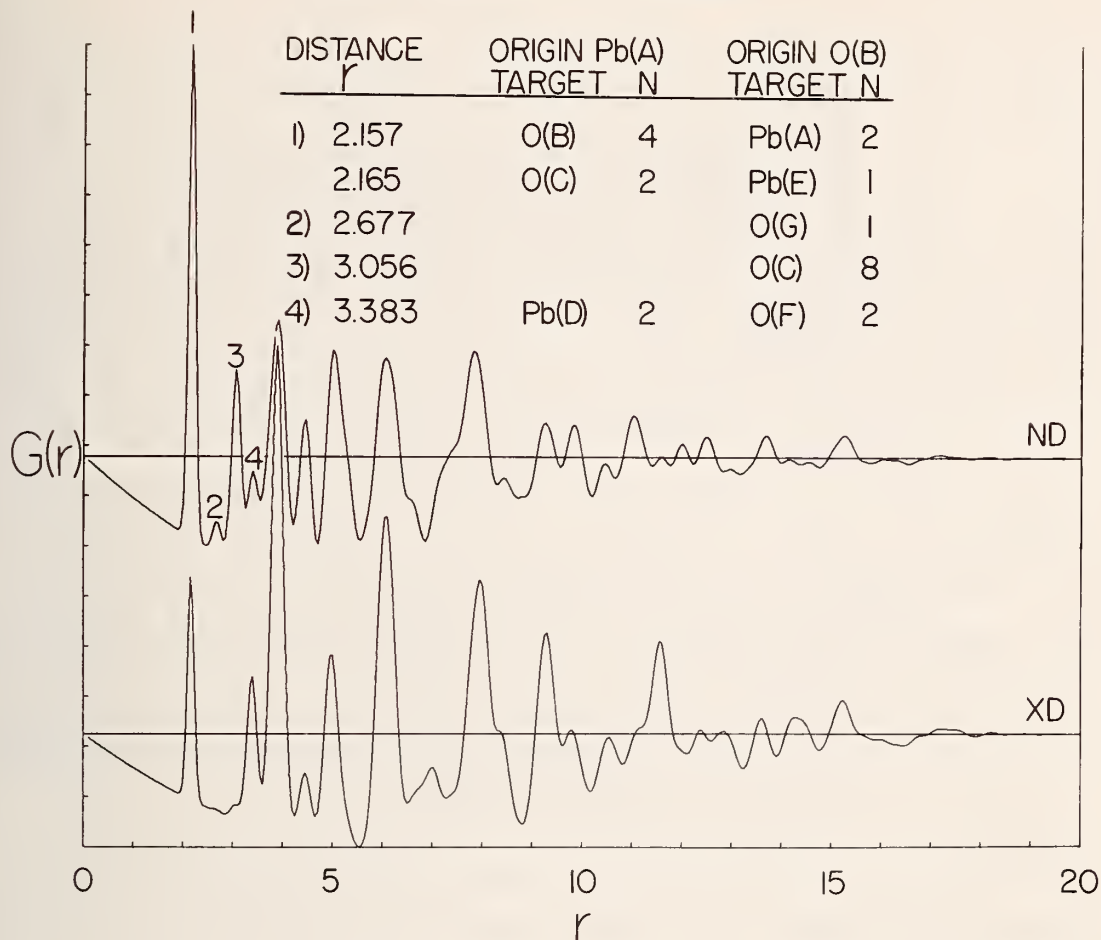


Figure 1. (Continued)

MIDDLE - Table listing atom pairs contributing to the first four peaks in the $G(r)$ curves and coordination numbers (N).

BOTTOM - Theoretical $G(r)$ curves computed for the atomic arrangement shown at the top of this figure. The ND curve is predicted for an x-ray diffraction experiment.

distribution curve, where the probability of finding an internuclear distance is zero. The procedure isolated the interatomic interference scattering from the total intensity scattered and also determines the interatomic distance thermal or disorder parameters, and coordination numbers of the short resolved distances in the sample. The bottom curve shows the isolated distances after they have been characterized by the analysis. The agreement between experiment and theory is quite good and further experiments are being carried out on actual formed and failed

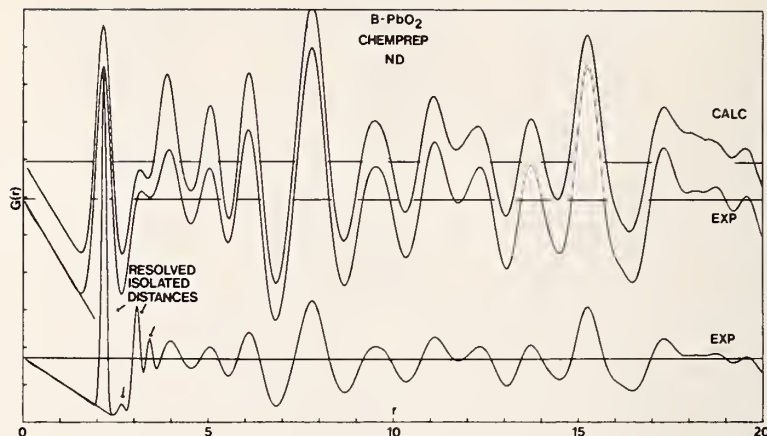


Figure 2.

TOP - Calculated $G(r)$ for beta- PbO_2 using atomic arrangement shown at the top of figure 1.

MIDDLE - Experimental $G(r)$ for chemically prepared beta- PbO_2 from a neutron diffraction experiment.

BOTTOM - This curve illustrates the resolution that can be achieved for the short resolved isolated distances in the sample once they are characterized.

battery plates in the hope of correlating electrochemical activity with electrode structure.

1. J. H. Konnert and J. Karle, *Acta. Cryst.* A29, 702 (1973).
2. P. D'Antonio, P. Moore, J. H. Konnert, and J. Karle, *Transactions of the American Crystallographic Association*, 13, 43 (1977).
3. H. M. Rietveld, *J. Appl. Cryst.* 2, 65 (1969).
4. A. Tolkalev, *Vestnik Leningradskogo Univ.* No. 4, 152 (1958).
5. J. Leciejewicz and I. Padlo, *Naturwissenschaften*, 49, 373-4 (1962).
6. R. W. G. Wyckoff, *Crystal Structures*, Volume 1, pg. 259, second edition, Interscience.

A STUDY OF THE PHASE TRANSFORMATION IN TRINITROTOLUENE

S. F. Trevino, C. S. Choi and H. Prask
(Energetic Materials Division, ARRADCOM, Dover, NJ)

Trinitrotoluene (TNT) can be crystalized from the melt into two phases, an orthorhombic phase and a monoclinic phase. Both phases are stable at 25°C but upon annealing at 70°C the orthorhombic phase transforms into the monoclinic. It has been thought that this transformation is the cause of cracking and void formation in castings of munition containing TNT. In the present study, neutron diffraction was used to detect the presence of the two phases in samples cast under varying conditions. The samples were cast in two containers one a 1 cm diameter aluminum tube and the second a thin wall large diameter (6 cm) aluminum cup. The orthorhombic phase could be obtained from the melt only if the TNT was quenched from 85°C in the melt to 0°C (ice bath) in ~ 2 sec. One can conclude that in the process of casting munitions, any orthorhombic TNT formed will very quickly transform to the stable monoclinic and therefore this phase transition is not the cause of the cracking and void observed. Further studies on samples from actual munition will be performed.

PHONON DISPERSION CURVES OF KN_3 AT 1 BAR AND 6.6 KBAR

N. J. Chesser

and

S. F. Trevino

(Energetic Materials Division, ARRADCOM, Dover, NJ)

The acoustic and low-lying optic modes of KN_3 have been determined

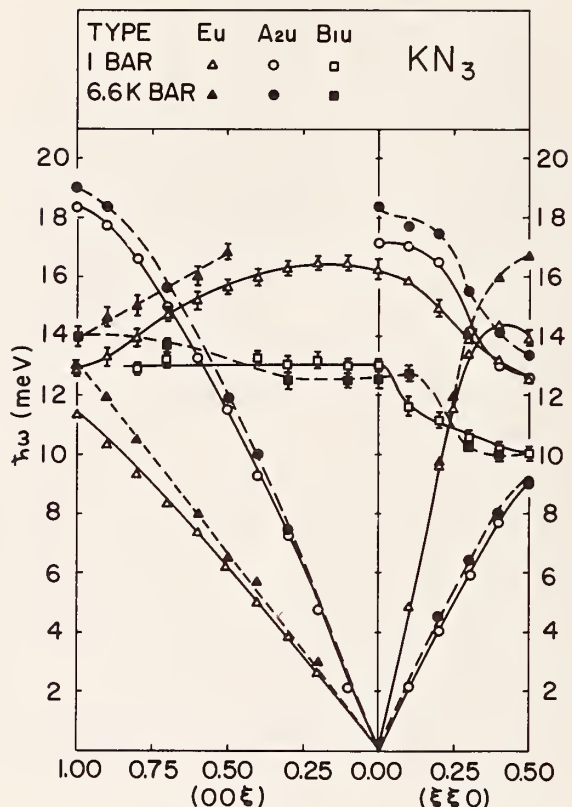


Figure 1. Measurements along the [110] and [001] directions for 1 bar and 6.6 kbar.

using inelastic neutron scattering. Measurements were made along the [110] and [001] directions at both 1 bar and 6.6 kbar. The results are shown in figure 1. The mode Grüneisen constants of several modes are found to be substantially larger than in KBr and very anisotropic. A rigid ion model is being formulated in an attempt to reproduce the measurements.

AMMONIUM-ION DYNAMICS IN NH_4ClO_4

N. J. Chesser and H. J. Prask
(Energetic Materials Division, LCWSL, ARRADCOM, Dover, NJ)

Our studies of ammonium-ion dynamics in ammonium perchlorate (AP)

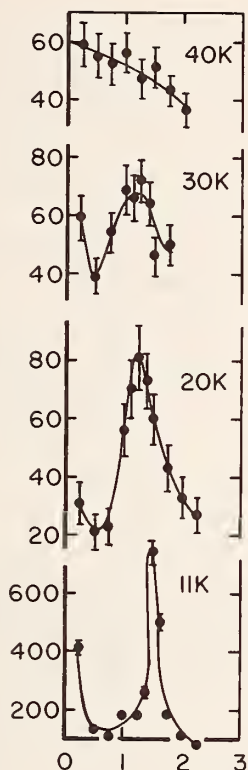


Figure 1. Temperature dependence of the very low-lying optic mode observed in d-AP, measured at the (0,2,1) zone-center lattice point.

have continued in two areas: 1) quasi-elastic neutron scattering (QNS) has been used to re-examine the character and directional dependence of NH_4^+ re-orientations in single-crystal AP in the 80 to 120K temperature range; 2) dispersion curves have been measured for the first time for deuterated-AP. In both cases analyses of the measurements are in progress; however, preliminary results are summarized below.

Earlier QNS measurements¹ made with ~ 0.09 cm thick crystals showed differences in the Lorentzian-component width for momentum transfers along the three crystallographic-axis directions ($|Q| \sim 1.5 \text{ \AA}^{-1}$). However, for higher Q s ($|Q| > 2.6 \text{ \AA}^{-1}$) expected differences were not observed. This was attributed to significant multiple scattering. In the present series of measurements, crystals ~ 0.04 cm in thickness were used. Multiple scattering still lessens the observed differences compared to expected

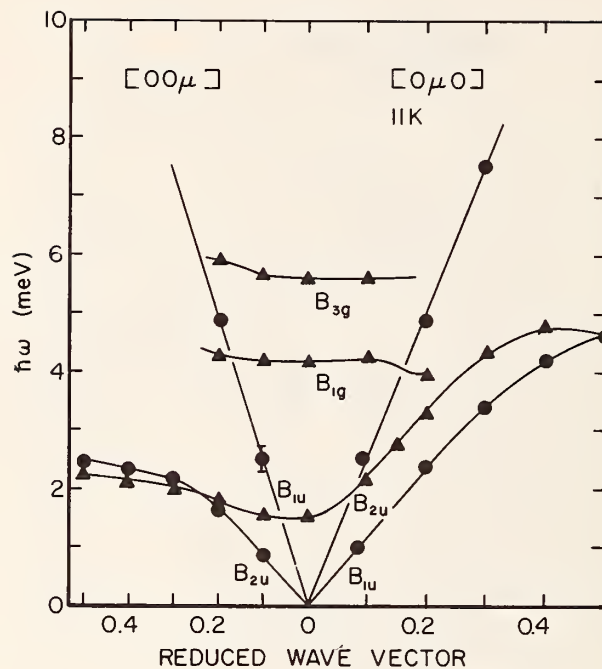


Figure 2. Partial dispersion curves of d-AP at 11K. The curves are guides to the eye.

values at higher Q s, but distinct differences are observed. At lower Q s, both magnitudes of Lorentzian widths and their "degree of anisotropy" differ from the values obtained with the thicker crystals. Results for 80 and 100K are compared in table 1.

Because of the complexity of AP (orthorhombic, $Pnma$, with four formula units per primitive cell) our dispersion curve measurements have focused, primarily, on two modes (B_{1g} at 4.2 meV, B_{3g} at 5.7 meV at Γ) the temperature-dependence of which was found to be anomalous in earlier Raman-scattering measurements.² We have made use of the neutron scattering selection rules formulated by Casella and Trevino³ to examine lattice points in deuterated AP at which the modes of interest would be expected to dominate the scattering. The results for several temperatures are consistent with the results of the Raman scattering study. In addition, we have observed a very low frequency optic mode (1.5 meV at 11K) not observed in the Raman measurements,⁴ the temperature dependence of which

Table 1. Lorentzian-widths of QNS profiles for single-crystal NH_4ClO_4

	80K		100K	
	Previous Work ¹	Present Results ²	Previous Work ¹	Present Results ²
Γ_1 (y-axis)	0.11 ± 0.01 meV	0.07 ± 0.01 meV	0.20 ± 0.02 meV	0.20 ± 0.02 meV
Γ_2 (x-axis)	0.14 ± 0.02	0.12 ± 0.01	0.28 ± 0.02	0.23 ± 0.04
Γ_3 (z-axis)	0.11 ± 0.01	0.12 ± 0.01	0.31 ± 0.03	0.29 ± 0.03

1. From Ref. 1; 0.09 cm thick crystals.

2. 0.04 cm thick crystals.

is also anomalous. The fact that the three modes "conserve" energy among themselves (i.e. $E_1 + E_2 - E_3 = 0$) and exhibit similar behavior with temperature is suggestive of a particularly strong cubic anharmonic interaction among the three modes. The temperature dependence of the previously unobserved mode is shown for the Γ -point in figure 1; partial dispersion curves are shown in figure 2.

1. N. J. Chesser and H. J. Prask, *Proc. of Conf. on Neutron Scattering*, Gatlinburg, TN, (1976).
2. G. J. Rosasco and H. J. Prask, *Sol. St. Comm.* 16, 135 (1975).
3. R. C. Casella and S. F. Trevino, *Phys. Rev.* 6B, 4533 (1972).
4. A peak has been observed in incoherent scattering spectra of polycrystalline AP at ~ 2 meV (H. J. Prask and J. J. Rush; H. G. Smith, M. Nielsen and H. A. Mook; unpublished work).

A SEARCH FOR THE CENTRAL MODE IN LITHIUM TANTALATE

S. F. Trevino
(Energetic Materials Division, AARADCOM, Dover, NJ)

and

J. M. Rowe

Lithium tantalate is a ferroelectric which undergoes a phase transition at $\sim 620^\circ\text{C}$. Penna, Chaves and Porto¹ have reported the

observation, by Raman scattering, of a very broad (~ 4 meV) central mode whose intensity increases as a function of temperature until it disappears at the phase transition. This central mode is only observed in the (zz) configuration thus corresponding to long range fluctuations along the z-axis. These observations are interpreted as the first experimental observation of a Debye-like relaxation in a ferroelectric.

In the present work, a single crystal of LiTaO_3 approximately cylindrical (10mm diameter, 25mm height) was aligned with the [110] zone axis vertical at the BT-6 triple axis spectrometer. The reciprocal lattice point (0,0,3) which has zero structure factor for Bragg scattering was used to search for the central mode as a function of \vec{q} and temperature. The incoherent elastic peak (at room temperature) from the Li was used to measure the resolution which was ~ 1.1 meV. The crystal was maintained at a temperature of 550°C and energy scans were made at Q's of (-.1,-.1,3), (-.3,-.3,3), (0,0,2.75) and (0,0,2.25). There was no sign of a broadened component in any of these scans. We are not certain as to the source of the central mode observed by the above authors but it is not due to a phenomenon associated with microscopic long range order. Perhaps very small Q inelastic measurements might reveal such a mode.

1. A. F. Penna, A. Chaves and S. P. S. Porto, *Sol. State Comm.* 19 491 (1971).

DEFORMATION OF UNIFORM POLYBUTADIENE
RUBBER NETWORK

C. Han
(Polymers Division)

and

B. Mozer

and

J. Hinkley and H. Yu
(University of Wisconsin, Madison, WI)

In this study, an attempt is made to compare the molecular deformation of a polymer chain in a rubber network with its macroscopic deformation in order to evaluate the affine postulation of the kinetic theory of rubber elasticity.

Uniform polybutadiene rubber networks have been prepared for this study. This is done by mixing anionically prepared polybutadiene (PB) with a certain fraction (1-3%) of molecular weight matched perdeuterated polybutadiene (dPB) and end cross-linked in bulk by tri-isocyanate. The radii of gyration of the same dPB molecule before and after cross-linking have been studied. A typical Zimm plot for the mixture (before cross-linking) is shown in figure 1. From this plot, a radius of gyration $\langle R_G^2 \rangle_0 = 44 \pm 10$ A has been obtained. This can be compared with the radius of gyration of dPB after cross-linking. Our preliminary data indicate the radius of gyration before and after cross-linking are approximately equal ($\langle R_G^2 \rangle_0 / \langle R_G^2 \rangle \sim 1$), which agrees with Floy's predication instead of Guth's predication ($\langle R_G^2 \rangle / \langle R_G^2 \rangle = 2$).

The 3% network was then subjected to a unidirectional deformation in the scattering plane and perpendicular to the incident beam. The 3% network with 0%, 22%, 43%, and 60% extension ratios has been studied. An inverse intensity plot for the 22% extension is shown in figure 2. Our initial data indicate the chain segment deformation is smaller than the affine prediction of a Gaussian chain.

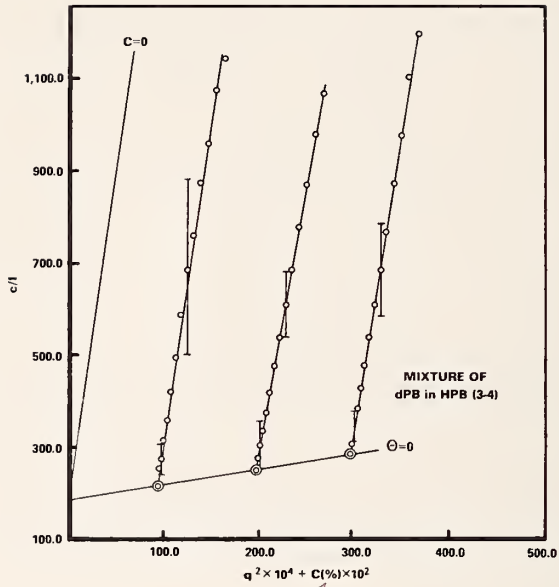


Figure 1. A Zimm plot for the mixture before cross linking.

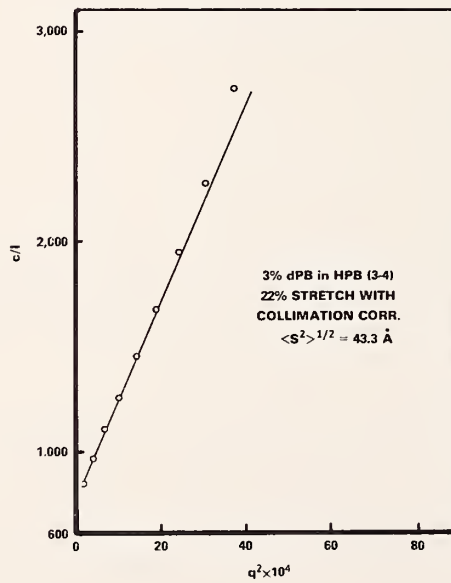


Figure 2. An inverse intensity plot for a 22% extension.

SMALL ANGLE MAGNETIC SCATTERING FROM
AMORPHOUS RARE-EARTH IRON ALLOYS

H. Alperin

(White Oak Laboratory, Naval Surface Weapons Center, White Oak, MD)

and

S. J. Pickart

(University of Rhode Island, Kingston, RI)

and

J. Rhyne

The anomalously large small-angle scattering reported previously, which appears at low temperatures in a sample of amorphous $\text{Tb}_{0.018}\text{Fe}_{0.982}$ has been analyzed further. This magnetic scattering below the curie temperature which is undoubtedly due to some sort of distribution of small magnetic "particles" (micro-domains), has an inverse power law dependence of the intensity on the scattering vector q with an exponent of 2.4 at 77K. After correction for vertical and horizontal resolution, the power law becomes q^{-3} which is the same as that observed previously for amorphous TbFe_2 and TbHo_2 . It is to be noted that this is not the correct dependence for a distribution of spheres (q^{-4}) nor the more general Porod Law dependence, (also q^{-4}) which would be valid for any shape of particle with random orientation as long as $qL \gg 2\pi$ (L = any particle dimension). This implies that some dimensions are as small as 40Å while others are much larger. The actual interpretation is therefore difficult and suggests that no distribution of simple particle shapes and sizes applies. An appealing possibility is an interconnected sponge-like arrangement with partially one-dimensional character.

MAGNETIC SCATTERING IN DILUTE Pd(Fe) ALLOYS

J. W. Lynn

(University of Maryland, College Park, MD)

and

J. J. Rhyne

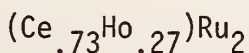
and

J. I. Budnick

(University of Connecticut, Storrs, CT)

Although pure palladium does not exhibit a magnetic phase transition, the high density of d-states at the Fermi level leads to a large magnetic susceptibility for the system. The introduction of magnetic impurities such as iron into a high susceptibility host matrix results in the formation of "giant-moment" clusters ($\sim 12\mu_B$ /Fe atom). In the range of concentration where individual clusters do not interact with each other the system is thought to form a spin-glass type of state at low temperatures, whereas for higher concentrations a transition to conventional ferromagnetism is observed. We have undertaken an investigation of the magnetic scattering in such a dilute ferromagnetic alloy: Pd(1.5% Fe). Preliminary measurements were taken on a polycrystalline sample $\sim 1/2$ ml in volume, with a measured Curie temperature of $T_c = 65\text{K}$. In the small wavevector ($Q < 0.3\text{\AA}^{-1}$) region the observed magnetic critical scattering was diffusive in appearance both above and below the phase transition, with the intensity peaking at $T \approx T_c$ in a conventional manner. The wavevector dependence of the scattering at fixed temperature obeyed an Ornstein-Zernike correlation function within experimental error. No evidence of spin wave excitations was observed at any temperature, although this aspect will be investigated in more detail. Quantitative measurements of the critical and spin wave scattering are now in progress on a new sample of larger volume.

CRYSTAL FIELD EFFECTS IN THE SUPERCONDUCTOR



J. W. Lynn

(University of Maryland, College Park, MD)

and

D. E. Moncton

(Bell Laboratory, Murray Hill, NJ)

and

W. Thomlinson and L. Passell

(Brookhaven National Laboratory, Upton, NY)

For most superconductors the introduction of magnetic impurities is very detrimental to the superconducting state since the magnetic impurities provide spin-flip scattering centers which can break the Cooper pairs. The most evident effect is a precipitous decrease of the superconducting transition temperature with increasing impurity concentration. It has thus been particularly intriguing that there are some superconducting materials, notably CeRu_2 , which readily accept large concentrations of heavy rare-earth metals substitutionally without adversely affecting the superconductivity. For example, $\sim 35\%$ of the Ce can be replaced by Ho before the superconducting state is suppressed, and small concentrations of Ho actually enhance T_S .¹ On the other hand, HoRu_2 is a ferromagnet with a Curie temperature T_C of 14 K, and the substitution of Ce for Ho gradually reduces T_C . The magnetic phase boundary as determined by susceptibility and Mössbauer measurements, however, appears to intersect the region of superconductivity at a finite temperature, raising the interesting possibility of these two cooperative phenomena coexisting.

The neutron scattering technique is ideally suited to study the magnetic properties of these superconductors since the magnetic state can be microscopically probed without being affected by the screening of the superconducting electrons. A particularly favorable system for study is $(\text{Ce}_{1-x}\text{Ho}_x)\text{Ru}_2$, both because of the large moment of the Ho and because the coexistence region has the highest concentration of rare-earth ions ($\sim 30\%$).

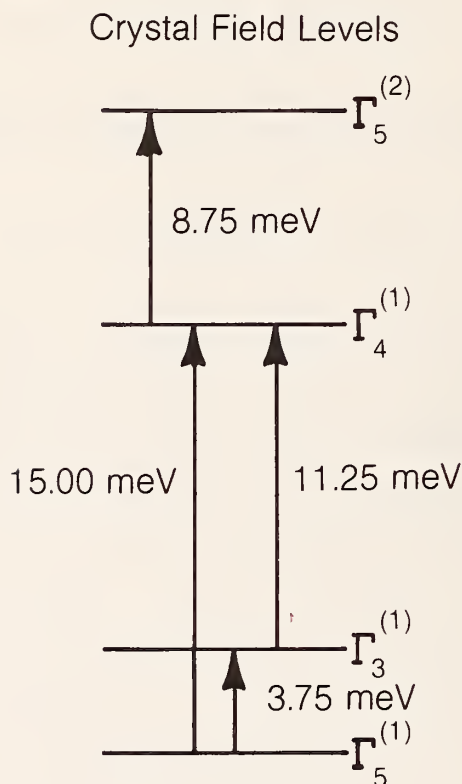


Figure 1: Crystal field levels for Ho^{3+} .

Our initial studies were on a sample with $x = 0.27$. The superconducting transition temperature was measured to be 1.6 K, and a Curie constant of 2.2 K was obtained from paramagnetic susceptibility measurements. Below ~ 4 K we observed² the appearance of small angle elastic or quasielastic scattering, indicating the development of ferromagnetic correlations. These correlations could be described to a first approximation by an Ornstein-Zernike correlation function, with the correlation range ξ ($=1/\kappa$) increasing steadily with decreasing temperature down to 0.5 K, but then saturating at a value of 80 Å. There was no evidence in the magnetic scattering of the onset of superconductivity, and there was no transition to long range ferromagnetic order.

One of the most important characterizations of this system is to determine the ground state of the 4f electrons of the Ho ion. The

degeneracy of the $J = 8$ Ho^{3+} free ion will be at least partially removed by the effects of the crystalline electric field, and we may expect this to be the dominant effect since the magnetic energy is small (~ 0.5 K). CeRu_2 and $(\text{Ce-Ho})\text{Ru}_2$ form the C15 structure for $x \leq 4$. In this structure the crystallographic point symmetry of the Ho (or Ce) site is cubic ($\bar{4}3m$), with 12 Ru ions as nearest neighbors and four next-nearest neighbors of Ce (or Ho). Locally the site symmetry of each Ho ion will be lower than cubic due to substitutional disorder on the Ce type of site, but since these are next-nearest neighbor (and more distant) sites we anticipate that the crystal-field splitting will reflect the cubic symmetry to a first approximation. We may then compare our observations with the predictions of Lea, Leask and Wolf³ (LLW) for Ho^{3+} in a cubic field.

Investigations of the inelastic neutron scattering at low temperatures revealed two transitions from the ground state at 3.75 meV and 15.0 meV. This is consistent with the LLW diagram if the LLW parameters $|X| \sim 1$, $W/X > 0$. We note that $|X| \sim 1$ implies that a triply-degenerate Γ_5 state is lowest, so the ground state is magnetic. With increasing temperature two additional transitions appear at 8.75 meV and 11.25 meV. This is only consistent with the LLW diagram if $X \sim 1$, and the appropriate crystal field levels and corresponding transitions are shown in figure 1.

Additional measurements were carried out on pure CeRu_2 to determine if any of the inelastic scattering could be due to the Ce. No crystal field transitions or magnetic inelastic scattering was detected up to an energy transfer of 35 meV.

Further measurements are in progress on a series of samples with differing Ho concentration to establish the concentration dependence of the magnetic correlation range and crystal field splittings, and the influence of the Ce site disorder on the Ho ground state.

1. M. Wilhelm and B. Hillenbrand, *Z. Nature* 26a, 141(1972).

2. J. W. Lynn, D. E. Moncton, W. Thomlinson and L. Passell, *Bull. Am. Phys. Soc.* 22, 339(1976). Measurements of the correlation range were carried out at Brookhaven National Laboratory.
3. K. R. Lea, M. J. M. Leask and W. P. Wolf, *J. Phys. Chem. Solids* 23, 1381(1962).

EXCITED STATE SPIN WAVES IN ErFe_2

J. J. Rhyne

and

N. C. Koon

(Naval Research Laboratory, Washington, DC)

The group of compounds RFe_2 , where R is a heavy rare earth, crystallize in the close packed Laves phase or MgCu_2 structure. These compounds have high Curie temperatures ($>550\text{K}$) and show extraordinarily large magneto-elastic interactions. The iron moments are ferromagnetically aligned, and are antiparallel to the R moment (ferrimagnetic order). The iron moment as determined from both bulk measurements¹ and neutron scattering² on polycrystalline samples shows an anomalous reduction from the expected $2\mu_B$ to approximately $1.6\mu_B$. The rare earth moments have their free ion values. We have studied in detail the magnetic excitations in the compound ErFe_2 .

ErFe_2 has 6 atoms per unit cell with the Er atoms arranged on sites of tetrahedral symmetry and the Fe atoms on octahedral sites. One thus expects six spin wave branches, one acoustic and five optic. As the results in figure 1 show, only three of these branches have energies easily studied by neutron scattering. The remaining three modes (two are degenerate) are expected to have energies of approximately 200-300 meV. The data in figure 1 for spin waves propagating in the $[q,q,0]$ and $[q,q,q]$ directions at room temperature show isotropic spectra consisting of (1) an acoustic mode with no measurable anisotropy energy gap, (2) a very flat optic mode of energy 5.1 meV degenerate with

the acoustic mode at the zone boundary and (3) a highly dispersive higher optic mode starting from an energy gap of 8.75 meV. This latter mode has quadratic dispersion ($\hbar\omega = D|q|^2$) in the q range shown with $D = 240 \text{ meV-A}^2$ only slightly smaller than pure iron metal³ ($D = 280 \text{ meV-A}^2$) and would represent the iron acoustic mode in the absence of rare earth spins and the R-Fe exchange interaction. This mode is shown

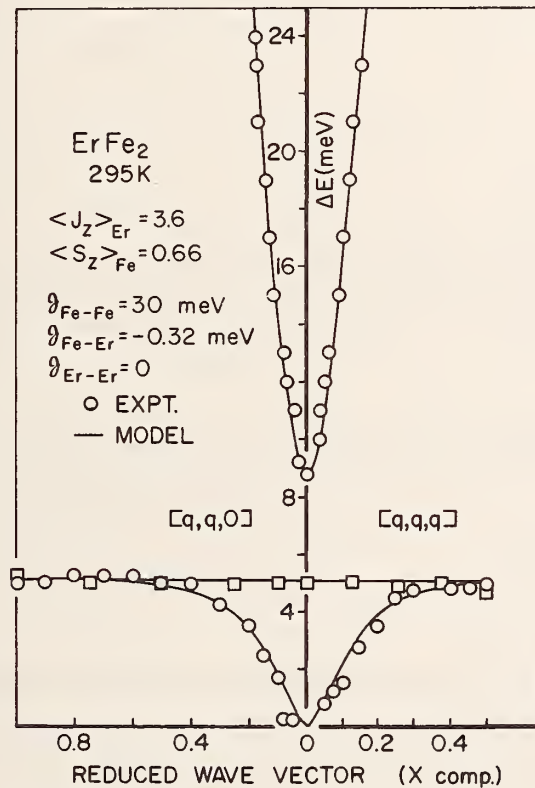


Figure 1. Magnon dispersion of ErFe_2 along $[q,q,0]$ and $[q,q,q]$ symmetry directions. The acoustic mode was measured about the (111) and (220) lattice reflections, the lower optic mode at (200), and the higher optic mode at (220) and (222) reflections. The solid line is the result of a nearest neighbor spin wave calculation described in the text.

over only a small portion of the Brillouin zone due to the very high energy transfers involved. The vanishing dispersion in the lower optic mode is a consequence of negligible Er-Er exchange in this compound; rather the Er simply sits in the molecular field from the iron spins.

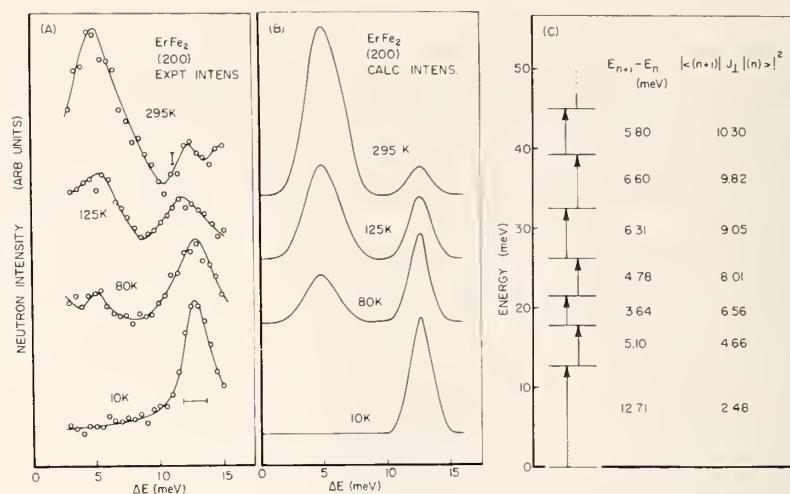


Figure 2. (a) Experimental lower optic mode neutron intensities for $q=0$.
 (b) Calculated neutron intensities.
 (c) Single ion energy levels and transition matrix elements.
 Parameters used in the calculation are $B_2^0 = 3.3 \times 10^{-2} \text{ meV}$,
 $B_4^0 = 1.5 \times 10^{-4} \text{ meV}$, $B_6^0 = -9.0 \times 10^{-7} \text{ meV}$, $g\mu_B H_{\text{exch}} = 5.1 \text{ meV}$.

At low temperatures the basic spectra remain essentially unchanged, except for a giant $q = 0$ gap of 8.3 meV for the spectra taken at 10K. It was expected that the 8.3 meV gap would simply decrease continuously as the temperature was raised. The data, however, show that the energies renormalize very little with temperature. Instead, the modes change in intensity, coexisting at all measured temperatures except 10K and below, where the two lowest energy modes vanish. Typical data on the zone center lower optic mode are shown in figure 2a as a function of temperature. At 10K the only transition observed has an energy of 12.7 meV and a width roughly equal to the experimental resolution. As the temperature is raised, however, another peak appears which has an energy of about 5 meV and which has a width considerably greater than the instrumental resolution. At room temperature the peak at 12.7 meV is much weaker than the one at 5 meV. Data for the acoustic mode are qualitatively similar except that the broadening appears to be somewhat greater. The intensity data shown in figure 2a are typical of those due to crystal field population effects, although in the present

case the overall level splitting due to exchange is much greater than that due to the crystal field. Since the q independent lower optic mode corresponds to localized excitations of the rare earth spins only, our initial attempt at explaining these results was to try to calculate the scattering intensity for that mode using the independent spin model assuming that the rare earth spins experience a crystal field plus an exchange field from the iron. The form of the Hamiltonian for cubic symmetry and a [111] easy axis is

$$H = g\mu_B \vec{H} \cdot \vec{J} + B_2^0 O_2^0 - \frac{2}{3} B_4^0 [O_4^0 - 20\sqrt{2} O_4^3] + \frac{16}{9} B_6^0 [O_6^0 + \frac{35\sqrt{2}}{4} O_6^3 + \frac{77}{8} O_6^6] \quad (1)$$

where O_ℓ^m are the Stevens operator equivalents.⁽⁴⁾ The term involving O_2^0 is included because of the spontaneous rhombohedral distortion due to magnetostriction. For independent spins in the dipole approximation the cross-section for the crystal field transition corresponding to the zone center optic mode scattering intensity including instrumental resolution is given approximately by

$$I(\omega, T) \propto \sum_n \rho_n |\langle n+1 | J | n \rangle|^2 \exp[-(\omega - E_{n+1} + E_n)^2 / \sigma^2] \quad (2)$$

where $|n\rangle$ are eigenstates of the Hamiltonian (1) and J is the component of the total angular momentum operator perpendicular to the scattering vector. ρ_n is the Boltzman population factor, and σ is the energy resolution width. Since the eigenstates are almost pure J^Z states, the only transitions with significant matrix elements are those between $|n\rangle$ and $|n+1\rangle$.

Values of the crystal field and exchange parameters were determined using a combination of magnetization and neutron data and led to the crystal field scheme shown in figure 2c. Using equation (2) the scattering intensity was calculated and is shown in figure 2b. The calculated curves are remarkably similar to the experimental data of figure 2a. Examination of the crystal field levels, gives an

immediate qualitative explanation of the observed data. The separation between the ground and first excited state is 12.7 meV, much greater than either the exchange splitting or the splitting between excited states, which fluctuates about an average value of approximately 5 meV. The observed low temperature optic mode is sharp because it involves only one transition. The high temperature lower optic mode, on the other hand, is significantly broadened because it consists of a number of excited state transitions with different energies. It is interesting to note that the transition matrix element from the ground state to the first excited state is several times smaller than those between the excited states which produces the observed intensity distribution.

-
1. A. E. Clark, *A.I.P. Conf. Proc. Series* 18, 1015 (1974).
 2. J. J. Rhyne, to be published; M. O. Bargouth and G. Will, *Journal de Physique* C1, 32, 675 (1971).
 3. H. A. Mook and R. M. Nicklow, *Phys. Rev.* B7, 336 (1973).
- K. W. H. Stevens, *Proc. Phys. Soc. London*, Sect. A, 65, 209 (1952).

MAGNETISM IN $\text{ErFe}_2\text{-H}$

J. J. Rhyne

and

S. G. Sankar and W. E. Wallace

(Chemistry Dept., University of Pittsburg, Pittsburgh, PA)

The close-packed Laves phase crystal structure compounds R Fe_2 (where R is a rare earth) have been shown to absorb hydrogen readily⁽¹⁾ forming stable hydrides. One such phase has composition near $\text{R Fe}_2\text{H}_4$. We have begun an investigation of the compound $\text{ErFe}_2\text{H}_{3.5}$ using elastic scattering techniques to examine the sublattice magnetization and its temperature dependence. At low temperature the magnetization does not

saturate even in fields as large as 120 kOe. This precludes an accurate determination of the sublattice magnetization from bulk magnetic measurements.

The Curie temperature of $\text{ErFe}_2\text{H}_{3.5}$ determined from neutron experiments is 450K which is significantly depressed from the 574K found for pure ErFe_2 . The sublattice magnetization also indicates several anomalies. At 10K, the Er moment was found to be only 5.5 Bohr magnetons (μ_B) which is significantly lower than the free ion value of $9 \mu_B$ found in pure ErFe_2 . The Er moment decreases rapidly as the temperature is raised and is essentially zero at 300K, well below the overall Curie temperature of 450K.

The iron moment on the other hand is $1.6 \mu_B$ at low temperatures in agreement with that found in pure ErFe_2 and remains essentially constant up to 350K before dropping rapidly to zero at the bulk Curie temperature. These results suggest a significant reduction in the Er-Er and Er-Fe exchange interactions on hydriding leading to a structure in which the rare earth is very loosely coupled. The marked reduction in low temperature Er moment also suggests a predominance of crystal field terms in the magnetic energy.

-
1. D. M. Gualtieri, K.S.V.L. Narasimhar, and W. E. Wallace. *AIP Conf. Proc. Series* 34, 219(1977).

APPLICATION OF NEUTRON DIFFRACTION TO NON-DESTRUCTIVE TESTING PROBLEMS

H. J. Prask and C. S. Choi
(Energetic Materials Division, LCWSL, ARRADCOM, Dover, NJ)

and

H. A. Alperin
— (Naval Surface Weapons Center, White Oak, MD)

and

E. Prince

The Army group at the NBSR has been engaged in a continuing program to use neutron diffraction to determine texture (i.e. grain orientation) in the copper liner component in shaped-charge munitions. The need for this information arose because of difficulties in procurement and quality control for these items. Our most recent work in this area has been directed toward the determination of texture as a function of depth. In principle, the penetrating power of neutrons and the ability to adjust incident wavelength continuously permits texture determination directly as a function of depth in extended samples. However, in the liner application, the thickness is only 0.28 cm so that a "difference" method has been developed and tested, which consists of the following. One makes use of the fact that for a given set of planes, and appropriate masking, different depths are sampled for different wavelengths, as illus-

SAMPLING DEPTH VS NEUTRON WAVELENGTH

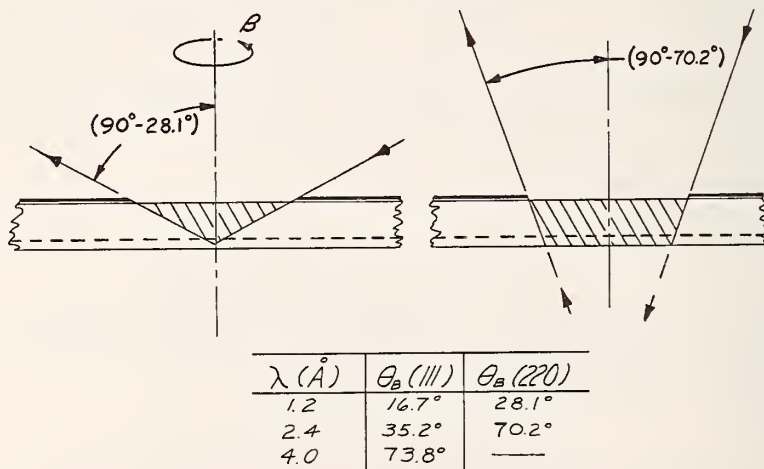


Figure 1A. Schematic illustrating "difference" technique for texture vs. depth measurement in shaped-charge liners. The cross-hatched area in each figure (defined by masking with Cd or Gd) corresponds to the volume examined for the (220) reflection for wavelengths of 1.2 and 2.4 Å, respectively. The angle α is between the normal to the surface and a vector perpendicular to the scattering plane. An appropriately weighted difference of the two measurements should give a rough profile of the pole figure for the lower part of the liner.

trated in figure 1A (alternatively, the same effect is achieved by examining different order reflections for the same plane).

This concept has been tested by examining grain orientation in two Cu plates each 0.08 cm thick. Texture was determined in each plate separately, and then together using (111) and then (222) reflections. The results are shown in figure 1B, for $45^\circ \leq \alpha \leq 90^\circ$; $0 \leq \beta \leq 360^\circ$. The agreement between the pole figures for the bottom plate determined alone and determined from the difference is reasonable. We attribute the discrepancies to the fact that optimum conditions (i.e. wavelength and planes) were not utilized and beam divergence was not taken into account.

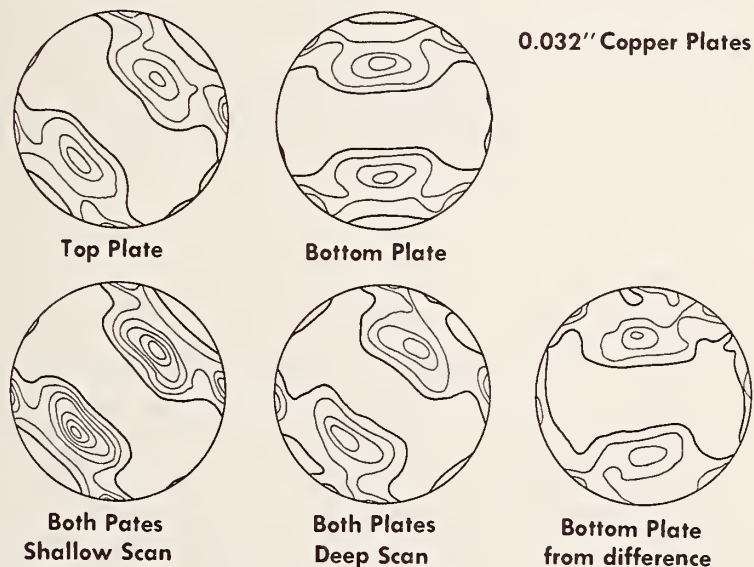


Figure 1B. Pole figures ($45^\circ \leq \alpha \leq 90^\circ$) for two copper plates (each 0.08 cm thick) taken together and separately. In this case the "shallow" scan corresponds to a (111) pole figure, the "deep" scan to a (222) pole figure. The heavier contour in each figure corresponds to "random" grain orientation; the lighter contours correspond to steps of 50% of random. $\alpha = 90^\circ$ is at the center of each figure.

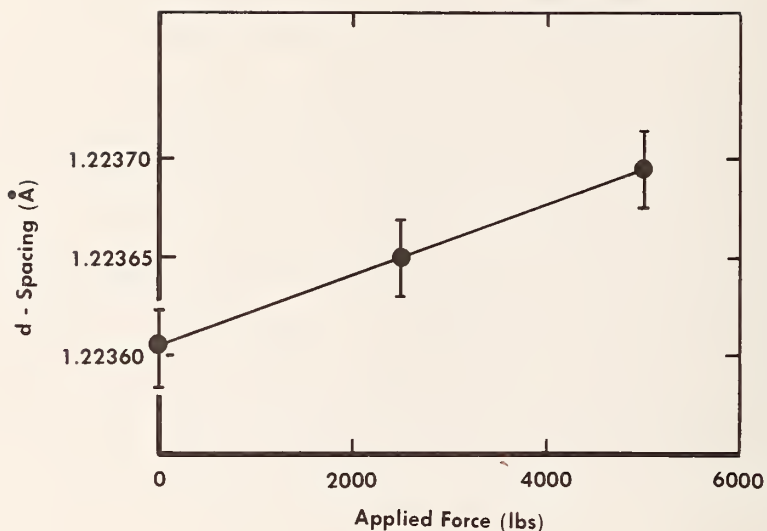


Figure 2. Change in d-spacing vs. loading for a 6061-T6 aluminum cylinder (2.54 cm diameter) as measured by neutron diffraction using the (113) reflection of aluminum. The scattering geometry was such that the measured change in d-spacing reflects the radial strain (tensile) in an axially compressed cylinder.

In the area of residual stress measurement with neutrons, results are very preliminary. The principal problem lies in the lower intensity - relative to x-ray sources - of even a high-flux research reactor. This necessitates relatively coarse collimation to achieve reasonable counting times. Our initial studies in this area have concentrated on careful lineshape analysis of Bragg peaks from samples of simple geometry to which an external load is applied. In figure 2 is shown results for a 2.54 cm diameter Al 6001-T6 cylinder loaded axially, with strains measured radially. The results suggest that the neutron technique may be sufficiently sensitive to strain as induced by residual stress to have practical utility.

ACTIVATION ANALYSIS: SUMMARY OF 1977 ACTIVITIES

Harry L. Rook and Thomas E. Gills
(Analytical Chemistry Division)

In the Act of Congress which provides the basic authority of the National Bureau of Standards (NBS), an essential function of the National Bureau of Standards is the "preparation and distribution of standard samples and their use in chemical analysis ..." and the "development of methods of chemical analysis ...". These two functions are basic to the Neutron Activation Analysis (NAA) program, at NBS. As a part of the Analytical Chemistry Division, Institute for Materials Research, the NAA Section has performed numerous measurements that require the systematic and random errors to be known sufficiently well enough to state the concentration of an analyte within required uncertainty levels. The majority of these measurements are in support of the Standard Reference Materials programs which include the certifications of inorganic and organic compounds for the chemical composition (major, minor, and/or trace elements). Congruent to the support of SRM certification, the NAA Section continually develops or modifies new procedures to insure that the necessary accuracy is obtained during the certification of SRM's.

In addition to rendering support to the NBS Analytical Chemistry Division's program, the NAA Section has made significant contribution to other agency programs wherein an improved methodology must be developed or demonstrated. Such interaction mechanism allows the NAA Section and NBS as well to transfer analytical expertise where needed.

This report summarizes the activities of the Activation Analysis Section during the period of July 1976-June 1977. Included are contributions in the areas of basic research, applied research, radiochemical separations, certifications, and non-NBS research programs.

1. Basic Research in Activation Analysis

a. Fast-Neutron Flux Determination and Optimized Measurement of Aluminum in High-Purity Silicon

R. M. Lindstrom and R. F. Fleming

Measurement of small quantities of aluminum in silicon of semiconductor or solar grade is complicated by production of Al-28 by an (n,p) reaction on the matrix, in competition with the (n, γ) reaction on the trace Al sought. In selecting the optimum irradiation facility, the conflicting requirements of high thermal flux for greatest signal and of low fast flux for smallest noise must be balanced. The present work outlines a simple experimental procedure for assessing and correcting for interferences. No a priori knowledge of fast fluxes or cross sections is required; these are often poorly known. The procedure is generally applicable to other cases of competing reactions.

For a given facility, relatively pure Si and Al monitors are irradiated both bare and cadmium covered. The ratio of observed activity bare to that in cadmium is determined for each of the two standards, from which an apparent Al concentration X_0 in absolutely pure Si may be calculated for that facility. Subsequently, an unknown Si sample is irradiated bare with an Al monitor and an apparent Al concentration in the sample (S_1) derived. The true concentration of Al is then $X = X_1 - X_0$. Except for sample weights and the well-determined half-life of Al-28, all parameters in the calculation are experimental numbers, usually ratios. Once X_0 has been determined, it need not be done again as long as the neutron spectrum in that facility is unchanged.

Once the facilities available have been characterized, the optimum one may be chosen. The "best" measurement is the one for which the relative error in the concentration X is a minimum. We assume that the uncertainty in X_0 can be made negligible, by replicate measurement if necessary. Therefore, if we ignore the half-life uncertainty and assume that counting statistical error is dominated by the sample and not the monitor, we can estimate the relative uncertainty in the measurement as

$$\frac{\sigma(X)}{X} = \frac{\sigma(X_1)}{X_1 - X_0} = \frac{\sigma(X_1)/X_1}{1 - X_0/X_1} = \frac{1/\sqrt{C_1}}{1 - X_0/Z_1}$$

where C_1 is the observed number of counts from the silicon sample. For samples with an aluminum concentration $X \gg X_0$ the relative uncertainty becomes $1/\sqrt{C_1}$ which is proportional to $1/\sqrt{\phi_{th}}$ for the given irradiation facility. For samples whose concentrations $X < X_0$, the uncertainty quickly becomes very large. For a given facility, the value of X_0 is proportional to the neutron flux above 4 MeV.

The present method has been used to characterize the pneumatic tube facilities in the RT4 facility ($\phi_{th} = 1.2 \times 10^{13}$, $R_{Cu} = 560$), $X_0 = 48 \pm 4$ $\mu\text{g/g Si}$, in excellent agreement with paired irradiations in RT4 and the thermal column ($R_{Cu} = 3400$), and also in agreement with calculation from the measured fission flux and the tabulated fission-averaged cross section.

The fission flux has been measured in four rabbit tubes, by irradiating bare titanium and silicon (quartz), counting on a calibrated Ge(Li) detector, and deriving fluxes from tabulated fission-averaged cross sections (Handbook on Nuclear Activation Cross Sections, Technical Reports series 156, IAEA, Vienna 1974). The results are as follows:

Fission Fluxes in Pneumatic Tubes					
Radionuclide	RT1	RT2	RT3	RT4	RT5
^{28}Al	2E12	-	1E12	7E10	4E8
^{29}Al	1E12	-	7E11	3E10	-
^{46}Sc	2E12	1E13	8E11	2E10	-
^{47}Sc	2E12	1E13	4E11	1E10	-
^{48}Sc	2E12	2E13	3E11	3E10	-

- b. The Quantitative Determination of Volatile Trace Elements in NBS Biological Standard Reference Material 1569, Brewers Yeast
H. L. Rook and W. Wolf.

The accurate analysis of chromium in biological samples has historically been difficult. Analytical methods such as atomic absorption spectroscopy and neutron activation have the required sensitivity to determine nanogram levels of chromium, but reported analytical data on biological materials, such as NBS Standard Reference Materials (SRM) 1577, Bovine Liver, has been widely discrepant (1). More recent data has indicated that the current status of chromium analysis has not greatly improved (2). It has been suggested that part of the analytical error may be due to the presence of a volatile organic species which may be lost upon certain preparation procedures in samples of biological origin (3,4).

Analytical verification of volatile trace elemental species in biological systems has been, in general, limited. Elements such as mercury and lead have been shown to form elemental or simple molecular species which vaporize upon mild thermal treatment. The awareness and confirmation of possible vaporization losses of other metals, which are not normally considered volatile, is becoming of increasing importance. Two recent studies have reported no chromium losses during ashing and acid digestion of biological samples to which radiotracers of Chromium-51 were added (1,2). A more recent study has reported as much as 30 percent volatilization loss of chromium from neutron activated brewers yeast samples during dissolution with concentrated acids (5).

Detectable amounts of six trace elements were observed in trapped fractions distilled from the brewers yeast. The amount of each element trapped was dependent upon the maximum temperature to which the sample was heated. The quantity of those trace elements observed was normalized to the weight of yeast used in individual experiments and is given in table I. The amount of each element in the trapped fraction increased with increasing temperature in all cases except silver. However, the quantity of the element volatilized and the dependence on temperature varied among the individual elements.

Table I. Trace Elemental Loss from Brewers Yeast by Vacuum Distillation
 --- μg Trapped/Gram Sample (Temperature $^{\circ}\text{C}$) ---

Element	150	190	205	250	295	305
Mercury	0.0014	0.006	---	0.017	0.10	0.055
Selenium	0.0013	0.0027	0.0018	0.036	0.16	0.23
Chromium	0.0028	0.0021	0.0021	0.0050	0.0038	0.0052
Arsenic	0.064	0.060	0.050	0.10	0.22	0.32
Silver	0.0045	0.0005	0.0028	0.0027	0.0010	0.0042
Gold	0.00010	---	0.00006	0.00040	---	---

The data in table II reflect elemental concentrations in the yeast residue relative to those in the initial unheated yeast sample. These data are corrected for total weight loss of material from the sample due to the vacuum distillation.

Table II. Relative Elemental Composition of Yeast Residue

-- Concentrations Relative to Unheated Yeast --

Temperature $^{\circ}\text{C}$

Element	0	0	200	265	290	305
Scandium	0.996	1.01	0.992	1.00	1.00	1.02
Iron	1.00	0.983	1.00	1.00	1.01	0.983
Cobalt	1.00	1.00	0.905	1.01	0.910	0.933
Chromium	1.01	0.990	1.06	0.920	1.02	1.06
Mercury	0.990	1.01	---	1.01	1.06	0.74
Selenium	1.04	0.960	1.12	0.64	0.44	0.57
Percent Weight Loss	0	0	7%	22%	39%	32%

The elemental data are given relative to initial yeast concentration because the absolute trace element content of the SRM Yeast has been determined only for chromium. Approximately 50 percent of the total selenium, about 25 percent of the total mercury, and less than one percent of the total chromium content was lost at the 300 $^{\circ}\text{C}$ temperature. This was with a total weight loss from the material of between 30

and 40 percent at that temperature. For chromium, these data are consistent with the observed volatility data. Although there was a volatile chromium component observed, the quantity, approximately .003-.005 $\mu\text{g/g}$, was within measurement error of the total certified chromium content in the yeast. For the elements scandium, iron, and cobalt, which were not detected in the trapped fraction, correspondently no difference was observed in the residue compared to the initial sample.

The analytical portion of the experiment was conducted by non-destructive neutron activation. For analysis, four of the sealed quartz tubes containing the condensed volatile material were irradiated together with one quartz tube containing 300 μl of a mixed trace element water standard. Samples were placed in one irradiation container so that one sample from each different temperature level, from 150-300 $^{\circ}\text{C}$, were irradiated together. The samples and standards were irradiated for four hours at a thermal neutron flux of $\sim 6 \times 10^{13} \text{ n} \cdot \text{cm}^{-2} \text{ sec}^{-1}$. After irradiation, the samples were allowed to decay for two days to eliminate short half-lived radioactivity, and counted on a large volume Ge(Li) detector coupled to a 4096 channel nuclear analyzer. The samples were then allowed to decay for two weeks and were recounted to determine those elements with half lives greater than a few days. The resultant gamma-ray spectra were output onto magnetic tape and processed off line by computer code QLN-1. The individual photopeaks were quantified by the total peak area method. Quantitative results were obtained by direct comparison of the specific activity of the samples and standards.

In an effort to resolve the question of chromium volatility, a vacuum distillation experiment has been designed and conducted on a new NBS Standard Reference Material, SRM 1569, Brewers Yeast, which is certified for total chromium content. The experimental design allowed for the collection of all volatile species in the range of 150 to 325 $^{\circ}\text{C}$, and for the quantitative determination of those elemental species amenable to neutron activation. In addition to chromium, volatile

losses were found and quantified for the elements Hg, Se, and As. Other elements such as Br and I were observed to volatilize but were not quantified due to experimental conditions of the neutron activation.

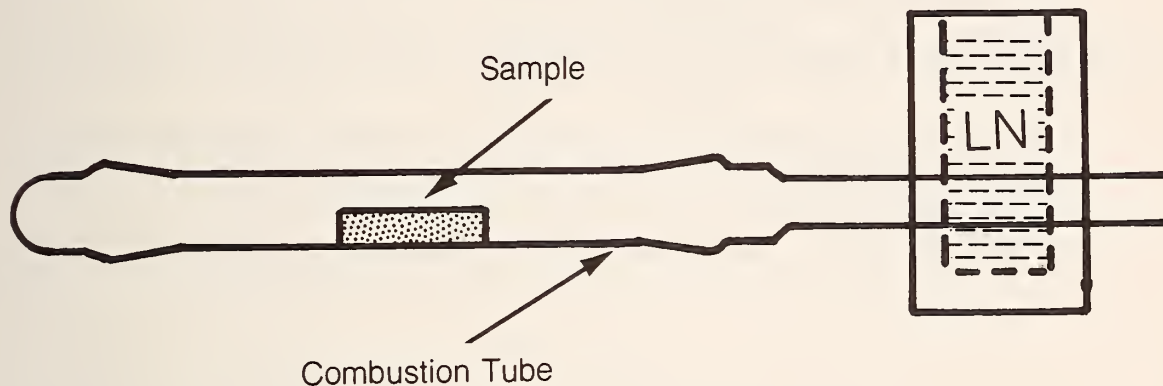


Figure 1. Vacuum Distillation and Collection System

The basic experimental system is pictured in figure 1. The system consists of a tube furnace used to heat a 19 mm i.d. quartz combustion tube containing the sample and a thermometer for temperature measurement. One end of the quartz tube was enclosed with a standard taper ground glass removable stopper. The other end was fitted with a second standard taper joint, the inner portion of which was tapered to an 8 mm i.d. quartz tube. A 10- to 12-inch piece of similar quartz tubing was fused to the 8 mm tube. This extension, which was used for collection of the distillate, was passed straight through a liquid nitrogen trap. The trap was constructed out of styrofoam with holes bored through the sides to seal to the collection tube. The collection tube was connected to a vacuum pump with rubber vacuum tubing. A second liquid nitrogen trap was placed between the pump and the collection tube to prevent back streaming of pump oil vapors and other contaminants.

1. McClendon, L. T., "Proceedings VIII Trace Substances Conferences," University of Missouri, Columbia, Missouri (1974).
2. Parr, R., International Conference on "Modern Trends in Activation Analysis," (to be published).
3. Wolf, W., W. Mertz, and R. Masironi, *J. Agr. Food Chem.*, 22, 1037 (1974).
4. Wolf, W., "Proceedings of 7th Materials Research Symposium," NBS Special Publication 422, 605-610. U.S. Government Printing Office (1976).
5. McClendon, L. T., *Radio Anal. Chem.*, 8, (to be published).

c. Study of the Chemical Dissolution of Different NBS Environmental Matrices. Recovery of Cd, As, Sb, Se, and Cr.

M. Gallorini, T. E. Gills, R. R. Greenberg

One of the most important problems in the field of trace elemental analysis using the nuclear activation technique coupled to radiochemical separation, is to dissolve the sample easily, completely, and without losses of volatile elements.

The purpose of this research is to find the most suitable conditions under which the complete dissolution of all environmental matrices can be obtained without losses of volatile elements such as arsenic, cadmium, antimony selenium, and chromium.

Because of different chemical composition of matrices several methods and techniques of dissolution will be tested so as to correlate the volatile elements losses with the chemical nature of the matrix.

For this study, a list of the environmental correlated matrices in different groups with similar chemical composition is grouped. The following general scheme shows a possible subdivision:

Biological Botanic [B. B. matrices]	:	Orchard Leaves, Spinach, Pine Needles, Wheat Flour, Rice Flour, Tomato Leaves, Brewers Yeast.
--	---	---

Biological Physiological: Serum, Blood, Urine.
 [B. P. matrices]

Biological Tissue : Tuna Fish, Bovine Liver, Human Tissue,
 [B. T. matrices] Oysters.

Environmental Related : Inorganic: Fly Ash
 Samples : Mixed: River Sediment, Air Particulate,
 Coals.

Typically, different matrices may require different dissolution methods, i.e. different acid mixtures, Teflon bomb, and fusion with appropriate flux.

Determination of Trace Element:

In order to determine As, Sb, Se, Cd, and Cr losses, a selective radiochemical separation is necessary to measure the losses of these elements after chemical dissolution. After dissolution of the sample, the next schematic procedure will be followed:

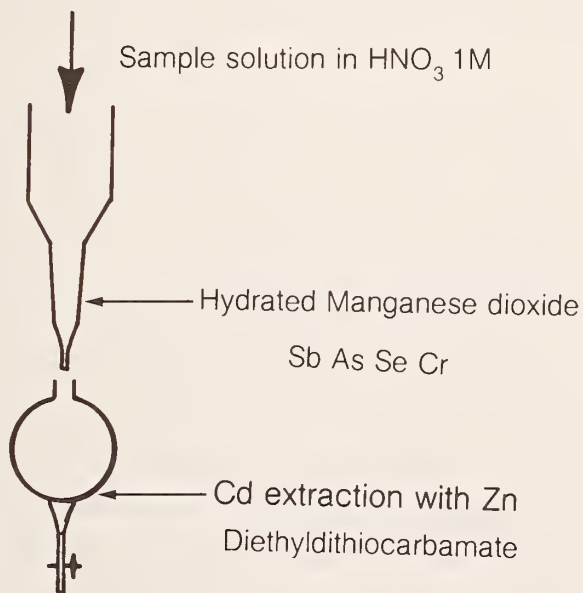


Figure 2. Radiochemical Separation Scheme

Proposed Study of different dissolution methods:

Biological Matrices Environmental Related Coals	}	1) HNO_3 HClO_4 HF (3:1:03)
		2) H_2SO_4 HNO_3 H_2O_2 HF (5:3:3:0.3)
		3) Teflon Bomb using H_2SO_4 , HNO_3 , HCl, HF
Environmental Related Fly Ash River Sediments Air Particulate	}	1) HNO_3 HClO_4 HF
		2) Teflon Bomb Na_2O_2 NaOH
		3) Fusion with Pyrosulfate (Bisulfate) Other

During the dissolution, parameters such as temperature, ratio and amount of acids, length of attack, fusion in a fused silica tube under different gases will be tested and measured. Using radioactive tracers and standards, recovery yield will be determined. This work should be valuable to many procedures currently used in the SRM Certification Program.

d. Determination of Os, Ru, and Hg in Inorganic Matrices and Environmental Samples by Destructive Neutron Activation Analysis.

M. Gallorini and T. E. Gills

Because of the very low concentrations in nature, elements such as osmium and ruthenium have been studied only by geologists and metallurgists. Consequently, the analytical methodology of those two elements must be developed to determine accurately their concentration in matrices such as rocks, particular alloys, and as impurities in noble metals (1,2,3). Recently, the noble metals have been found in many environmental related materials (such as air particulate and ashes) and their determination have become very interesting in relation to many environmental problems. For this research, a method for analysis, at trace levels, of mercury, osmium, and ruthenium using thermal neutron activation analysis followed by radiochemical separation has been developed.

Different kinds of matrices of geological interest, e.g. (rocks PCC-1, G-2, DTS-1 from U. S. Geological Survey) and inorganic-environmental materials (Air Particulate, Fly Ash, from the National Bureau of Standards) were analyzed. Because of the low contents of Hg, Os, Ru, and the matrix radioactivity from neutron irradiated materials, a radiochemical separation was necessary. Thus, the dissolution of the very difficult matrices was required. During sample dissolution procedure, the most delicate step is to prevent the losses by volatilization of mercury as metal and osmium and ruthenium as tetroxides (4). A fusion with sodium peroxide and sodium hydroxide in a quartz tube under particular conditions was developed so as to obtain, simultaneously, a quantitative separation of mercury and an easy dissolution of the matrices followed by distillation of osmium and ruthenium tetroxides. The general procedure followed can be subdivided into two subsequent stages:

- a. A fusion attack and quantitative separation of mercury. The samples with carriers and the fusion mixture were carefully mixed in a quartz boat which was placed in a Vycor tube joined to a liquid nitrogen cold trap. During the fusion, the mercury is quantitatively distilled and condensed while the matrix is completely dissolved.
- b. Distillation of OsO_4 and RuO_4 : The boat and the melt content were then placed in a distillation flask and ruthenium and osmium tetroxides were distilled from sulfuric acid by the addition of a sodium bromate solution.

In order to ascertain the quantitative separation of mercury and the complete retention of osmium and ruthenium during the fusion step, a study using radioactive tracers of Os-191, Ru-103, and Hg-197 was carried out. The temperature, length of fusion, different kinds of transporting gas, amount of reagents were tested. The results are shown in table 1. For the distillation procedure, a similar test using radioactive tracers was carried out, obtaining a complete recovery of two tetroxides.

Table 1. Results of a Series of Fusions in Different Conditions.

Os Retent %	Ru Retent %	Hg Recovered %	Oven Temp* °C	Length* Min.	Trasp. Gas*	Sample g	Na ₂ O ₂ g	NaOH g
97.82	99.8	100	900	5	Air	River Sed. 0.367	2	-
97.97	100	100	850	5	Air	River Sed. 0.273	1.5	-
99.91	100	100	850	5	N ₂	River Sed. 0.300	1	0.150
99.92	100	100	800	5	N ₂	PCC-1 0.380	1.2	0.200
99.90	100	100	800	8	N ₂	PCC-1 0.305	1.2	0.200

*Parameters measured during the oven heating phase.

Conclusions.

In conclusion, this fusion-distillation method is rapid, simple, and quantitative. It permits the determination of mercury and the simultaneous control of eventual losses of osmium and ruthenium as tetroxides. Analysis of materials such as rocks, dust, and fly ashes can be completed in 2-3 hours. Furthermore, accuracy can be achieved even at the nanogram level.

1. Nadkarui, R. A., and G. H. Morrison, *Anal. Chem.*, 46, 2, (1974).
2. Chung, K. S., and F. E. Beamish, *Anal. Chem.*, 43, 357-368 (1968).
3. Gijbles, R., and H. Hoste, *Anal. Chem.*, 41, 419-429 (1968).
4. Apt, R. E., and E. S. Gladney, *Anal. Chem.*, 47 (1975).

e. Lithium Analysis by Use of Tritons

B. S. Carpenter and L. J. Pilione

A method of lithium analysis is accomplished by allowing alpha particles from the thermal neutron induced ${}^6\text{Li}(n,\alpha){}^3\text{H}$ reaction to damage a nuclear track detector which is then chemically etched to enlarge the damaged region to a size easily discernable in an optical microscope. The measurement of the etched track density yields information on the amount and distribution of lithium in the host matrix. Unfortunately, elements such as boron and oxygen also undergo (n,α) reactions which can lead to serious background problems if they occur in significant amounts relative to lithium.

Below is a listing the characteristics of the above mentioned reactions:

<u>Element</u>	<u>Isotopic Abundance</u>	<u>Reaction</u>	<u>Thermal Neutron Cross Section(barns)</u>	<u>Alpha Particle Energy (MeV)</u>
${}^6\text{Li}$	7.5%	${}^6\text{Li}(n,\alpha){}^3\text{H}$	942	2.05
${}^{10}\text{B}$	19.8%	${}^{10}\text{B}(n,\alpha){}^7\text{Li}$	3838	1.41(96%); 1.78(4%)
${}^{17}\text{O}$	0.04%	${}^{17}\text{O}(n,\alpha){}^{14}\text{C}$	0.24	1.41

The damage produced by the B-10 and O-17 alpha particles is not sufficiently different from that of the lithium alphas to be easily recognized with the nuclear track technique. Therefore, unless one can identify the different alphas a serious error can be made in the determination of lithium.

A technique recently developed at the NBS facilities utilizes the ${}^3\text{H}$ (triton) particle from the ${}^6\text{Li}(n,\alpha){}^3\text{H}$ reaction. The lithium-triton is a penetrating particle as compared to the alpha particle and is unique since thermal neutrons do not produce exothermic nuclear reactions for light elements where a by-product is triton. The lithium reaction is an exception since the second product particle is an extremely well bound alpha particle.

This new technique used an absorber between the host matrix and the plastic detector thus stopping all the alpha particles from reaching the

plastic detector but allows some of the tritons to pass through with degraded energies.

The initial studies had to resolve the following related problems:

- (a) to find a plastic detector sensitive to triton damage,
- (b) to find an absorber free of oxygen and boron and be of sufficient thickness to stop the alpha particles and allow penetration by some of the tritons.

Two track recorders (cellulose nitrate and cellulose acetate) were chosen for this study because of their reported ability to register triton particles. However, it was found that the triton energy needed to damage the plastics was ≤ 0.6 Mev. This critical energy was determined by slowing down lithium tritons with various thicknesses of absorber and measuring the triton energy with a solid state detector. The plastic detectors were then exposed to the different energy tritons and subsequently etched. It was found that tritons with energies >0.6 Mev did not cause sufficient damage in the plastics.

This energy constraint placed a range on the absorber thicknesses from 35-45 μm . Two readily available plastics were used as absorbers: a polycarbonate and a linear polyethylene. The polycarbonate was not free of oxygen but was available in a wide range of thicknesses. The linear polyethylene was free of oxygen (<100 ppm) but is currently available in one thickness (25 μm). Even though the polycarbonate has an oxygen content the range of the ^{17}O alpha particles is <25 μm . Thus the configuration of the system is as follows:

Host matrix	10 to 20 μm	-25 μm	-plastic detector:
(Li)	polycarbonate	linear polyethylene	(cellulose nitrate or cellulose acetate)

This combination has been used to successfully form triton images of an aluminum backed ^6LiF target ($.0.1 \mu\text{g}/\text{cm}^2$); a 21% ^6Li glass and a NBS glass standard (SRM-961).

f. Non-Destructive Determination of Trace-Element Concentrations by Neutron-Capture γ -Ray Spectrometry

D. Anderson, M. Failey, W. H. Zoller, G. E. Gordon and W. B. Walters (Dept. of Chemistry, University of Maryland, College Park, MD 20742)

R. M. Lindstrom

Instrumental neutron activation analysis (INAA), in which one irradiates samples with neutrons and observes γ -rays from the radioactive products formed, is a very powerful technique that is capable of measuring concentrations of typically 30 to 40 elements in complex environmental or geological samples. However, there are some important elements that are difficult or impossible to measure even with INAA. There are several reasons why some elements don't lend themselves easily, if at all, to INAA: neutron-capture cross sections may be too small, the products may have extremely short half lives or such long half lives (or they are stable) that they can't be observed, or their decay may involve emission of few or no observable γ -rays.

One of the great strengths of many nuclear methods of analysis is the fact that matrix effects such as self-absorption of radiations by the sample are usually negligible, since both the projectiles and the emitted radiations have very long ranges in the material. Thus, when an element of interest cannot be measured by one nuclear technique it is often helpful to try a different projectile. For example, some of us, in collaboration with Dr. George Lutz of the Activation Analysis Section, developed instrumental photon activation analysis (IPAA) in which one bombards samples with high-energy bremsstrahlung from an electron linac and observes decay of the products (1,2). In general, one produces a different set of products by (γ,n) , (γ,p) , etc. reactions than are produced in INAA. We found that IPAA could be used to measure concentrations of about 17 elements in environmental samples, of which about half were difficult or impossible by INAA, including Pb, Ni and Si.

Even with INAA and IPAA combined, there are still some important elements that cannot be measured routinely to the desired accuracy, e.g., Cd, B and S. Therefore, we are investigating the potential of neutron-capture γ -ray spectrometry as a new analytical tool. Instead of looking at γ -rays from radioactive decay, we will observe prompt γ -rays emitted from the samples while undergoing neutron irradiation. It may make possible the observation of many elements that are not observable by INAA and IPAA. Take Cd as an example: it has one of the highest cross sections of any element, but is not usually observable in INAA because most of that cross section leads to stable ^{114}Cd . However, we can take advantage of the high cross section by observing prompt γ -rays during irradiation. One of us (William Zoller) observed Cd, as well as Na, Cl, B and Gd, in a variety of samples via prompt γ -rays in preliminary experiments at Lawrence Livermore Laboratory in 1973. Gladney et al. have also reported measurements of Cd, B, S, C, N, H, Si, Al, Fe and Na in various samples (3).

We have designed and are now setting up a system at the NBS Reactor in order to thoroughly investigate the prompt γ -ray technique and, if successful, to use the set-up for routine measurements on many classes of samples. We will use a vertical beam tube in the reflector, which will give a reasonably high flux ($\sim 2.2 \times 10^8$ n/cm²-sec) with good thermalization ($\text{CR}_{\text{AU}} \sim 20$) and a low flux of scattered γ radiation. Targets will be external to the reactor, which will allow for unusual sample size and shape, good counting geometry, cooling if needed for unstable materials, etc. The γ -ray spectra will be taken with a Ge(Li) detector that can be surrounded with a NaI(Tl) anti-Compton shield. The detectors will be coupled to a computer-based pulse-height analyzer system capable of storing "singles" spectra Compton-suppressed spectra, pair-escape spectra, etc. in order to give maximum flexibility for observing γ rays from about 100 keV up to 8 MeV. The analyzer system, which is programmable, will also be used for reduction of most of the data.

The components of the beam facility are nearing completion. The beam thimble and shutter inserts, consisting mainly of steel, lead, boral, borated polyethylene and ^6Li -loaded polystyrene annuli have been fabricated and/or machined. Only the machining down of a few welds on the outer Al beam tube and the final working of the Hevimet shutter plug remain to be done before insertion into the reactor, which is scheduled for 3-5 September 1977.

The beam stop is now being assembled. A large block of (natural) Li_2CO_3 -loaded polystyrene containing $^6\text{Li}_2\text{CO}_3$ -loaded polyethylene plug has been fabricated. A Pb jacket and the supporting structure will be added over the next few weeks. Aluminum tubing and a slit box have been obtained for use as the upper beam tube and sample holder.

A TP-5000 pulse-height analyzer system delivered in March, 1977 has been undergoing de-bugging. The system is built around a PDP-11/34 computer with 80K words of core and uses an LA-34 Decwriter for programming and output, as well as magnetic tapes and discs. Software has been written which is easily adaptable for complete analysis of singles, Compton-suppressed and pair spectra. A NaI(Tl) Compton-suppressor shield has been ordered. Until it is installed preliminary experiments will be conducted with a smaller suppressor already available at the University of Maryland. As soon as the system is operational we will irradiate many pure elements and a wide variety of typical complex samples in order to explore the capabilities of the method.

-
1. N. K. Aras, W. H. Zoller, G. E. Gordon and G. J. Lutz, *Anal. Chem.*, 45, 1481 (1973).
 2. I. Olmez, N. K. Aras, G. E. Gordon and W. H. Zoller, *Anal. Chem.*, 46, 935 (1974).
 3. E. S. Gladney, E. T. Journey and D. B. Curtis, *Anal. Chem.*, 48, 2139 (1976); Gladney, Curtis and Journey, Paper presented at American Chemical Society National Meeting, New Orleans, (1977).

2. Applied Research in Activation Analysis

a. Standardization of Thin Gold Films

R. M. Lindstrom and S. H. Harrison

A set of seven gold films on silicon substrates have been calibrated for absolute gold content, in conjunction with the surface physics research group of the California Institute of Technology. These calibrated films are now being used by the Cal Tech group to substantially improve the worldwide intercomparison of Rutherford-backscattering film thickness measurements.

The gold assay was performed by instrumental neutron activation in the RT4 position of the NBSR, followed by gamma-ray counting with a Ge(Li) detector. Sources of systematic of error in the procedure were eliminated or compensated, with the result that the average total error was 0.3%, as determined by independent gravimetric analysis of the sample set. Bias due to unequal neutron flux for the sample, as compared with the standard, was compensated by reversing the rabbit and for end midway during irradiation; this procedure reduces the longitudinal flux gradient to less than 0.5%. Matching the weights of standards to the samples was necessary to compensate changes in counting efficiency due to pileup losses, which may amount to as much as 10% at 10^4 counts/sec (25% dead time).

The results obtained by activation analysis and by gravimetry are given in the accompanying table. Agreement is excellent.

A Comparison of Results Obtained by Activation Analysis and Gravimetry

Sample	Au Measured (μg)		NAA/Grav
	NAA*	Grav	
A	356.3 ± 1.0	355.7 ± 0.7	1.0017 ± 0.0034
B	835.8 ± 1.6	836.1 ± 0.7	0.9996 ± 0.0019
BB	832.4 ± 1.7	834.4 ± 0.7	0.9976 ± 0.0019
C	1067.8 ± 2.0	1060.2 ± 0.7	1.0072 ± 0.0020
CC	872.8 ± 1.8	878.0 ± 0.7	0.9941 ± 0.0022
D	1384.2 ± 2.3	1377.8 ± 0.7	1.0046 ± 0.0017
DD	1491.7 ± 2.4	1491.7 ± 0.7	1.0000 ± 0.0017

mean = 1.0007 s = 0.0043

* Errors quoted for NAA determinations are the standard deviations based on counting statistics alone.

b. Trace Elements in Solar Cell Silicon

R. M. Lindstom, R. F. Fleming and H. L. Rook

The process by which silicon solar cells are currently made requires silicon of "semiconductor grade", as a starting material. This high purity material is very expensive, costing about \$70 per kilogram. It is possible to make solar cells from less pure, therefore less expensive silicon, but usually the efficiency of the resultant solar cells decreases as the general impurity level increases.

In an effort to reduce the cost of producing silicon used in solar cells while maintaining a reasonable efficiency, the Jet Propulsion Laboratory (JPL) has undertaken a project to define the quantitative affects of selected trace elements on the conversion efficiency of silicon solar devices. One fundamental requirement of this project is the ability to accurately measure trace element concentration at the 10^{13} to 10^{15} atoms/ml level. Methods for accurate analyses at these levels are not presently available for all trace elements of importance. The NBS program is designed to develop and provide credible analytical procedures for materials specific to JPL's needs. These procedures

should provide a mechanism to generate accurate data from all contractor laboratories. The elements to be included in this study will be Cu, Ni, Al, Cr, V, Ti, Fe, Mn, Mg, Zn, Sn, and Zr. The established procedures will be evaluated for the accurate measurements of elemental concentrations in 10^{13} to 10^{15} atoms/ml range.

c. National Environmental Sample Bank

T. E. Gills, S. H. Harrison and H. L. Rook

The United States as well as many other Nations, has been concerned about the potential dangers to human health and the environment by the ever increasing influx of new man-made substances into our ecosystem. The U.S. Environmental Protection Agency is especially aware of this situation and is presently studying the feasibility of establishing a program, the National Environmental Specimen Bank (NESB), that would provide a formalized, systematic approach to assess the environmental impact of these substances at a national as well as an international level.

The concept of the NESB is that of a well defined system of collection, analysis and long term storage of selected environmental samples. This system would provide two important outputs. First, the analytical portion of the NESB will provide real time monitoring data for pollutant trend evaluation. Second, the specimen bank will provide properly stored samples for retrospective analysis enabling health scientists to determine accurate levels of substances that would be either undetectable or poorly analyzed by today's less sensitive techniques.

For an NESB type of system to be of any value, the credibility of the scientific protocols must be above reproach. Research into analytical methodologies has been undergoing extensive laboratory testing over the past three years. The scientific effort is at the point now where it is necessary to scale up the developed protocols from the "lab-bench" operation to a modified banking program--the Environmental Pilot Bank. This pilot bank effort will give the scientists actual working experience through all stages of the banking effort. The specimen

program would concentrate on a limited number of samples, collected, analyzed and stored in a central facility. This approach would allow for strict control and constant evaluation over all operational procedures. Problems encountered in any aspect of the program would undergo extensive review in order to determine the areas of deficiencies so that corrective measures may be taken.

The specimen bank concept was recently evaluated at two workshops, one sponsored by NBS and EPA, the other, an international workshop, sponsored by the World Health Organization, the Commission on European Communities and the Environmental Protection Agency. The conclusions of both workshops were in agreement; that the NESB is a viable concept, both from the standpoint of need and by the availability of present specific knowledge. However, it was felt by scientists at EPA and NBS that it would be premature to initiate a full scale storage and analysis banking effort until a pilot bank program had been initiated and all aspects of sample banking had been fully evaluated.

The interaction of the Neutron Activation Analysis Program has been primarily in obtaining the best possible assessment of proper long-term storage and proper analysis of important samples through accurate measurement of the trace constituents, a critical need which has mandated the Section's involvement. The overall research plan or objectives for neutron activation analysis program can be formalized as following:

- (1) Tissue sampling and sample handling techniques will be investigated to insure that during the process of sampling, alteration of trace components within the sample does not occur.
- (2) The development and evaluation of tissue storage techniques has been and will continue to be investigated for short-term and long term storage. These techniques will minimize changes in chemical constituents within the sample.
- (3) Improved analytical techniques have been and will be developed for the determination of trace elements of interest in human and animal tissues. These techniques allow the accurate determination of trace constituents of importance to human health.

(4) The accuracy and precision of the proposed analytical techniques have been and will be determined on real samples so that appropriate errors may be applied to data in future banking systems evaluating long-term storage systems. This program is concurrent with existing research programs in analytical measurement carried on in the Analytical Chemistry Division, and therefore there is a natural mating of scientific interest within NBS with that of the EPA.

The benefits of the sample bank research will be most readily evident in the continuing programs on health related research within EPA. However, other agencies will have direct benefit from the program, including the Department of Agriculture and the Food and Drug Administration. The NBS sample bank research will greatly benefit their programs in assessing the effects of changes in human diet patterns required in studies over long periods of time.

The main support for this program is derived from an interagency agreement of support and understanding between the EPA and NBS.

d. Environmental Effects of Used Oils

R. F. Fleming and H. L. Rook

The disposal of used oils has become a significant environmental problem in modern society. A recent article stated that waste oil from automobiles and industrial machinery alone accounted for over 40 percent of the total amount of crude oil and petroleum products introduced into the ocean each year [Science, 194, 791 (19 November 1976)]. These used oils contain high concentrations of inorganic elements and organometallic compounds from lubricant additives, fuel additives, and wear debris. Consequently, the deleterious effects on the ocean environment due to used oils may very well exceed the harmful effects of all other sources of crude petroleum and petroleum products, including oil tanker accidents and cleaning operations, all offshore oil drilling and production, and all natural seepage.

Alternatives of disposal of used oil include: (1) removal of the decomposition products, additives and contaminants from the used oil to

allow improved disposition of the concentrated impurities and reuse of the petroleum basestock (reprocessing or re-refining); or (2) burning of used oil with minimal or no pretreatment to recover the heat energy, with concurrent increased production of toxic species which may be emitted to the environment. Both the above alternatives appear to be an improvement over straight disposal of the used oil in the environment. However, both of the alternatives also suffer from a lack of basic information on the chemical contaminants of used, virgin, processed, and re-refined lubricating oils including, especially, their source, speciation, and ultimate fate in the environment.

Neutron Activation Analysis techniques have been developed or modified for non-destructive analysis for a variety of trace elements in virgin, used, processed, and re-refined lubricating oils. In particular, correlation of trace element content with chemical speciation is being attempted in conjunction with other speciation techniques. Efforts to establish the degree of processing by means of the trace element concentration will also be made. Finally, preliminary studies will be made on samples of typical oils in preparation for selecting one or more for lubricating oil research materials.

e. Radiochemical Separation for Cd

Robert R. Greenberg

A radiochemical separation using the diethyldithiocarbamate (DDC) ion was adopted for the analysis of Cd. The procedure involves the extraction of Cd by $Zn(DDC)_2$ in $CHCl_3$. Tracer experiments indicated that this procedure was >99 percent quantitative for a shaking time of two minutes over a pH range of 1-12.

In addition to Cd, several other elements were found to be extracted by $Zn(DDC)_2$. In some instances, Cu was found to interfere with the determination of Cd by producing a high background level of radiation. This problem was eliminated by first extracting with $Bi(DDC)_3$, which removes Cu. Cd in SRM 1571 (Orchard Leaves) and Atmospheric Particulate material was determined using an extraction with $Bi(DDC)_3$, followed by extraction with $Zn(DDC)_2$. Good results were obtained.

In addition to the determination of Cd, several other elements can be determined using this two-extraction procedure. Preliminary results indicate that Ag, Cu, and Hg are extracted quantitatively (>99%) by $\text{Bi}(\text{DDC})_3$ for a pH of 1, and a shaking time of 30 minutes. This group separation can also be used as part of a larger multielement analysis scheme by using an ion exchange resin, such as HMD, prior to the extractions.

3. Cooperative Research Projects

- a. Boron Measurements in Silicon using the Nuclear Track Technique.
B. Stephen Carpenter and W. Robert Thurber

In the semiconductor field, boron is used as a dopant to make p-type silicon devices. These devices are usually single crystal of Czochralski-processed silicon wafers with polished $\langle 111 \rangle$ faces. In each wafer the resistivity is a function of the boron dopant concentration and homogeneity. Electrical methods of four-probe, metal-oxide-semiconductor, and capacitance-voltage measurements are used for resistivity and concentration determination of active boron sites and not the total dopant in the silicon wafers. However, the total boron dopant concentration and distribution is determined in this study by the nuclear track technique (NTT). Silicon wafers with boron concentrations ranging over five orders of magnitude, 10^{15} to 10^{20} atoms cm^{-3} , were analyzed and correlated with the resistivity measurements. Figure 1 indicates the extent of the correlation of the results. In addition, comparisons of the NTT characteristics to other methods of determining boron are given in table 1.

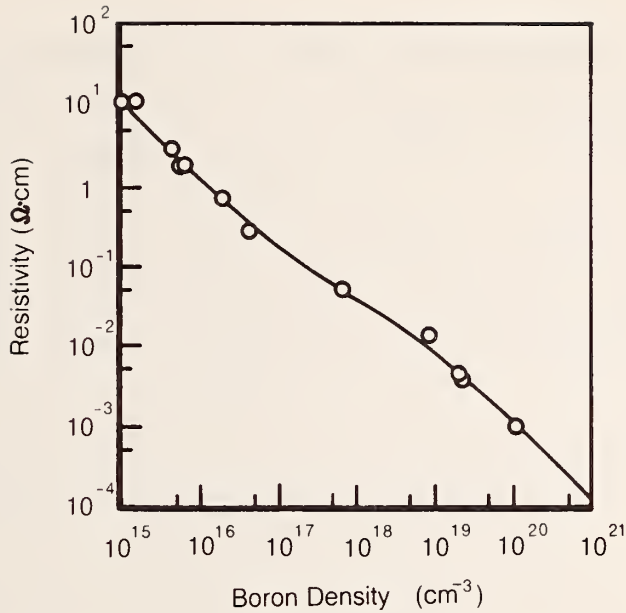


Figure 1. Resistivity Versus Boron Doping in Silicon Semiconductors.

Table 1. Characteristics of Methods Used to Determine Boron in Doped Silicon Wafers

Technique Characteristic	Secondary Ion Mass Analyzer	Nuclear Track Technique	Resistivity Measurement
Detection Limit (B Atoms/CM ³)	10 ¹⁷	10 ¹⁵	<10 ¹⁴
Spatial Resolution	Excellent	Good	Good
Specificity	Excellent	Excellent	Poor
Quantitation Requirements	Material Standards	Material Standards	R Calibrated Probes & Irvin-Wagner Curve
Precision	5-10%	2-5%	1%
Accuracy	20%	10%	≤20%

4. Other Agency Research Programs with Activation Analysis.

a. Nuclear Safeguards - NDA-NRC Research Program.

B. S. Carpenter, R. F. Fleming and H. L. Rook

Current measurement technology is neither accurate nor precise enough to meet the national (and international) goals of insuring the safety of fissionable materials. Through this program NBS is to provide leadership in the improvement of this measurement technology, as well as to provide the access of standards to transfer this technology. NBS was requested to provide the necessary standards to ensure traceability to NBS. At the present time there are no SRM's specifically for NDA of nuclear materials (although a few counting standards may be applicable in some cases). To provide these, along with the appropriate methodology, is clearly an NBS role.

The procedure to be used is to establish an NDA counting facility at NBS and to complete a priority assessment of the needed SRM's. Following this, prototype standards will be produced and after both laboratory and field evaluation, certified SRM's will be produced. The effective utilization of the SRM's will be assessed by providing a Measurement Assurance Program (MAP).

NBS personnel in the Activation Analysis Section are experienced in state-of-the-art nuclear measurements and in addition are currently advising on suitable techniques that may be used for NDA. The Section has extensive experience in the production and certification of a wide variety of Standard Reference Materials for a wide variety of elements in a wide range of matrices. Below is listed an outline of NDA safe-guard objectives for the coming year:

- (1) Establish an NDA Gamma-Ray Spectrometry System (i.e., modified Segmented Gamma Scan),
- (2) Measure attenuation and absorption coefficients of various matrix materials,
- (3) Design and prepare homogeneous standards - relative to density (bulk and tap), particle size, etc.,
- (4) Design and prepare heterogeneous standards
 - a) variation of density
 - b) variation of geometry and configuration
- (5) Gamma Scan-Segmented, and Others
 - a) transmission measurements
 - b) direct measurements
 - c) evaluation of gamma/x-ray coincidence counting,
- (6) Study absorption edge measurements,
- (7) Investigate limited applications of the nuclear track technique.

The most urgent transfer of technology will be through the certification of SRM's. Effective utilization of SRM's will be aided by providing a Measurement Assurance Program for users.

b. Adhesive Bonding of Various Materials to Hard Tooth Tissues
 XVII Tracer Study of Mordant Adsorption on Enamel.

T. E. Gills and R. L. Bowen

For improving adhesion between resins and hard tooth tissues, a mechanism has been proposed which calls for chelate bonding of poly-functional monomers with surface calcium ions or, preferably, with cations that have higher chelate stability constants. For clinical utility, the substitution (ion exchange) must be very rapid and relatively irreversible. The present study evaluated selected metal ions simultaneously for their sorption (adsorption or absorption) on enamel

surfaces. The test solution contained 2M phosphoric acid and 1/6 M each of cupric, zinc, cobaltous, and ferric chloride, spiked with radioactive tracers. Eight noncarious premolar tooth crowns were cleaned, exposed to the solution for 60 seconds, rinsed with water, and then dried. The residual radioactivity was measured to quantify each element sorbed. The copper ion concentration was as high after a second, extensive washing as it was before, indicating irreversible adsorption. The copper was slightly higher than the zinc, and more than ten times higher than the retained cobalt ions. That these ions can be sorbed during an etching or "conditioning" treatment from a phosphoric acid solution is very important to the development of practical therapeutic measures for both restorative and preventive dentistry.

c. The Analysis of Archaeological Obsidian and Geological Source Sample

M. J. Blackman

The use of trace and minor element profiling to determine the geological sources of archaeological obsidian is well established in the archaeological literature. A variety of analytical techniques have been used, including XRF, AA, INAA, and optical emission spectroscopy. Many of the studies, while internally valid, have suffered because data has not been published in concentration units or lacked an indication of the precision of the analysis. Both of these shortcomings result in the necessity of duplicating source analyses for each new investigation.

In this project thirty-two obsidian artifacts from the archaeological site of Tall-i Malyan, Iran, and twenty geological source samples from central and eastern Turkey were analyzed for nineteen elements by instrumental neutron activation analysis (table 1). The objectives of the research

Table 1. List of Elements Determined

<u>Nuclide</u>	<u>Half-Life</u>	<u>Gamma-Ray Energy (KeV)</u>	<u>Decay Time</u>
⁵⁶ Mn	2.587 H	846.7	1 hour
²⁴ Na	14.96 H	1368.6	1 hour
⁴⁶ Sc	83.9 D	889.26	14 days
⁵⁹ Fe	45.6 D	1099.22	14 days
⁸⁶ Rb	18.66 D	1076.77	14 days
⁹⁵ Zr	65.5 D	756.72	14 days
¹²⁴ Sb	60.4 D	1690.94	14 days
¹³¹ Ba	12.0 D	496.37	14 days
¹³⁴ Cs	2.046 Y	795.84	14 days
¹⁴⁰ La	40.22 H	1596.17	14 days
¹⁴¹ Ce	32.5 D	145.44	14 days
¹⁵³ Sm	46.8 H	103.18	14 days
¹⁵² Eu	12.7 Y	1408.02	14 days
¹⁶⁰ Tb	72.1 D	879.36	14 days
¹⁷⁵ Yb	4.21 D	396.29	14 days
¹⁷⁷ Lu	6.74 D	208.36	14 days
¹⁸¹ Hf	42.5 D	482.18	14 days
¹⁸² Ta	115.1 D	1221.38	14 days
²³³ Pa	27.0 D	311.9	14 days

project were: 1) to determine the number and location of geological sources of obsidian used to make artifacts found at the site; 2) to evaluate the usefulness of the published source data in the identification of obsidian sources; and 3) to compare the precision and accuracy of the twenty geological source samples previously analyzed at the University of Michigan (Keene and H. T. Wright, n.d) and reanalyzed in this study.

Two irradiations and counting schemes were employed (table 1). Elements whose nuclides have half lives of less than 24 hours were determined by irradiating about 20 mg of the samples and standards for 30 seconds in the RT-3 facility of the NBSR. Samples and standards were allowed to decay for one hour and counted twice for 10 minutes each. The standards used in the short irradiations were U.S.G.S. rock standard GSP-1 and NBS SRM 1633 "Fly Ash". Elements whose nuclides had half lives of greater than 24 hours were determined by irradiating about 100 mg of the samples and standards for 8 hours in the RT-3 facility. Samples and standards were allowed to decay for 14 days and counted for 100 minutes. The standards used in the long irradiations were U.S.G.S. rock standards AGV-1, GSP-1, and BCR-1, and NBS SRM 1633 "Fly Ash".

The concentration of each element was determined by taking the mean of the standard values was determined by the counting statistics or the standard deviation of the mean of the standard values, whichever was the higher.

The artifacts could be assigned to one of five compositional groups consisting of two or more members, representing five separate sources (table 2). Three samples did not fit well into any of these groups and therefore may represent three additional sources. Caution should, however, be used when postulating a separate source based on only one sample.

Comparison of the artifact groups with the analyses of the geological source samples allowed artifact group A (table 2) be assigned to the Nemrut Dag obsidian source (table 3). The remaining four artifact groups and the three unassigned samples could not be identified with any of the six geological sources available for analysis. Attempts

to compare the results of this project to published obsidian source data proved unsuccessful.

The work of Renfrew et al. (1966 and 1968) employed optical emission spectroscopy. The set of elements determined in these studies was, therefore, somewhat different from those determined in this project. Where the same elements were reported (Ba, Zr, La, Rb, and Fe) lack of statement of the precision in the Renfrew et al. analyses hampered comparisons. In the other major published work (G. A. Wright, 196), although instrumental neutron activation analysis was the analytical technique used, only a limited number of elements were reported in concentration units. The remainder of the elemental data was given as ratios of counts. This method of reporting data made meaningful comparisons impossible.

Table 3. Concentration Data for Source Sample SND/105/521

<u>Element</u>	<u>This Study (ppm)</u>	<u>Keene and Wright (ppm)</u>
Sc	0.35 ± 0.02	0.32 ± 0.02
Fe	24376 ± 245	24987 ± 299
Co	not detected	1.89 ± 0.25
La	110.3 ± 1.9	94.9 ± 1.5
Sm	20.0 ± 0.9	19.4 ± 0.2
Yb	14.8 ± 2.4	2.3 ± 1.9
Lu	2.25 ± 0.16	3.26 ± 0.91
Hf	28.4 ± 2.1	22.9 ± 1.6
Ta	5.01 ± 0.62	5.26 ± 1.03
Th	31.7 ± 1.5	33.9 ± 2.0
Na	41890 ± 801	38477 ± 158

The geological source samples analyzed in this study were part of a group of source samples analyzed at the University of Michigan and reported by Keene and H. T. Wright (n.d.). The two studies compare favorably in precision and accuracy for most elements, however, there are some discrepancies (cf Table 3 for an example). Cobalt, reported in

NON-RRD NBS PROGRAMS

Table 2. Obsidians: Malyan Artifact Groups (given in ppm)

Group (No.)	Sc	Sigma	Mn	Sigma	Fe	Sigma	Rb	Sigma	Na	Sigma	Zr	Sigma	Sb	Sigma
A (18)	0.241	0.008	—	—	21121	986	223.3	8.4	38331	412	943.0	110.3	1.32	0.14
B (2)	1.95	0.03	456.0	26.7	5301	101	181.4	5.4	31413	9	165.8	13.4	0.275	—
C (3)	0.583	0.019	459.7	14.1	16532	828	118.7	4.7	37547	67	599.8	73.5	0.428	0.057
D)	2.56	0.22	307.2	15.5	13494	902	227.0	19.1	36083	580	311.9	69.0	0.932	0.043
E (3)	2.07	0.10	552.4	14.9	10045	562	198.6	8.2	36939	365	238.4	25.5	0.422	0.068
Sample	Sc	Sigma	Mn	Sigma	Fe	Sigma	Rb	Sigma	Na	Sigma	Zr	Sigma	Sb	Sigma
003a	3.33	0.23	571.4	—	8858	435 ⁺	153.0	17.43	29814	—	224.0	26.1	0.438	0.085
012	1.76	0.10	510.6	—	16528	511	122.9	14.04	35120	—	390.3	32.2	0.611	0.105
026	0.182	0.017	—	—	25825	1883	251.6	19.3	—	—	962.7	54.8	2.32	0.156
Group	Ba	Sigma	Cs	Sigma	La	Sigma	Ce	Sigma	Sm	Sigma	Eu	Sigma	Tb	Sigma
A (18)	84.1	26.8	8.77	0.89	100.4	1.8	194.5	18.3	21.16	1.28	0.486	0.047	4.03	0.52
B (2)	121.7	7.0	5.83	0.28	40.3	1.8	57.6	6.1	2.75	0.10	0.205	0.010	0.260	0.059
C (3)	681.3	7.8	1.53	0.15	81.5	3.0	172.7	10.3	18.64	0.53	2.66	0.05	4.04	0.92
D (3)	509.3	15.7	11.93	0.53	47.8	1.9	78.0	9.2	7.51	0.95	0.493	0.047	0.846	0.163
E (3)	171.1	45.4	11.24	0.39	37.4	2.6	71.4	4.7	8.81	1.33	0.436	0.030	1.73	0.10
Sample	Ba	Sigma	Cs	Sigma	La	Sigma	Ce	Sigma	Sm	Sigma	Eu	Sigma	Tb	Sigma
003a	517.0	34.12	6.10	0.38	35.8	1.15	63.1	7.68	3.92	0.19	0.561	0.041	0.693	0.137
012	723.3	51.2	1.54	0.06	110.1	3.23	196.8	23.94	17.94	0.84	2.132	0.116	3.76	0.745
026	140.7	13.5	17.23	1.55	110.5	4.0	192.6	10.77	22.24	2.51	0.652	0.037	4.61	0.482
Group	Yb	Sigma	Lu	Sigma	Hf	Sigma	Ta	Sigma	Th	Sigma				
A (18)	14.94	0.77	2.28	0.15	25.13	3.24	4.36	0.35	27.20	0.73				
B (2)	1.92	0.04	0.339	0.006	4.37	0.25	2.64	0.00	33.33	0.68				
C (3)	12.08	0.31	1.85	0.14	19.69	2.41	8.37	0.89	17.46	0.57				
D (3)	4.31	0.10	0.701	0.029	8.24	0.77	1.73	0.19	26.73	1.20				
E (3)	6.53	0.56	1.04	0.073	8.30	0.30	2.57	0.20	24.53	0.36				
Sample	Yb	Sigma	Lu	Sigma	Hf	Sigma	Ta	Sigma	Th	Sigma				
003a	3.08	0.58	0.527	0.062	5.43	0.85	3.51	0.34	14.94	1.56				
012	10.15	1.84	1.50	0.129	15.37	2.39	8.47	0.81	19.93	2.08				
026	16.41	2.74	2.53	0.30	24.69	1.93	4.08	0.28	34.48	2.67				

the Keene and Wright analyses, was not detected, and the lanthanum and sodium concentrations were significantly higher in this study. Work is presently underway in an attempt to explain these differences.

5. Standard Reference Materials Certification Program in Activation Analysis

a. NBS Food Grain SRM (Rice and Wheat Flour)

H. L. Rook, T. E. Gills and M. Gallorini

Increasing concern with possible toxic trace elements in the food chain plus growing recognition of the importance of a number of trace elements in nutrition makes the accurate determination of these trace elements essential. The National Bureau of Standards is an interagency agreement with the Food and Drug Administration are in the process of developing and certifying certain elements in food grain as part of their Standard Reference Materials Program. These SRM's Rice and Wheat flours, will allow the FDA to trace the results of their district and regional laboratories to SRM's in support of their regulatory programs. This will increase accuracy, and hence the comparability of these analyses.

Neutron Activation Analysis was used for both the homogeneity testing and certification analyses of those SRM's. Both destructive and instrumental NAA using radiochemical separations were used for analysis.

b. Surveys of Proposed SRM's by Instrumental Neutron Activation Analysis

R. R. Greenberg

Surveys of four proposed SRM's were performed to determine the approximate levels of various elements in these materials, and to determine which of these elements could be certified using this technique. The proposed SRM's included oil shale, urban atmospheric particulate material and two different coals. Approximate concentration of elements having intermediate or long-lived neutron irradiation products were determined using primary standards and SRM 1632 (Coal). The elemental concentrations used for SRM 1632 were the certified values and those appearing in the literature. The results of these surveys are listed in table 1.

NON-RRD NBS PROGRAMS

Table 1. Approximate Concentration¹ ($\mu\text{g/g}$ unless % indicated)

	<u>Eastern Coal</u>	<u>Western Coal</u>	<u>Oil Shale</u>	<u>Air Particulate</u>	<u>SRM² 1632</u>
Na(%)	0.089	0.22	1.6	0.42	0.040
K(%)	0.39	0.12	1.0	0.95	0.27
Rb	30		63	52	20
Cs	2.2	0.012	3.4	3.4	1.4
Ba	140	73	540	920	330
Br	56	0.76		510	19
Sc	5.9	0.53	4.6	6.6	3.7
Cr	35	2.4	32	400	20.2
Fe(%)	1.1	0.20	1.8	3.8	0.87
Co	6.3	0.53	9.0	18	5.6
Zn(%)				0.45	
As	9.1	0.35	64	110	5.9
Se	2.4	0.79	3.5	25	2.9
Ag				6.4	
Cd				71	
Sb	0.52	0.12	2.8	45	
La	16	1.7	20	38	11.3
Ce	30	2.9	34	55	20.4
Sm	2.6	0.23	2.5	4.0	1.83
Eu	0.55	0.058	0.52	0.83	0.38
Tb				0.45	0.22
Yb	0.91	0.15	0.85	1.6	0.70
Lu	0.19	0.030	0.18	0.29	0.14
Hf	1.7	0.22	1.5	4.4	0.95
Ta	0.34	0.34	0.30	5.9	0.21
W				4.9	
Th	4.4	0.52	4.7	7.4	3.0

¹ As Received (not dried).

² Reference values used.

c. SRM-Na in Bovine Serum

S. H. Harrison

The objective of this work was to determine the concentration of Na in the proposed SRM-Na in bovine serum to an accuracy and precision of less than 0.6% relative. Instrumental neutron activation analysis (INAA) is not routinely used for high accuracy and precision analyses. However, for carefully chosen matrices, INAA has been shown to be capable of the accuracy and precision desired in this study (1). Before the actual analysis of the proposed SRM Na in bovine serum, it was necessary to demonstrate that this matrix could be analyzed to produce the desired statistical criteria. The precision was demonstrated by analyzing 13 samples from a pooled lot of bovine serum for the relative $A_0(^{24}\text{Na})/\text{g soln}$. The results showed that precisions of 0.5% or better could be achieved.

To assess the accuracy, the primary solution standard made from NBS-SRM 919 NaCl was used to analyze to other standard solutions, one made from NBS-SRM 40h $\text{Na}_2\text{C}_2\text{O}_4$ and the other from a commercial source of high purity NaCl. The relative difference between the experimentally determined concentration of the sodium oxalate solution and the gravimetrically calculated value was .0.4%. For the high purity NaCl standard solution, the relative difference between the experimentally determined concentration and the gravimetrically calculated value was .0.2%. Potential sources of error from a sample and standard preparation, irradiation and counting were investigated during the course of the experiment. Finally, the SRM-serum with nominally 3000 $\mu\text{g/g}$ Na was accurately analyzed for Na content on duplicate samples of six bottles.

d. SRM's for Water Pollution Program

H. L. Rook and L. T. McClendon

The national effort in water pollution abatement involves municipal and state government agencies, industries, water suppliers, and nearly every department of the federal government. Although all industry and government have been engaged in water pollution measurement since the previous century, added urgency has resulted from the passage of the

Federal Water Pollution Control Act Amendments of 1972 (P. L. 92-500) and the Safe Drinking Water Act of 1974 (P. L. 93-523). The later legislation (P. L. 92-523) set limits on the concentration of some trace elements in water. Thousands of analyses for trace inorganic elements in water are performed annually, both by governmental and industrial laboratories. However, due to the lack of standards, many of these analyses are of questionable accuracy, casting serious doubts on the intercomparability of data between laboratories. Without accurate measurements, scientists cannot relate health efforts to levels of pollution correctly, engineers cannot assess the effectiveness of control techniques correctly, and regulatory agencies cannot relate levels of pollution effluents with ambient water quality correctly, nor can compliance with water pollution regulations be fairly and equitably tested.

The National Bureau of Standards (NBS) was asked (by the Environmental Protection Agency) to develop a multi-element in water Standard Reference Material (SRM) which would consist of 16 trace elements and 4 major elements and be representative of trace element concentrations found in the natural environment. Additionally, the NBS was asked to develop an industrial sediment SRM for testing the methodology of 16 elements and selected bulk properties in polluted water sediments. These two materials will make it possible to evaluate the accuracy of methods for the elements certified in the presence of interfering substances.

Two different analytical methods were used: instrumental neutron activation analysis (INAA) for the determination of some elements (Na, K, Mn, Al, V and As) and a "semi-destructive" neutron activation technique (DNAA) for other elements (Cu, As, Co, Mo and Cr).

1. Multielement, instrumental
 - a. Short Half-Lives

Vandium was determined instrumentally. Approximately 6 gram samples of the water were placed in precleaned polyethylene vials. Standard solutions of vandium were made by dissolving the metal in high purity acid and diluting to volume with high purity water. Standards

were then packaged in same manner as samples. Each sample and standard was irradiated for 60 seconds in RT-3 of the NBSR and allowed a constant three minute decay. This decay period allowed the analyst time to transfer the samples into clean counting vials and positions on the 66 ml Ge(Li) detector system for assaying. Data were recorded on magnetic tape and quantified using QLN-1 computer program.

b. Medium Half-Lives

Manganese, sodium and potassium were determined simultaneously. Approximately 1.5 gram samples of the water were placed in polyethylene bags, and the air evacuated. Four samples and one standard were placed in a "rabbit" and irradiated for 30 minutes in RT-3 of the NBSR. The samples were allowed to decay for five hours to minimize short-lived activities. The samples were transferred to petri dishes, post-weighed and counted on the 75 ml Ge(Li) detector-automatic sample changer system. Data was recorded on magnetic tape and quantified using the QLN-1 computer program with the exception of potassium which was hand calculated.

2. Multielement, radiochemical separation

High levels of gold, sodium and arsenic made it difficult to determine other elements of interest in the water sample without some radiochemical separation. Therefore, a procedure using a multiple inorganic ion exchange technique based on work by Girardi, et. al., and further developed in this laboratory by Gills, was adopted to separate elements of interest in the water. The procedure was as follows: Standards and samples were double sealed in polyethylene bags, irradiated for 1 hour in RT-3 and decayed 8 hours. The samples were post-weighed into 100 ml beakers five milligrams of appropriate carriers added, 5 ml concentrated HClO_4 added and heated to near dryness. Samples were allowed to cool and 5 ml of 6M HClO_4 added to each column mounted in series. Two 10 ml portions of 6M HClO_4 was used to wash columns. Copper and gold are retained on the CUC column, As and

Mo on the TDO column and the remaining elements in the effluent. The effluent was allowed to decay for an additional seven days to reduce Na-24 activity and then counted on the 75 ml Ge(Li) detector system.

The results for those elements determined using INAA are shown in table 1. The results for those elements determined using radiochemical separation are shown in table 2. Arsenic and zinc will be re-determined in the water samples and the results reported at a later date.

Table 1. Elemental Concentrations in Low-Level Multielement Water
(INAA) μg of Element/Gram Water

<u>Sp1</u>	<u>Na</u>	<u>K</u>	<u>Mn</u>	<u>V</u>
1001 A	10.052	1.871	0.0306	0.0500
1001 B	10.155	1.813	0.0301	0.0510
1078 A	10.319	1.758	0.0300	0.0510
1078 B	10.473	1.745	0.0306	0.0507
1121 A	10.120	1.810	0.0296	0.0512
1121 B	9.971	1.803	0.0303	0.0509
1186 A	10.269	1.858	0.0295	0.0510
1186 B	10.427	1.928	0.0297	0.0506
1228 A	9.879	1.831	0.0299	0.0501
1228 B	9.926	1.878	0.0297	0.0503
\bar{x}	10.159	1.829	0.0300	0.0507
	± 0.028	± 0.056	± 0.0004	± 0.0004

NON-RRD NBS PROGRAMS

Table 2. Elemental Concentration in Low-Level Multi-element Water (w/separation).

µg of element/gram water					
<u>Sp1</u>	<u>Cu</u>	<u>As</u>	<u>Co</u>	<u>Mo</u>	<u>Cr</u>
1001 A	0.0167	0.0707	0.0186	0.100	0.0141
1001 B	.0171	.0711	.0184	0.099	.0150
1078 A	0.0174	0.0703	0.0198	0.100	.0156
1078 B	.0168	.0702	.0184	0.105	.0148
1121 A	0.0160	0.0707	0.0181	---	.0140
1121 B	---	.0715	.0184	---	---
1186 A	0.0168	0.0695	0.0184	0.099	0.0146
1186 B	.0164	0.0690	.0182	---	.0155
1228 A	.0164	0.0735	0.0186	0.099	0.0147
1228 B	.0163	.0710	.0184	---	---
\bar{x}	0.0166	0.0707	0.0185	0.100	0.0148
	±0.0004	±0.0012	±0.0005	±0.002	±0.0006

e. Analysis of Copper Benchmarks SRM's

G. J. Lutz

In response to industrial needs for standards for determination of trace elements in scrap copper, which is to be recycled, NBS has prepared a series of eleven copper "Benchmark" Standard Reference Materials (SRM's). Using instrumental neutron activation analysis, it is possible to determine in many of the samples, selenium, chromium, silver, zinc, antimony, cobalt and iron, the activation products of these elements being long lived and hence measurable after Cu-64 ($t_{1/2} = 12.9\text{hr}$) has decayed to low levels.

Since the matrix in all cases is copper and the samples only vary in trace element composition, a different approach to their analysis was taken. Only the first group of the series was analyzed by primary methods, i.e., those known or assumed to be reliable for the seven elements. This group is then used as a standard for the other ten with an enormous saving of effort.

These standards are available in both rod and chip form. A major consideration in the analysis is homogeneity of the various constituent samples of each group of the series. We are conducting homogeneity testing for the seven elements in approximately 150 samples. Duplicates are run on each of the these rod and chip samples. The variance of value obtained for the duplicates is statistically compared with the variance of the individual component samples of each group. The use of automatic sample changers in gamma ray counting and computers for data reduction keep the time involved for these determinations within reasonable bounds.

6. Multielement Standard in Neutron Activation Analysis
 - a. Preparation of Multielement Standards for Instrumental Neutron Activation Analysis

R. R. Greenberg

For accurate instrumental analysis it is essential to have good standards. Concentrated stock solutions of each element were prepared from pure materials. A small portion of each solution was irradiated and counted to check for contamination. Contamination of one element with a second element to be used in the same multielement standard is especially significant. While preparing these standards, the concentration of Cs in one bottle of high purity RbCl was found to be comparable to the amount of Cs required for the standard. This bottle of RbCl was therefore rejected and another Rb compound was used. Various multielement standards were prepared in the following manner. Appropriate amounts of the stock solutions were combined to form various mixed standard solutions. These solutions were then pipetted onto Whatman 41 filters and allowed to dry. The blank values in the filters were determined and the standards checked by analyzing SRM 1632 (Coal) and comparing the results with the certified and published values.

- b. Freeze-Drying Studies of Oysters and Salt Water

S. H. Harrison

In conjunction with the National Environmental Specimen Bank project on evaluating sample storage procedures, a study of freeze-drying as a pre-treatment for room temperature storage of oyster and water samples has begun. For oysters, the concern is whether some trace elements are volatilized during the freeze-drying process. For salt water there are several different reasons for investigations. First, is the possible loss of trace elements from the sample due to actual mass loss (sputtering during freeze-drying). The second is the loss of some trace elements which may exist in volatile chemical forms. (These first two factors have been investigated for fresh water by Harrison et al.) (1). A final reason for studying freeze drying of salt water is an interest in the ability to reconstitute the sample to the original

volume while retaining properties such as salinity.

Fourie and Pusach (2) have evaluated freeze drying and oven drying oysters using radioactive tracer techniques. In their study, oysters were placed in water containing various radioactive species for 1 month and then counted before and after preconcentration. It must be pointed out that one possible difficulty with this method is in shucking the oyster in such a way that only oyster meat and body fluid are collected and water (usually greater than 50% of the volume inside the shell containing the radioactive tracer, is drained off. Fourie and Peisach find that only for cadmium are significant losses from freeze drying detected.

It was felt that in this laboratory a similar, but perhaps more definitive, study could be made without the use of radioactive tracers. By careful sample packaging techniques, instrumental analysis of wet tissues could be done with the NBS Reactor. Therefore, in this experiment a collection of 40 oysters about the same size and from the same bed would be split into two groups; 20 will be freeze dried and analyzed and 20 will be analyzed wet. A comparison of elemental concentration means and standard deviations should definitively determine if losses from freeze-drying occur for these biologically incorporated trace elements. Colby et al. (3) have studied the variability of Zn in oysters for individuals from a single bed and groups from different beds and conclude that 20 individuals is a valid sampling of oysters.

The salt water study will entail a similar comparison of a set of freeze-dried samples to liquid samples, all from the same bottle.

-
1. S. H. Harrison, P. D. LaFleur and W. H. Zoller, *Anal. Chem.*, 47, 1685 (1975).
 2. H. O. Fourie and Max Peisach, *Analyst*, 102, 193 (1977).
 3. D. R. Colby, F. A. Cross and R. J. Huggett, "Variability of Zinc in Oysters (*Crassostrea virginica*): Implications for Sampling Design," (to be published).

THE INTERMEDIATE-ENERGY STANDARD NEUTRON FIELD (ISNF)

D. M. Gilliam, C. M. Eisenhauer, J. A. Grundl
(Center for Radiation Research)

The Intermediate-Energy Standard Neutron Field (ISNF) Facility has become operational and initial experimental results have been reported,^{1,2} The objectives of this measurement program are as follows: to develop an irradiation facility which will produce a well-characterized neutron field with a strong spectrum component in the energy range 5 keV to 4 MeV relevant for studying fast neutron reaction rates. Specific applications include:

1. Measurement of basic fission and capture cross sections.
2. Calibration of activation and other passive neutron detectors employed in reactor fuels testing.
3. Long-term measurement assurance and detector performance studies for power reactor neutron dosimetry.
4. Validation of neutron spectrometers and related energy-sensitive neutron detectors.

The ISNF arrangement is fundamentally simple as can be seen in figure 1: a spherical cavity in the graphite thermal column of the NBS reactor, a thin shell of boron-10 lightly supported at the cavity center, and fission source disks of U-235 placed symmetrically around the periphery of the cavity. Thermal-neutron-induced fission neutrons in the source disks - both the uncollided and those returning from the graphite - are transmitted by the boron-10 shell and give rise to the ISNF field at the center of the cavity. Summary properties of the ISNF field are as follows:

Total neutron flux intensity: $\sim 7 \times 10^8 \text{ n} \cdot \text{cm}^{-2} \cdot \text{s}^{-1}$

Typical maximum fluence: $\sim 0.5 \times 10^{14} \text{ n} \cdot \text{cm}^{-2}$

Neutron field gradient: < 2% over 4 cm

Spectrum:

average and median neutron energies: 1.0 MeV and 0.56 MeV,
respectively

energy range: 90% of spectrum between 8 keV and 3.5 MeV
Response range of $1/v$ -detector: 90% between 0.5 keV and
1.5 MeV

Initial measurements of fission cross section ratios for U-235, U-238, and Pu-239 have been completed. The flux and spectral gradients along the axis of the system have been checked, and thermal-neutron-induced background and leakage have been measured, also. These results are presented in tables 1, 2, and 3 below.

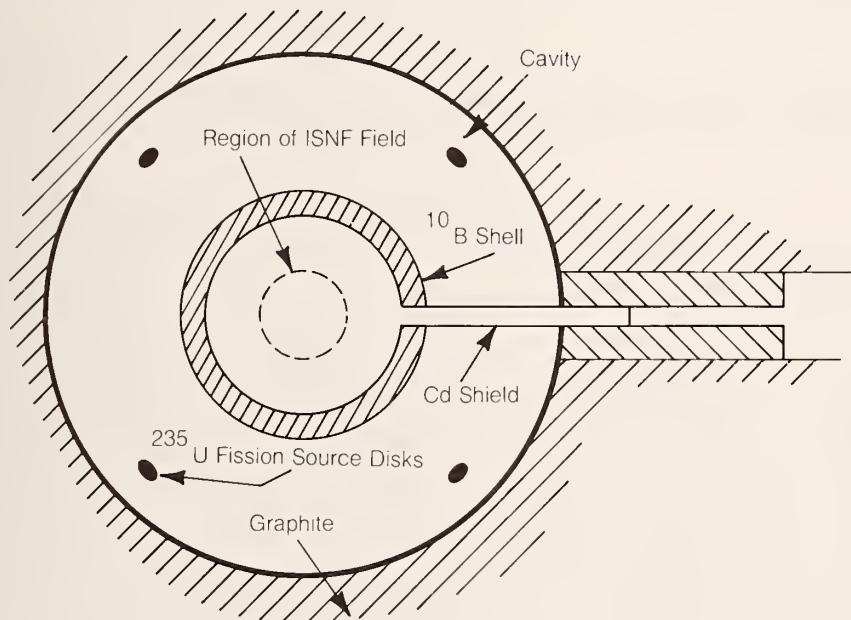


Figure 1. A schematic drawing of the ISNF spherical cavity.

NON-RRD NBS PROGRAMS

Table 1. Measured Fission Cross Section Ratios and Comparisons with Calculated Values.

	$\bar{\sigma}_f(x)/\bar{\sigma}_f(\text{U-235})$		
	Measured*	Calculated†	(Calc/Meas -1) x 100%
x:U-238	0.0923 \pm 1.1%	0.0843	8.7%
x:Pu-239	1.155 \pm 1.8%	1.113	3.6%

*The cross section values and error estimates given here were derived without taking into account possible perturbations due to epithermal neutron leakage.

†Calculated cross section ratios are derived by folding together the ENDF/B-IV cross section data and the neutron energy spectra given in the compendium by Grundl and Eisenhauer (Ref. 2).

Table 2. Measured Residual Thermal-Neutron-Induced Response with Fission Source Disks Removed.

Fissionable Isotope	Fission Rate in ISNF Spectrum (s ⁻¹ mg ⁻¹)	Fission Rate Due to Thermal Neutrons plus Background (s ⁻¹ mg ⁻¹)	Background and Thermal-Induced Fission Rate/ Fast-Induced Fission Rate
U-235	3170	45 \pm 11	1.4%
U-238	290	8 \pm 0.5	2.8%
Pu-239	3660	47 \pm 10	1.3%

Table 3. Spatial Gradients in the ISNF Central Test Region.

	Isotope Observed	
	U-235	U-238
Measured Fission Rate Change from ISNF center to a point 2.5 cm away from the center	-(2.3 \pm 0.5)%	-(2.9 \pm 0.8)%

1. D. M. Gilliam, "Integral Measurement Results in Standard Fields," Proceedings of the International Specialists Symposium on Neutron Standards and Applications, Gaithersburg, MD (1977).
2. J. S. Grundl and C. M. Eisenhauer, "Benchmark Neutron Fields for Reactor Dosimetry," Proceedings of the IAEA Consultant's Meeting on Integral Cross Section Measurements in Standard Neutron Fields for Reactor Neutron Dosimetry, Vienna, (1976).

FISSION RATE INTERCOMPARISONS WITH THE REACTOR PHYSICS GROUPS AT ARGONNE NATIONAL LABORATORY

D. M. Gilliam
(Center for Radiation Research)

and

R. J. Armani
(Argonne National Laboratory, Argonne, IL)

A round robin test series was undertaken to intercompare fission rate measurement capabilities at NBS-Neutron Standards and ANL-Reactor Physics. The first series of planned intercomparison measurements have been made, and some results are reported here from NBS and ANL-E (Argonne National Laboratories; Argonne, IL). A set of 18 fissionable deposits was prepared by R. J. Armani of ANL-E including the three isotopes U-235, U-238, and Pu-239. Six deposits of each isotope were made with nominal masses ranging from 23 μg to 85 μg . Armani also alpha counted the entire set. Two deposits of each isotope were compared to the NBS Reference Deposits by fission counting. For the U-238 deposits, this comparison was carried out at the NBS Cf-252 facility. For the other isotopes, the comparison was carried out in a beam from the thermal column of the NBS Research Reactor. All six of the U-235 and Pu-239 deposits were counted relative to NBS Reference Deposits and alpha emission standards, but corrections for alpha emissions from minor isotopic constituents have not been completed as yet so that only relative masses, normalized to the fission comparison results can be given from the alpha

NON-RRD NBS PROGRAMS

Table 1: Comparison of results: NBS vs. ANL-E

Intercomparison Fission Deposit Label	Total Elemental Mass*		Discrepancies (NBS/ANL-1) (%)
	NBS Value (μg)	ANL-E Value (μg)	
N-U5-1	27.11(38)	26.92(13)	0.7
N-U5-2	28.62(39)	28.51(14)	0.4
N-U5-3	53.1(7)	52.67(25)	0.8
N-U5-4	50.8(7)	50.39(24)	0.8
N-U5-5	75.2(11)	74.51(36)	0.9
N-U5-6	73.7(10)	73.19(36)	0.7
N-P9-1	22.79(30)	22.81(13)	-0.1
N-P9-2	24.37(32)	24.52(14)	-0.6
N-P9-3	43.0(6)	43.38(24)	-0.9
N-P9-4	45.2(6)	45.13(26)	0.2
N-P9-5	69.6(9)	70.17(39)	-0.8
N-P9-6	74.5(11)	75.00(42)	-0.7
N-U8-5	80.4(13)	80(Nominal)	0.5
N-U8-6	84.0(14)	85(Nominal)	-1.2

*The number in parentheses is the uncertainty in the least significant digit.

data at this time.

As may be seen in table 1, the ANL-E and NBS mass comparisons agree within 1.2%, well within the estimated errors of the comparison.

U-235 CAVITY FISSION IRRADIATION FACILITY

V. Spiegel, Jr.
(Center for Radiation Research)

The U-235 thermal-neutron-induced fission neutron spectrum is a key standard neutron field¹ for the validation of differential nuclear data needed for fast reactor physics or for neutron dosimetry. At the NBS this fission spectrum is produced in a 30 centimeter diameter spherical cavity in the reactor thermal column. As an example cadmium-covered nickel-iron detectors of 1/2 inch diameter were sandwiched between two U-235 disc of 5/8 inch diameter, which weighed about 500 milligrams each. For a separation distance between the two U-235 discs of about 8 millimeters, the average source to detector separation is about 1 centimeter. Since the average source-to-detector separation is small relative to the size of the cavity, a negligible fraction of fission neutrons produced in the uranium discs were returned to the detectors from the cavity walls compared to the direct flux. The U-235 neutron flux obtainable in this facility was about 100 times more intense than is available from our Cf-252 irradiation facility.²

Three discs of SRM-1158 (36% nickel, 63% iron) were irradiated in the U-235 Cavity Fission Irradiation Facility for approximately 24 hours. The ratio of the nickel to iron cross section in the U-235 fission spectrum is to be determined by three participating laboratories of the Interlaboratory Reaction Rate (ILRR) program, namely, Argonne National Laboratory, Idaho National Engineering Laboratory, and Handford Engineering Development Laboratory.

-
1. A. Fabry, J. A. Grundl, and C. Eisenhauer, "Fundamental Integral Cross Section Measurements in the Thermal-Neutron-Induced Uranium-235 Fission Neutron Spectrum," Proceedings of the Conference on Nuclear Cross Sections and Technology, (1975).
 2. J. A. Grundl, V. Spiegel, C. M. Eisenhauer, H. T. Heaton II, D. M. Gilliam, and J. Bigelow, "A Californium-252 Fission Spectrum Irradiation Facility for Neutron Reaction Rate Measurements," *Nucl. Tech.*, 32, 315 (1977).

ABSOLUTE MEASUREMENT OF THE DT THICK TARGET YIELD AT 191.3 KeV USING A THERMAL NEUTRON BEAM

R. F. Fleming and R. B. Schwartz
(Center for Radiation Research)

The thick target yield of the reaction $D(t,\alpha)n$ for tritons of initial energy 191.3 KeV slowing down in deuterium gas has been measured. This yield is defined as the number of DT reactions occurring per triton and can be expressed as

$$\psi(E_0) = \int_0^{E_0} \frac{\sigma(E)}{S(E)} dE \quad (1)$$

where $\sigma(E)$ is the reaction cross section and $S(E)$ is the stopping power for tritons in deuterium. This reaction ¹ is important since deuterium-tritium will be the fuel in any foreseeable first generation fusion reactor.

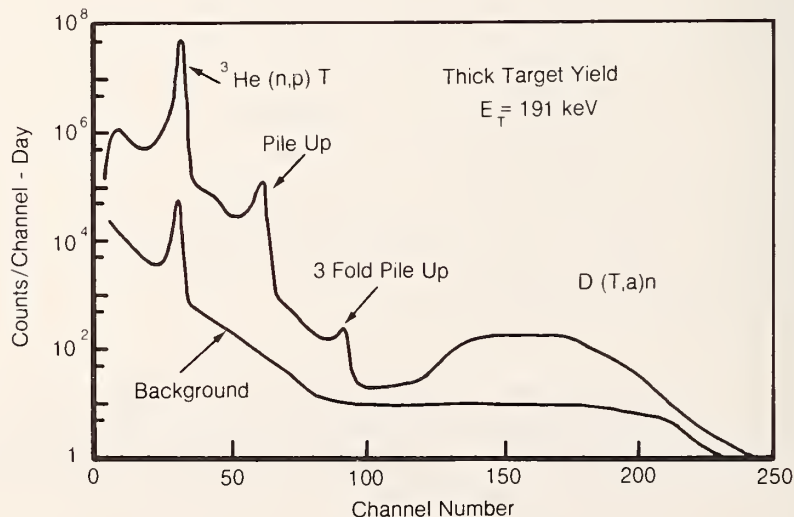


Figure 1. Pulse height spectrum from thermal neutrons on gas proportional counter filled with 5 atm. of D_2 and 10 torr of He-3.

The measurement was done by placing a standard end-window, gas proportional detector filled with five atmospheres of D_2 and about 10 torr of He-3 in a Bragg-scattered thermal neutron beam. The tritons are produced by the reaction $He-3(n,p)T$ which gives a count in the 763.8 keV peak for each reaction. About once in every 10^4 times the triton, in slowing down, reacts with a deuterium atom to give a $D(t,\alpha)n$ event. The "14 MeV" neutron escapes the detector without interacting, but the alpha particle will produce a broad high energy distribution in the pulse height spectrum. The ratio of the number of alpha counts to the number of He-3 counts is an absolute measure of the thick target yield. (See figure 1.) The preliminary result is in reasonable agreement with the value calculated from equation 1. The final result will be available as soon as we calculate the correction for the counter end effect.

-
1. Stewart, L. and G. M. Hale, "The $T(d,n)He-4$ and $T(t,\alpha n)$ Cross Sections at Low Energies," LA-5828-MS (1975).

FILTERED BEAM FACILITY

Robert B. Schwartz
(Center for Radiation Research)

1. Improvements to 25 keV Beam

The 25 keV beam has been rebuilt using larger diameter collimators and higher purity aluminum. We now have a neutron intensity of 1.0×10^6 neutrons/sec, which represents a factor of 12 improvement over the previous configuration.

2. Measurement of the B-10 ISNF Shell

The low energy flux distribution of the ISNF (Intermediate-Energy Standard Neutron Field) is carefully "tailored" by means of the B-10 content of the shell. Knowledge of this flux distribution is essential for proper interpretation of the results from this facility. The flux distribution must be calculated, since direct measurement is a formidable

problem. The calculations in turn, require accurate knowledge of the B-10 content of the shells. While this datum was supplied by the shell fabricators at LASL, it is obviously desirable to check both the B-10 content and its uniformity experimentally. A simple transmission experiment is probably the most reliable method. The B-10 shells are (by design) black to thermal neutrons; hence a transmission measurement at thermal won't give any information. The transmission at 2 keV is, however, almost ideal: $\sim 30\%$.

Accordingly, a transmission experiment was done at the 2 keV filtered beam. The results of the uniformity measurements were most gratifying: the B-10 content does not vary by more than $\pm 0.5\%$ over the shell surface. Our measured value for the absolute B-10 content differs from that given by LASL by $\sim 4\%$. This difference, while small, is significant and will be remeasured.

3. Use of the Filtered Beams for Dosimeter Calibrations

The filtered beams have been funded by ERDA as a dosimeter calibration facility. Although the facility is not yet quite open for business, several calibrations have been performed by ERDA contractors. In general, the facility seems to serve the function for which it was funded. The 144 keV beam provides an overlap with existing calibration facilities, the 24 keV beam fixes the low energy end of these facilities, and the 2 keV beam allows calibrations to be extended a decade lower in energy than had previously been possible. There is good agreement (where appropriate) with other calibration facilities and with calculations. Work is continuing to improve the quality of the beams and our calibration of them.

-
1. R. B. Schwartz, "Calibration and Use of Filtered Beams," Proc. Int. Specialists Symp. on Neutron Standards and Applications. Gaithersburg, MD, to be published.

PRECISION MEASUREMENT OF THE WAVELENGTH OF
NUCLEAR GAMMA LINES AND THE COMPTON
WAVELENGTH OF THE ELECTRON

R. D. Deslattes, E. G. Kessler, W. C. Sauder, and A. Henins
(Optical Physics Division)

A unique facility has been established at NBS which permits precision measurement of wavelengths of spectral lines in the 50 keV to 1 MeV range in terms of the wavelength of a visible molecularly stabilized laser. The radiation is diffracted by nearly perfect Ge and Si crystals in a two crystal transmission spectrometer. The lattice spacings of the crystals have been accurately determined in terms of the stabilized laser in a separate experiment, while the diffraction angles are measured with angle interferometers. Experimental arrangements have been documented in more detail elsewhere.^{1,2,3}

Most precision measurements require detailed investigation of systematic errors, and this experiment is no exception. During the past year we have made significant progress in understanding the vertical divergence correction, the shape of recorded line profiles, and the dependence of the angle interferometer calibration on temperature and the aging of the invar interferometer structure.

Because the radiation cannot be sufficiently confined parallel to the plane of dispersion without unacceptable loss of intensity, we must work with an appreciable vertical divergence. The effect of vertical divergence on the line profile is to introduce a slight asymmetry in the dispersive position which has now been modeled in an analytical form. We have used a convolution of this vertical divergence smearing function, the crystal diffraction patterns and an empirically determined Gaussian component to fit the observed data and thereby extract directly the Bragg-Laue angles. In early trials, the fit for data recorded with Si crystals was satisfactory, while data recorded with Ge crystals showed an asymmetry which could not be explained by other than imperfection in at least one of the Ge crystals which was subsequently

replaced with good effect.

The angle interferometers were calibrated at different temperatures and at different times of the year in order to determine the temperature coefficient of the calibration and the growth of the invar corner cube arm with time. Improvements of the analysis of the calibration data to compensate for second order errors resulting from the tip of the optical polygon and the autocollimator slit have provided a calibration constant accurate to 0.1 ppm.

Understanding of the above mentioned systematics brought to light a significant discrepancy between wavelengths measured with Ge and Si crystals. The Ge lattice spacing was then remeasured in a more carefully controlled experiment with the result that the discrepancy has been eliminated.

During the past year we irradiated three Au samples for additional measurements on the 412 keV line and new measurements on the 675 keV line. By employing the combination principle, a precise standard at 1.09 MeV is thereby available. Final wavelengths for the Au lines along with 9 lines from Ir-192 (205, 295, 308, 316, 468, 484, 588, 604, 612 keV) will soon be available and will provide accurate standards in the 100 keV to 1 MeV range.

Our measurement of the Au 411 keV γ -ray line brought to light a difficulty involving the $W\text{K}\alpha_1$ line. Another route to the 411 keV line is as follows: A previous (1 ppm) measurement of $\lambda(\text{MoK}\alpha_1)$ in terms of a visible standard⁴ is combined with the (2 ppm) ratio $\lambda(\text{WK}\alpha_1)/\lambda(\text{MoK}\alpha_1)$ from Bearden et al.⁵ to obtain a value for $\lambda(\text{WK}\alpha_1)$. When this is combined with the ratio $\lambda(^{198}\text{Au } 411)/\lambda(\text{WK}\alpha_1)$ from Borchert et al.⁶ a value for $\lambda(^{198}\text{Au } 411)$ results which differs by more than 100 ppm from our measurement.

In order to resolve this difficulty we directly measured the wavelength of the $W\text{K}\alpha_1$ line first with Ta-182 radioactive source and later and more successfully with a W x-ray tube. Our measurements suggests that the ratio $\lambda(\text{WK}\alpha_1)/\lambda(\text{MoK}\alpha_1)$ is in error in that combining the new measurement of $W\text{K}\alpha_1$ with Au/W ratio of reference 6 gives quite satis-

factory agreement with the direct route.

Very recently a Tm foil was activated and profiles of the 84 keV line from the decay of Tm-170 were recorded. Measurements of this line were undertaken because it has been used as a secondary energy standard^{7,8} particularly in measurements of pionic x-rays from which pion mass values are deduced.⁹

-
1. R. D. Deslattes, E. G. Kessler, W. C. Sauder, and A. Henins, *Atomic Masses and Fundamental Constants 5*, J. H. Sanders, A. H. Wapstra, eds., Plenum Press, New York, p.48 (1976).
 2. R. D. Deslattes, E. G. Kessler, W. C. Sauder, and A. Henins, *Nat. Bur. Stand. (U.S.), Tech Note 896*, 114 (Jan. 1976).
 3. R. D. Deslattes, Course #LXVIII, "Metrology and Fundamental Constants", Enrico Fermi School of Physics, July 12-24, 1976.
 4. R. D. Deslattes and A. Henins, *Phys. Rev. Lett.* 31, 972 (1973).
 5. J. A. Bearden, A. Henins, J. G. Marzolf, W. C. Sauder and J. S. Thomsen, *Phys. Rev.* 135, A899 (1964).
 6. G. L. Brochert, W. Scheck, and O. W. B. Schult, *Nucl. Instr. and Meth.* 124, 107 (1975).
 7. W. Beer and J. Kern, *Nucl. Instr. and Meth.* 116, 183 (1974).
 8. G. L. Borchert, W. Scheck, and K. P. Wieder, *Z. Naturforsch* 30a, 274 (1975).
 9. R. E. Shafer, *Phys. Rev. D* 8, 2313 (1973).

D. SUMMARY OF REACTOR OPERATIONS

All aspects of reactor operations continued to be excellent. Once again, outstanding on-line performance and full utilization efficiency were achieved. A new major in-core facility located in the center of the reactor was installed and is already being utilized. A summary of the overall operating statistics for this and previous years is presented in the following table.

NBSR Operating Summary

	<u>1974</u>	<u>1975</u>	<u>1976</u>	<u>1977</u>
Reactor Operations to date, MWh	290,000	328,000	396,000	459,000
Reactor Operations for year, MWh	61,000	38,000	68,000	63,000
Hours Reactor Critical	6,000	3,900	6,900	6,400
Number of Days at 10 MW	254	157	283	262
On-line Time at 10 MW	70%	43%	78%	72%
Number of fuel elements used	24	16	24	24
Average U-235 Burnup	54%	53%	55%	56%
Number of Refueling Operations	6	4	6	6
Number of Unscheduled Shutdowns	6	0	2	3
Number of Irradiations	3,000	1,550	2,360	2,255
Irradiations, Total Hours	4,300	1,800	7,250	7,400
Hours per irradiation	1.4	1.2	3	3.3
Number of Visitors	5,000	3,000	7,000	3,000

SUMMARY OF NBS REACTOR HEALTH PHYSICS ACTIVITIES AND SERVICES

T. Hobbs
(Health Physics)

During the past year, the NBS Reactor Health Physics group provided radiation safety surveillance and support services for all radiological activities which occurred at the reactor facility. Among the activities and services performed on a continuing basis by NBSR Health Physics were the following:

SUMMARY OF REACTOR OPERATIONS

- (1) Film badge monitoring of all personnel at the NBSR for radiation exposure control;
- (2) Routine bioassay sampling of all Reactor Operations personnel and, as necessary, other individuals for internal nuclide monitoring and exposure control;
- (3) Radiation surveys of areas and equipment and monitoring of irradiated samples;
- (4) Contamination control at the facility by regular swipe surveys of the radiological laboratories, experimental and maintenance equipment, and other areas of the reactor;
- (5) General sampling and surveillance activities required for NBSR effluent monitoring; personnel exposure control, and environmental monitoring;
- (6) Consultation on all matters involving radiation safety at the NBSR;
- (7) Indoctrination of all new employees in the radiological safety practices and emergency procedures to be followed at the facility; and
- (8) Health physics activities and services of a general nature, such as radioactive waste collection and disposal, laundering and decontamination of anti-contamination clothing, and calibrating radiation survey instruments.

Table 1 presents a summary of NBSR Health Physics surveillance and sampling activities for the five-year period, 1972-1976.

SUMMARY OF REACTOR OPERATIONS

Table 1: Summary of NBS reactor health physics surveillance and sampling activities, 1972-76

<u>Surveillance/ Sampling Activity</u>	<u>1972</u>	<u>1973</u>	<u>1974</u>	<u>1975</u>	<u>1976</u>
Persons monitored with film badges	128	110	150	129	137
Radiation surveys	165	190	170	210	115
Total no. smears taken for contamination control	7,600	6,500	5,300	7,000	7,500
Particulate air samples collected and evaluated	41	51	67	32	12
Gaseous grab samples collected and evaluated	93	147	88	121	59
Samples assayed for tritium by LSC	1,700	1,100	1,365	1,125	925
Bioassay samples collected and evaluated	420	310	437	375	304
Stack cold trap samples for tritium	20	18	18	18	19
Liquid effluent samples collected and evaluated	54	33	33	33	25
Environmental water samples collected and counted	65	82	84	83	84
Primary system samples	19	14	5	6	3
Secondary system samples	360	480	258	410	374
Storage pool samples	13	9	27	17	19

THE NEUTRON ACTIVATION ANALYSIS PROGRAM OF THE
FOOD AND DRUG ADMINISTRATION AT THE NBSR

J. T. Tanner and M. H. Friedman
(Food and Drug Administration, Washington, DC)

The activation analysis unit of the Food and Drug Administration (FDA) is located at the National Bureau of Standards in the Reactor Building. Neutron activation analysis (NAA) has been used by the FDA for trace metal analysis of foods, drugs, hair, laundry aids, and cosmetics. The service of this group is available to anyone within the FDA both in the headquarters laboratory and in the field. The program described below accounts for the main effort of NAA at the FDA during the past year.

Solid waste from farm animals has traditionally been used as cropland fertilizer. In recent years municipal sewage sludge is also being increasingly used as crop fertilizer. The safety with respect to animal and human health of cropland application of sewage sludge is currently the subject of considerable research activity.¹⁻⁵ The broader aspects concerning management of sludge use on land to assure safety and wholesomeness of the food supply have also been discussed.⁶

While an environmentally and energy conscious public seeks to maximize waste production utilization, the volume of solid waste from animal feedlot operations and municipal waste treatment plants is growing steadily. Because of the large amount of undigested protein and high levels of several nutrient elements in these wastes, they are currently being considered as animal feed ingredients to be mixed with the more traditional grain and forage animal feeds.

The practices of feeding "wastelage" (derived from ensiling ground grass hay and manure), or mixtures of dried animal waste and feeder lot rations appears to be commonplace.⁷⁻⁹ Although several states have approved use of animal waste as a feed ingredient for meat producing animals sold in intrastate commerce, the U. S. Food and Drug

SERVICE PROGRAMS

Administration has recently decided to delay issuing proposed guidelines for the safe use of animal waste in feed, because legitimate questions about safety remain unanswered.¹⁰ While sewage sludge has not been formally approved for use in feed by any governmental agency, several federal and state supported projects are studying the effects of feeding sewage sludge to animals on an experimental basis.¹¹

Most feeding studies with animal wastes or sewage sludge being fed to animals have been conducted with the objective of showing the nutritive value of the material being fed, and not for the purpose of determining possible effects on human health.¹² Blattacharga and Taylor¹² have recently reviewed the use of recycled animal waste as a feed ingredient. Their review summarizes available information on: (i) the nutritional value of different kinds of animal waste; (ii) the possible human and animal health hazards from pathogens, drug and nutritional supplement residues, pesticides, and contaminant industrial chemicals, and (iii) the effects of processing methods on the safety of animal waste feed. They also give literature referenced levels of Al, As, B, Ca, Cl, Co, Cu, Fe, K, Mg, Mn, Na, P and Zn in poultry, swine, and cattle manure with respect to the nutrient composition of these wastes. Their review indicates that little work has been done to determine typical trace element content of animal wastes for other elements. Nor has much work been done to determine whether trace elements accumulate in edible tissue, or edible products, from animals fed diets containing animal wastes. Studies of the potential for tissue accumulation in steers of As, have been done in which feeding of broiler litter containing As as a feed additive residue resulted in tissue levels proportional to the amount of As ingested.¹³ Smith and Calvert¹⁴ have recently reported on the levels of Cu, Zn, Fe, Cd, and Pb in diets containing 88% corn meal supplemented with either cottonseed meal (control diet) or dried poultry excreta (DPE), and on the effects of accumulation of these metals in liver, kidney, muscle, and blood from steers fed the two diets. Reported levels of Zn, Cu, and Fe were

2-4 higher in the DPE diet than in the control diet, but were essentially the same for Cd and Pb. The levels of Cu in liver and Fe in kidney were significantly higher for steers on the DPE diet. Otherwise no other significant differences in tissue levels were seen. The levels of elements in the bones of the animals on the two diets were not reported.

In another recent study Furr, et al.¹⁵ fed swiss chard grown on soil treated with municipal sewage sludge to guinea pigs for 28 days. The swiss chard had elevated levels of many trace metals compared to swiss chard grown on a control soil containing no sludge. Analyses of liver, kidney, muscle, adrenal and spleen from the guinea pigs showed increased deposition of specific elements (including As, Cd, Ce, Co, Cr, Cs, Cu, Hg, K, La, Mg, Mn, Na, Pb, Sb, Sn, Ti, V, and W) in tissues from animals fed the sewage sludge amended swiss chard compared to those fed the control swiss chard. Depending on the element and the tissue, increased deposition ranged up to the high of a 10.8 fold increase for Sn in the kidney. The authors concluded that similar feeding studies over longer time periods for a greater number of animals are needed.

Numerous papers have appeared in the literature reporting the elemental content of sewage sludges for various numbers of elements.^{1-5,15-17} However, the most comprehensive report is that of Furr, et al.,¹⁵ who reported the levels of 68 elements in sewage sludges from 16 American cities and in a dehydrated bagged commercial cow manure product. The mean value for the 16 cities for each element determined by Furr, et al. is shown in table 1. The analytical techniques for the 68 elements included spectrophotometry, neutron activation, emission spectroscopy, spark source mass spectrometry, anode stripping voltammetry, furnace atomic absorption, flameless atomic absorption and fluorescence. In that study each element was determined by the alternate analytical technique. The authors state that the samples were air-dried, mixed in a Lucite twin shell blender, and

subsampled for analysis. However, no precision data is reported to indicate the homogeneity of the samples analyzed.

The macroelement (Ca, P, Mg, S, K, Na, and Cl) and the microelement (Co, Cu, I, Fe, Mn, Se and Zn) contents of traditional animal feeds and mineral supplements are available in the literature along with the dietary levels of most of these elements required for normal growth in cattle, horses, sheep, swine, rats and dogs.^{18,19} However, little information is available on typical levels of many other elements in traditional animal feeds.

The purpose of our study was to determine the levels of as many elements as possible in typical dried animal wastes having a documented history and to compare these levels with those of the same elements in animal feeds and sewage sludges. From this comparison we hoped to develop the data necessary to support conclusions about the desirability or relative safety of using animal wastes and sewage sludges and animal feed ingredients. Such data should assist in choosing among the various possible alternatives for beneficial use of animal wastes and sewage sludge, including cropland application, conversion to methane, and animal feed ingredients.

1. Samples

The samples analyzed were all received from the same source (Colorado State University) and included: (I) A typical feedlot ration without animal waste products added. The dry weight composition of this ration was 70% corn, 3% hay, 5% beet pulp, 20% corn silage and 2% mineral supplement; (II) oven dried cattle manure from feeder lot heifers fed a low fiber diet containing 59% corn, 2% alfalfa hay, 3% molasses, 33% corn silage and 3% mineral supplement; (III) oven dried cattle manure from feeder lot heifers fed a high fiber diet containing 24% corn, 29% alfalfa hay, 3% molasses, 41% corn silage and 3% mineral supplement; (IV) a commercial high-protein feeder lot animal waste product similar to (III) in which a portion of the fiber and ash was

removed and the product was pelletized; (V) dried poultry waste with litter consisting of wood shavings mixed with excreta from hens fed a layer ration; (VI) dried poultry waste from caged laying hens without any litter; (VII) dried sewage sludge from Denver Metro District. These samples correspond to columns I through VII respectively in table 1.

2. Sample Preparation

The feedlot ration was analyzed without further homogenization. Portions of the animal wastes and sludge samples (100 g) were initially blended with a blender and subsamples were analyzed by neutron activation analysis (NAA), flame atomic absorption spectrometry (AAS), and anodic stripping voltammetry (ASV) as described below. However, because most of the waste samples were still visibly inhomogeneous, additional portions of the as received unhomogenized waste and sludge samples (70 to 105 g each) were mixed in the ratio of 4 parts distilled deionized water to 1 part dry material and homogenized at high speed with a homogenizer equipped with sonic probe type generator until a homogeneous slurry was obtained (usually about 5 minutes). The slurries were then freeze dried. The resulting dry samples were analyzed using AAS, ASV, NAA, and induction coupled plasma optical emission spectroscopy (ICP). Details of the NAA analyses were reported in last years NBSR report and will not be repeated here. Information about the other analytical methods may be found elsewhere.²⁰⁻²³

3. Results

The analytical results from determination of 30 elements in the animal feeder lot ration, animal wastes, sewage sludge, and the NBS Reference Materials Orchard Leaves, Bovine Liver, and Spinach are reported in table 1. Values are reported only for those elements whose concentrations fell in the reliable quantitation range for the method indicated. In the case of the highly toxic elements Be and Hg less-

than values are reported when quantitation was not possible.

The mean levels of the same elements in sewage sludges from the 16 city study reported by Furr, et al.¹⁵ are also tabulated in table 1 for comparison with the data obtained in this study.

Among the animal wastes, the low fiber diet manure has a slightly lower content of most metals than the high fiber diet manure. The processed waste pellets, which were derived from a high fiber diet manure, also contained a lower content of most metals than did the high fiber diet manure. During processing of the pellets, some of the fiber and ash was removed from the manure, which probably accounts for the lower metals content.²⁴ In general the poultry waste without litter contains higher levels of most elements than the poultry waste with litter. The lower levels in waste with litter probably are due to dilution by the litter (mostly wood chips).

The order of magnitude of the levels of elements found in the Metro Denver sewage sludge compares well with the average level calculated from the 16 city study by Furr, et al.¹⁵ With a few exceptions the levels of elements found in the NBS Reference Materials agree well with the certified or uncertified NBS values.

Whenever comparisons of the levels found in the same sample by different determinative step techniques are possible the results are generally in good agreement. Two exceptions are the lower Se and Sb values obtained by AAS compared to NAA. Because AAS analyzes only the acid soluble portion of the sample while NAA analyzes the whole sample, these analyzes indicate that part of the Se and Bb is associated with the acid-insoluble portion of the samples.

Considering the gross inhomogeneity of the samples as received by the laboratory, including the wood chips, feathers, undigested grain, small rocks, and other identifiable particles normally present in animal waste and sewage sludge, the precision of the analytical results and the agreement of analyses of a given sample by several techniques are quite good. The extensive amount of data does not permit re-

porting precision data for individual elements by all techniques.

One problem with trying to achieve homogeneity with the waste and sludge samples is that abrasion of the homogenizer blade metal by small rocks or other solid material can contaminate the sample. Homogenization of the waste and sewage sludge samples with the homogenizer resulted in measurably higher levels of Co, Cr, and Ni compared to the unhomogenized samples. Thus the values reported for Co and Cr in table 1 are for blended samples. The blender does not produce the shear action of the homogenizer and thus does not produce measurable contamination due to abrasion.

4. Discussion

The levels of the macroelements Ca, Cl, Mg, P, K, and Na, and of the microelements Co, Cu, Fe, Mn, Se, and Zn found in the animal wastes and sewage sludge are considerably above the levels of these elements reported in the literature¹⁸ as being necessary for normal growth in cattle, horses, sheep, swine, rats and dogs. The levels of As, Cd, Co, Cr, Cu, Fe, Mn, Mo, Pb, Sn, Ti, V, and Zn are all at least a factor of 5 higher in animal wastes than in the feeder lot ration. The levels of some of these may be high enough to raise concern about continuous use of animal wastes as a animal feed ingredient. The levels of Al, As, Cd, Co, Cr, Cu, Eu, Fe, Hg, Pb, Sb, Sn, Ti, and Zn are all at least a factor of 100 higher in sewage sludge than in the feeder lot ration. Toxicity could be expected to occur in some animals if feeds were fed having the levels of Cd, Cr, Cu, Fe, Mn, Pb, Se and Zn shown in table 1 for sewage sludge.^{19,25,26} Whether any of the above elements would concentrate in animal tissues, similar to that demonstrated in previous studies^{1,6,13,14} sufficiently to present a human health hazard can only be determined by appropriate feeding studies with animal wastes or sewage sludge as feed ingredients. It is known that Cd accumulates in beef liver and kidney²⁷ and that the current level of Cd in the American food supply already approximates

SERVICE PROGRAMS

Table 1. Elemental Content of Animal Feed, Animal Waste, Processed Waste Pellets, Sewage Sludge, and Reference Materials a, b
(ppm in dried samples)

Element	Analytical Method	I		II		III		IV		V		VI		VII		16 Cities c			Reference Materials d			
		Feeder Lot	Ration	Cattle Manure Low Fiber Diet	Cattle Manure High Fiber Diet	Processed Cattle Waste Pellets	Poultry Waste With Litter	Poultry Waste Without Litter	Poultry Waste	Metro Denver Sewage Sludge	Metro Denver Sewage Sludge	NBS Orchard Leaves	NBS Bovine Liver	NBS Spinach	NBS	NBS	NBS	NBS	NBS			
As	AAS	0.10	0.88	2.2	0.60	0.57	0.66	8.1	14.3	0.50	0.16	(11+2)	(.055)	(.15+-.05)								
Ba	NAA	18.	105.	305.	70.	54.	57.	1066.	621.	45.	<45.	NV	NV	<30.	<45.							
Be	ICP	<0.03	<0.03	<0.03	<0.03	<0.03	<0.03	<0.45	<8.5	<.06	<.06	NV	NV	<.06	<.06							
Br	NAA	10.	34.	29. d	66.	9. d	31.	30. d	45.5	11.	11.	(10)	NV	11.	48.							
Cd	AAS ASV ICP	NA 0.05 <1.3	NA 0.28 <1.3	NA 0.24 <1.3	NA 0.14 <1.3	NA 0.42 <1.3	NA 0.58 <1.3	26.0 NA 25.4	104.	NA NA 25.4	NA NA 25.4	NA NA 25.4	NA NA 25.4	NA NA 25.4	NA NA 25.4	NA NA 25.4	NA NA 25.4	NA NA 25.4	NA NA 25.4	NA NA 25.4	NA NA 25.4	
Co e	NAA	0.10	1.7	2.2	1.1	2.0	1.2	7.1	9.6	0.13	0.29	(.2)	(.18)	(1.5)								
Cr e	NAA	0.75	20.	31.	5.	6.	4.9	280.	1441. f	2.7	<.4	(2.3)	NV	(4.6+0.3)								
Cu	AAS ICP	3.0 2.6	24.0 22.3	21.0 19.5	18.7 15.9	30.7 30.6	20.0 18.1	816. 905.	1346.	11.6 11.4	185. 210.	(12+1)	(193+10)	(12+2)								
Eu	NAA	0.012	0.12	0.4	0.06	0.03	0.07	0.6	3.7	<.05	0.003	(.027)	NV	<.02	(.027)							

SERVICE PROGRAMS

2.

Table 1. (Continued)

Element	Analytical Method	I		II		III		IV		V		VI		VII		C					
		Feeder Lot	Ration	Cattle Manure Low Fiber Diet	Cattle Manure High Fiber Diet	Processed Cattle Waste Pellets	Poultry Waste With Litter	Poultry Waste Without Litter	Metro Denver Sewage Sludge	16 Cities Average Sewage Sludge	16 Cities Average Sewage Sludge	16 Cities Average Sewage Sludge	16 Cities Average Sewage Sludge	16 Cities Average Sewage Sludge	16 Cities Average Sewage Sludge	16 Cities Average Sewage Sludge	16 Cities Average Sewage Sludge	16 Cities Average Sewage Sludge	16 Cities Average Sewage Sludge	16 Cities Average Sewage Sludge	
Hg	NAA	<0.01		0.05	<0.03	<0.09	0.06	<0.04	7.8	8.6	NA	NA	NA	NA	NA	NA	NA	NA	NA	NA	
La	NAA	0.5		5.0	18.6	3.2	5.5	9.	56.	35.7	1.2 (1.2)	0.07 NV	<.7 (.37)								
Mn	AAS ICP NAA	16.8 17.2 17.		117. 111. 115.	161. 158. 185.	100. 90. 92.	166. 167. 176.	242. 246. 273.	220. 222. 262.	194.	81.3 80.0 85.0 (91±4)	10.4 9.7 11.5 (10.3±1.0)	155. 157. 171. (165±6)								
Mo	ICP	<2.5		29.9	49.2	15.6	5.0	7.2	84.9	14.3	<5. NV	<5. (3.2)	<5. NV								
Pb	AAS ASV ICP	NA 0.36 <2.5		NA 2.10 3.6	NA 3.28 5.9	NA 3.29 4.5	NA 2.08 2.5	NA 3.45 5.8	950. NA 885.	1832.	52.6 NA (45±3)	NA NA (-34±.08)	NA 1.25 <3.5 (1.2±0.2)								
Rb	NAA	2.3		17.	46.	15.	7.0	12.	42.	32.6	10.5 (12±1)	17.8 (18.3±1.0)	10. (12.1±0.2)								
Sb	AAS NAA	<0.08 <0.03		<0.08 0.14	<0.08 0.26	<0.08 0.10	<0.08 0.10	0.10 0.19	7.07 11	10.6	NA 2.5 (2.7)	NA <.02 NV	NA 0.05 (.04)								
Sc	NAA	0.065		0.54	1.41	0.44	0.21	0.44	2.6	2.5	<.004 NV	<.004 NV	0.16 (.16)								
Se	AAS NAA	0.19 0.21		0.35 0.5	0.32 0.6	0.36 0.7	0.38 0.5	0.66 0.9	4.57 7.2	3.1	0.07 0.20 (.08±.01)	1.06 1.1 (1.1±0.1)	0.025 <.6 NV								
Sn	ICP	<.8		4.73	7.40	3.74	2.04	4.05	93.5	216.	<1.5 NV	<1.5 NV	3.1 NV								
Tl	ICP	8.1		54.9	129.	50.0	12.1	27.4	398.	2331.	7.6 NV	<0.15 NV	16.5 NV								

SERVICE PROGRAMS

3.

Table 1. (Continued)

Element	Analytical Method	I		II		III		IV		V		VI		VII		16 Cities		Reference Materials ^d		
		Lot	Ra-ion	Manure	Low Fiber Diet	Cattle Manure	High Fiber Diet	Processed Cattle Waste Pellets	Poultry Waste With Litter	Poultry Waste Without Litter	Poultry Waste	Metro Denver Sewage Sludge	Poultry Waste Without Litter	Poultry Waste With Litter	16 Cities Average Sewage Sludge	NBS Leaves	NBS Orchard	NBS Bovine Liver	NBS Spinach	
V	NAA	0.57	3.2	3.2	8.0	3.0	3.9	4.3	20.	40.6	0.8	0.46	1.7							
Zn	AAS	20.0	115.	86.	76.7	155.	158.	158.	1672.	2132.	25.9	145.	59.7							
	ICP	20.9	101.	79.2	69.2	142.	143.	143.	1717.		23.1	135.	48.							
	NAA	19.0	114.	110.	80.	133.	133.	141.	1978.		23.	124.	48.							
											(25+3)	(130+10)	(50+2)							
% (or ppm if noted) in dry weight sample																				
Al	ICP	0.023	0.17	0.38	0.18	0.047	0.07	0.07	1.12	1.83	157. ppm	<15ppm	482. ppm							
	NAA	0.065	0.51	1.56	0.28	0.087	0.20	0.20	1.96		383. ppm	65. ppm	881. ppm							
Ca	ICP	0.46	2.03	2.16	2.32	4.88	9.42	9.42	5.90	3.62	2.63	140. ppm	1.62							
	NAA	0.31	1.85	1.78	1.90	3.70	7.10	7.10	4.50		2.15	309. ppm	1.46							
											(2.09+3)	(123. ppm)	(1.35+ .03)							
Cl	NAA	0.17	1.01	0.85	0.71	0.35	0.65	0.65	0.71	0.38	675. ppm	2530. ppm	6290. ppm							
											(700. ppm)	(2600. ppm)	(6400. ppm)							
Fe	AAS	0.023	0.22	0.51	0.20	0.073	0.18	0.18	1.51	3.06	246. ppm	253. ppm	494. ppm							
	ICP	0.024	0.22	0.48	0.20	0.071	0.17	0.17	1.61		235. ppm	254. ppm	478. ppm							
	NAA	0.025	0.27	0.65	0.21	0.077	0.18	0.18	1.73		259. ppm	257. ppm	510. ppm							
											(300 ppm)	(270+20)	(550+20)							

Table 1. (Continued)

4.

Element	Analytical Method	I		II		III		IV		V		VI		VII		Reference Materials ^d		
		Feeder Lot	Ration	Cattle Manure Low Fiber	Cattle Manure High Fiber	Cattle Manure Diet	Processed Cattle Waste Pellets	Poultry Waste With Litter	Poultry Waste Without Litter	Poultry Waste With Litter	Poultry Waste Without Litter	Metro Denver Sewage Sludge	Average Sewage Sludge	16 Cities	NDS Orchard Leaves	NDS Bovine Liver	NDS Spinach	
K	NAA	0.80	1.94	4.70	2.80	1.80	2.30	1.40	1.22	1.42	7420 ppm	3.73	(1.47±.03)	(9700±600) ppm	(3.56±.03)			
Mg	AAS	0.156	0.46	0.42	0.50	0.26	0.46	0.35	0.60	0.53	566 ppm	0.84	0.49	613 ppm	0.70			
	ICP	0.155	0.45	0.41	0.50	0.26	0.43	0.35		0.63	94.9 ppm	0.98	0.63	94.9 ppm	0.98			
	NAA	0.180	0.55	0.63	0.68	0.28	0.65	0.74		(.62±.02)	(603 ppm)	NV						
Na	NAA	0.088	0.69	0.91	0.47	0.21	0.57	0.44	0.44	1.55	2438	1.44	(82±6)	(2430±130 ppm)	NV			
P	ICP	0.29	0.61	0.39	0.41	0.89	1.34	1.46	1.56	0.156	0.98	0.45	(.21±.01)	NV			(.55 ±.02)	

Notes: ^a Abbreviations: AAS - atomic absorption spectroscopy
ASV - Anodic stripping voltammetry
ICP - Induction coupled plasma
NAA - neutron activation analysis
N.A. - not analyzed
N.V. - no NBS value available

^b All values for samples I through VII average of triplicate analyses

^c Calculated mean from Reference 15 values. See Reference 15 for method used.

^d NBS values in parentheses

^e Waring blended samples. Co and Cr contamination from Polytron homogenizer prevented analysis of samples homogenized with Polytron

^f Milwaukee 14,000 value excluded in calculating 16 cities mean for Cr

SERVICE PROGRAMS

the World Health Organization maximum tolerable intake.⁶ Multiple recycling of animal wastes should also be studied for the effects on animal health and tissue elemental levels. Assuming a more or less constant concentration factor for each element with each pass through the animal and a more or less constant fractional absorption of each element during each pass, the potential exists for significantly elevated absorption for most elements after only a few passes. Whether multiple recycling of animal wastes actually results in elevated tissue elemental levels can only be determined by appropriate feeding studies.

Any widespread use of animal wastes or sewage sludge as animal feed ingredients could be expected to be accompanied by a need for periodic multielement and multiresidue organic analysis of the mixture being fed. Because of the gross variability, both with time and location, of animal wastes and especially sewage sludge, obtaining representative samples for analysis, which accurately reflect the average level of each element or residue being fed, would be a difficult problem. The cost of such representative analyses would detract from the economic gain of using these waste products as animal feed ingredients.

The results of this work indicate that the levels of most inorganic elements are considerably higher in animal wastes and sewage sludge than in traditional animal feeds. These findings suggest that the safety of using animal wastes, sewage sludge, and multiple recycled animal wastes, both with respect to animal and human health, should be thoroughly investigated by animal feeding studies.

Acknowledgement

This report is a condensed version of paper submitted to Environmental Science and Technology entitled, "Multielement Analysis of Animal Feed, Animal Wastes, and Sewage Sludge," by S. G. Capar, J. T. Tanner, M. H. Friedman, and K. W. Boyer from the Division of Chemistry and Physics, U. S. Food and Drug Administration, Washington, DC, 20204.

1. A. F. Furr, C. S. Sloewsand, C. A. Bache, and D. J. Lisk, "Study of Guinea Pigs fed Swiss Chard Grown on Municipal Sludge-Amended Soil," *Archives of Environmental Health*, 31, 87 (1976).
2. M. B. Kirkham, "Trace Elements in Corn Grown on Long-Term Sludge Disposal Site," *Environ. Sci. Technol.*, 9, 765 (1975).
3. W. J. Garcia, C. W. Blessin, G. E. Inglett, and R. O. Carlson, "Physical-Chemical Characteristics and Heavy Metal Content of Corn Grown on Sludge-Treated Strip-Mine Soil," *J. Agr. Food Chem.*, 22, 810 (1974).
4. T. D. Hinesly, R. L. Jones, E. L. Ziegler, and J. J. Tyler, "Effects of Annual and Accumulative Applications of Sewage Sludge on Assimilation of Zinc and Cadmium by Corn (*Zea mays* L.)," *Environ. Sci. Technol.*, 11, 182 (1977).
5. A. K. Furr, W. C. Kelly, C. A. Bache, W. H. Gutenmann, and D. J. Lisk, "Multielement Absorption by Crops in Pots on Municipal Sludge-Amended Soil," *J. Agric. Food Chem.*, 24, 889 (1976).
6. C. F. Jelinek and G. L. Braude, "Management of Sludge Use on Land, FDA Considerations," Presented at Third National Conference on Sludge Management, Disposal and Utilization, Miami, Florida, December 14-16, 1976.
7. E. F. Knight, T. A. McCaskey, W. B. Anthony and J. L. Walters, "Microbial Safety of Fermented Manure-Blended Feed," Presented at 71st Annual Meeting American Dairy Science Association, North Carolina State University, Raleigh, N. C., June 20-23, 1976.
8. L. W. Smith, "Waste Utilization as Animal Feed in the U. S.," Conference Proceedings: *Commercial Uses of Wastes as Animal Feed*, p. 185, Toronto, April 24-25, 1975.
9. L. W. Smith, "Animal Waste Reuse-Nutritive Value and Potential Problems from Feed Additives - A Review," Agricultural Research Service, USDA, Publication APS 44-224, February 1971.
10. J. C. Taylor, "Provisions of State and Federal Regulations on Refeeding," presented at the Seminar on Feedlot Manure Recycling for Nutrient Recovery, East Central University, Ada, Oklahoma, April 7, 1977.
11. G. S. Smith and H. D. Sivinski, "Recycling Sewage Solids as Feedstuffs for Livestock," presented at the Third National Conference on Sludge Management, disposal and Utilization, Miami, Florida, December 14-16, 1976.

SERVICE PROGRAMS

12. A. N. Bhattacharya and J. C. Taylor, "Recycling Animal Waste as a Feedstuff: A Review," *J. Animal Science*, 41, 1438 (1975).
13. C. C. Calvert, "Feed Additive Residues in Animal Manure Processed for Feed," *Feedstuffs*, 45, 32 (1973).
14. C. C. Calvert and L. W. Smith, "Heavy Metal Differences in Tissues of Dairy Steers Fed Either Cottenseed Meal or Dehydrated Poultry Excreta Supplements," Presented at American Dairy Science Association 71st Annual Meeting, Raleigh, N. C., June 1976.
15. A. K. Furr, A. W. Lawrence, S. S. C. Tong, M. C. Grandolfo, R. A. Hofstader, C. A. Bache, W. H. Gutenmann and D. J. Lisk, "Multi-element and Chlorinated Hydrocarbon Analysis of Municipal Sewage Sludges of American Cities," *Environ. Sci. Technol.*, 10, 683 (1976).
16. A. Chattopadhyay, "Optimal Use of Instrumental Neutron and Photon Activation Analyses for Multi-element Determinations in Sewage Sludges," *Proceedings of 1976 International Conference on Modern Trends in Activation Analyses*, p. 493, Munich, Germany, 13-17 Sept., 1976.
17. D. S. Scott and Harry Horlings, "Removal of Phosphates and Metals from Sewage Sludge," *Environ. Sci. Technol.*, 9, 849 (1975).
18. E. S. E. Hafez and I. A. Dyer, Editors, *Animal Growth and Nutrition*, p. 385 Lea and Febiger, Philadelphia, (1969).
19. *Nutrient Requirements of Domestic Animals*, 5th Rev. Ed. National Academy of Sciences, Washington, D. C., (1976).
20. J. W. Jones, Gajan, K. W. Boyer and J. A. Fiorino, *J.A.O.A.C.*, 60, in press (1977).
21. J. A. Fiorino, J. W. Jones and S. G. Capar, "Sequential Determination of Arsenic, Selenium, Antimony, and Tellurium in Foods via Rapid Hydride Evolution and Atomic Absorption Spectrometry," *Anal. Chem.*, 48, 120 (1976).
22. M. H. Friedmann and J. T. Tanner, "An Automated Activation Analysis Data Acquisition System," *J. Radioanal. Chem.*, 25, 269 (1975).
23. M. H. Friedmann, E. Miller and J. T. Tanner, "Instrumental Neutron Activation Analysis for Mercury in Dogs Administered Methylmercuric Chloride: Use of a Low Energy Photon Detector," *Anal. Chem.*, 46, 236 (1974).
24. G. M. Ward, personal communication, March 1976.
25. L. A. Maynard, and J. K. Loosli, *Animal Nutrition*, 6th Ed., p.193, McGraw-Hill, N. Y., (1969).

26. J. J. Dulka and T. H. Risby, "Ultratrace Metals in Some Environmental and Biological Systems," *Anal. Chem.*, 40, No. 8., 640A (1967).
27. M. R. S. Fox, "Cadmium Metabolism - A review of Aspects Pertinent to Evaluating Dietary Cadmium Intake by Man," in *Trace Elements in Human Health*, A. A. Prasad, Ed., p 26, Academic Press, N.Y., (1976).

ACTIVATION ANALYSIS PROGRAM OF THE U. S. GEOLOGICAL SURVEY

J. J. Rowe, P. A. Baedeker and J. W. Morgan
(U. S. Geological Survey, Reston, VA)

The Geological Survey is actively involved in a large scale program providing analytical data for coals from various parts of the U. S. Coals are being analyzed for Na, Fe, As, Ba, Br, Co, Cr, Cs, Hf, Rb, Sb, Se, Ta, Th, Zn, W, Sc, La, Ce, Nd, Sm, Eu, Tb, Yb and Lu at the rate of more than 1,000 samples per year. Other geochemical studies involve neutron activation analysis of about 1,000 samples of rocks and minerals per year.

The rare-earth elements have been useful in characterizing the magmatic history and crystallization-differentiation for use in wide variety of studies of ore deposition, alteration and trace element distribution in coexisting minerals. The computer generated reports of analysis now include a plot of chondrite: sample rare earth ratios as shown in figures 1 and 2,

The analytical procedure routinely determines uranium, via Np-239 to apply corrections for fission product interference. These corrections are processed via a modification of the computer data reduction procedure of Baedeker. If the uranium content is low or near detection limits, the correction is negligible. For higher uranium contents an asterisk indicates those results which have a fission product correction of 20% or more of the concentration of that element.

A study was made of the effects of thermal and epithermal neutron irradiation of rocks using both Ge(Li) and LEPD detector systems. The use of epithermal irradiation improved the determination of tungsten, cesium, rubidium, barium, uranium and thorium in rocks, minerals and coals.

SERVICE PROGRAMS

instrumental neutron activation analysis summary report

submitted by: Simon & Wright analyst: Louis J. Schwarz

job number:

irradiation number: 221

sample description:

sample:	0103972 75-35 ()	0103973 75-36 (a)	0103974 75-46 (b)	0103974 75-46 (a)	0103974 75-46 (b)	BCR-1 (a)	BCR-1 (b)
weight:	0.10866	0.15093	0.10318	0.10581	0.11694	0.11604	0.11605
FE (%)	8.68	13.55	13.47	11.43	11.79	12.34	12.19
sigma (PPM)	1(6)	1(2)	1(2)	1(2)	1(2)	1(2)	1(2)
BA (PPM)	148	376	844	703	735	581	614
sigma (PPM)	24(1)	4(1)	5(1)	5(1)	5(1)	5(1)	5(1)
CO (PPM)	44.8	36.8	72.2	42.3	43.4	43.4	48.4
sigma (PPM)	1(6)	1(2)	1(2)	1(2)	1(2)	1(2)	1(2)
CR (PPM)	298.4	37.1	39.5	120.4	125.9	163.3	155.7
sigma (PPM)	1(6)	3(2)	3(2)	2(2)	1(2)	1(2)	1(2)
CS (PPM)	< 1.4	< 1.0	< 0.5	< 1.1	< 1.0	< 1.0	< 1.2
sigma (PPM)	0(6)	0(2)	20(1)	0(2)	0(2)	0(2)	0(2)
HF (PPM)	4.0	11.2	10.7	6.7	7.1	5.6	6.5
sigma (PPM)	1(6)	2(2)	2(2)	2(2)	2(2)	2(2)	3(2)
RB (PPM)	< 34	30	18	19	22	23	28
sigma (PPM)	0(6)	12(1)	20(1)	13(1)	17(1)	0(1)	0(1)
SB (PPM)	< 0.8	< 0.8	< 0.8	< 0.8	< 0.8	< 0.8	< 1.0
sigma (PPM)	0(6)	0(2)	0(2)	0(2)	0(2)	0(2)	0(2)
TA (PPM)	1.26	2.24	3.12	1.78	1.80	2.00	1.95
sigma (PPM)	3(7)	3(3)	4(3)	4(3)	4(3)	3(3)	4(3)
TH (PPM)	1.3	4.1	4.0	3.2	3.6	1.9	2.4
sigma (PPM)	4(6)	4(2)	4(2)	5(2)	5(2)	8(2)	5(1)
ZN (PPM)	172	224	234	185	194	198	192
sigma (PPM)	1(6)	1(2)	1(2)	1(2)	1(2)	1(2)	1(2)
ZR (PPM)	278	286	439	341	360	386	352
sigma (PPM)	10(3)	15(2)	14(2)	11(2)	17(2)	10(2)	11(2)
SC (PPM)	36.51	38.28	38.72	38.72	40.22	40.88	40.30
sigma (PPM)	1(6)	1(2)	1(2)	1(2)	1(2)	1(2)	1(2)
LA (PPM)	15	53	55	28	39	34	25
sigma (PPM)	5(6)	8(1)	11(1)	17(1)	5(1)	5(1)	16(1)
CE (PPM)	37	150	149	91	92	90	89
sigma (PPM)	1(6)	1(3)	2(3)	2(3)	2(3)	2(3)	2(3)
ND (PPM)	31	77	75	57	42	48	57
sigma (PPM)	12(3)	9(1)	10(1)	15(1)	15(1)	14(1)	12(1)
SM (PPM)	6.3	20.2	21.7	11.6	12.3	12.3	12.5
sigma (PPM)	7(1)	7(1)	5(1)	10(1)	10(1)	6(1)	6(1)
EU (PPM)	2.01	5.55	5.59	5.27	3.54	5.57	3.52
sigma (PPM)	1(3)	1(3)	1(3)	1(3)	1(3)	1(3)	1(3)
GD (PPM)	6.3	23.1	26.3	13.7	13.8	13.7	13.4
sigma (PPM)	10(1)	4(1)	6(1)	5(1)	6(1)	6(1)	6(1)
TR (PPM)	0.90	3.33	3.44	1.42	1.94	2.04	1.85
sigma (PPM)	5(5)	2(2)	2(2)	3(2)	4(2)	3(2)	3(2)
TM (PPM)	0.36	1.40	1.51	0.82	0.91	1.85	1.56
sigma (PPM)	19(1)	4(1)	4(1)	5(1)	5(1)	5(1)	5(1)
YH (PPM)	1.7	9.2	9.3	5.4	5.6	5.4	5.7
sigma (PPM)	3(6)	2(1)	3(1)	3(1)	3(1)	3(1)	4(1)
LU (PPM)	0.53	1.57	1.69	0.46	0.90	1.93	0.96
sigma (PPM)	3(6)	4(1)	2(1)	2(1)	2(1)	2(1)	2(1)

SERVICE PROGRAMS

The analytical facilities of the U.S.G.S. in Reston, Va. consists of 5 Ge(Li) detectors (18%-2.0 keV; 12%-2.3 keV; 11%-1.9 keV; 11%-1.7 keV; 12%-1.7 keV) and 3 planar intrinsic germanium detectors. All detectors are equipped with sample changers. Samples are counted twice on planar and Ge(Li) detectors to utilize the maximum gamma and x-ray spectra. Instruments operate 24 hours/day, seven days/week.

Method developments in process include group separations of rare earths to permit the analysis of ultramafics: separations of Cs, Rb, Ta, As and Sb for application to studies of submarine basalts and methods for the analysis of fluid inclusions.

THE USE OF ACTIVATION ANALYSIS IN SCIENTIFIC CRIME DETECTION BY THE FEDERAL BUREAU OF INVESTIGATION

J. W. Kilty
(Federal Bureau of Investigation, Washington, D. C.)

The FBI Laboratory continues to use neutron activation analysis (NAA) to analyze for antimony and barium in cotton swabs which have been applied to the hands of suspected shooters. The reliability of NAA for these measurements in materials which are often heavily contaminated with soil, blood, grease, etc., makes it our method of choice. From July 1976, to June 1977, the FBI Laboratory has conducted these examinations on over 1,000 persons.

NAA is used extensively in doing compositional analyses of lead, copper, steel and aluminum. A recent application of the technique has been to analyze small ore samples for gold, silver and platinum. The concentrations of these metals in these ores is so low and the amount of sample so limited that the conventional assay methods are inadequate.

The value of NAA in conducting trace element analysis in materials such as synthetic fibers and biologicals is well known.

The FBI Laboratory considers NAA to be a valuable tool in determining elemental composition of evidentiary materials.

ATF'S ACTIVATION ANALYSIS PROGRAM

J. M. Hoffman, W. Kinard and L. Reid
(U. S. Treasury Department, Washington, DC)

Neutron Activation Analysis (NAA) continues to be a valuable tool in the crime laboratory. The ability to analyze microscopic amounts of evidentiary material non-destructively is a distinct asset in those cases where evidentiary materials must be preserved for courtroom presentation.

During the fiscal year 1977, the following types of evidentiary materials were examined by NAA. The irradiation time shown represents the total reactor utilization for samples of each type.

<u>Sample/Type</u>	<u>Number of Samples</u>	<u>Total Irradiation Time (Hours)</u>
Hair	40	136
Paint	17	42
Gunshot Residue	96	2
Explosives	8	4
Glass	6	1

In addition to our use of NAA for forensic purposes, wines and distilled spirits were examined for their trace elemental content using the NAA technique. This work was done in connection with our regulatory enforcement program of monitoring the composition of alcohol containing products.

On-going research using NAA includes the examination of writing inks for the purpose of identifying the product, its manufacturer, and the date of the ink's production. This is accomplished by tagging the inks during the production process with selected elements amenable to detection by NAA and other techniques.

The value of NAA in examining paints and human hair is being critically assessed. Additional analytical data will be accumulated during FY78 for this purpose and it is intended that this work will be reported in mid-1978.

TRACE ELEMENTS IN THE ENVIRONMENT
AND RADIOACTIVE DECAY STUDIES

W. H. Zoller, G. E. Gordon and W. B. Walters
(Department of Chemistry, University of Maryland,
College Park, MD)

Our group has made extensive use of the NBSR for the irradiation of numerous samples for trace-element analysis using instrumental neutron activation analysis (INAA). We have had our computer-based analyzer system and two Ge(LI) γ -ray detectors at the Reactor for periods of several weeks during the last year to count short-lived radioactive products. Most of the other samples are returned to the university for counting long-lived activities.

1. Urban Air Pollution Studies

For several years we have been using instrumental neutron activation analysis (INAA) at the NBS reactor, augmented with other analytical methods, to measure concentrations of 30 to 40 elements in atmospheric particulate material and in suspended particles released from several classes of major air pollution sources. In past years we have measured size distributions and compositions of particles released by two coal-fired power plants, an oil-fired power plant, three municipal incinerators, two sewage-sludge incinerators, and by vehicles passing through the Baltimore Harbor Tunnel.

In order to determine if the particles from these sources can account for the composition of material present in urban atmospheres, we analyzed samples collected from ambient air in Washington, D. C. during the Summer of 1974. We then "resolved" the average elemental concentration pattern of Washington aerosols into six components: soil, marine aerosols (sea salt), and particles released by coal and oil-fired plants, refuse incineration and motor vehicles. Except for marine aerosols, the elemental compositions of particles from these sources, were obtained mainly from our own studies that made use of the NBS reactor, including the soil component, which was an average of

SERVICE PROGRAMS

28 soil samples from around the Washington area. The strengths of the six sources were determined by a weighted least-squares fit to the observed concentrations of eight elements listed at the top of table 1. Columns 2-7 show the predicted contributions of each source to the atmospheric concentration of each element. Columns 8 and 9 list the total predicted concentrations and the observed concentrations and the final column gives the observed/ predicted ratio. The first eight elements are forced to fit rather well by the least-squares procedure. Most of the 15 non-volatile elements among the remaining 19 are fitted to within a factor of two - a considerable improvement over previous attempts to account for these very minor, but important elements in the atmosphere.

Despite the generally good fits obtained by the resolution, there are some outstanding problems that must be investigated more carefully and much of our current work at NBS is directed towards that end. First, we are obtaining much more detailed information on the Washington atmosphere. An extensive set of samples was taken at several sites during the Summer of 1976, including both whole-filter and cascade-impactor samples, the latter to give us more information about the size distributions of particles bearing the elements. Most of these samples were analyzed at the reactor during the present year. We're soon going to collect more samples from the Baltimore Harbor Tunnel to look for recent changes in emissions. W. R. Pierson of Ford Motor Company has found increases in emissions of Mg and Ca from trucks that may account for some of the unexplained amounts of these elements in Washington. Also, a manganese additive, MMT, is being phased into some gasolines as a replacement for tetraethyl lead and we need to monitor that change. Furthermore, the group of sources included in the resolution is incomplete. We know that some air-filter samples taken in Frederick County, Maryland, contain contributions from a cement plant. Samples in Washington may have contributions from a large steel mill in Baltimore when the wind is from the Northeast. For these reasons, we have collected filter samples with an airplane from the plumes of a cement plant and a steel mill and analyzed them with use of the reactor and will be collecting and analyzing more

samples soon.

One of the problems implicit in our analysis is the assumption that, once particles leave a plant, they are not modified. But we know, for example, that some elements from coal combustion are on large particles and other, preferentially on small particles. The former would be expected to settle out of the atmosphere more rapidly than the latter after release, thus altering the composition of particles from that source. To investigate those and related questions we have collaborated with Dr. John Ondov et al. of Lawrence Livermore Laboratory (LLL) on a study of emissions from a large, isolated power plant in New Mexico. The LLL Group did collections in the stack and our group collected particles at various distances in the plume. One set of experiments was done in February 1976 and a second in August 1976. Most samples from the first set were analyzed at LLL, as well as the in-plant samples from the second set. The plume samples from the second set are now being analyzed at the NBS reactor. A preliminary report on the February 1976 experiment was presented at the Spring Meeting of the American Chemical Society in New Orleans, March 1977 and a final report on both sets of studies will be written when sample analysis is complete.

Two other small projects are now in progress. For some years it has been known that lichens (fungi that are attached to trees and other objects) are sensitive indicators of air pollution such as SO_2 . A group at University of Maryland-Baltimore County is studying damage to lichens in the vicinity of the Dickerson Generating Station. We have obtained samples of healthy and damaged lichens from the UMBC group and are irradiating them for INAA. We want to see if the diseased lichens show evidence for collection of trace elements that we know are associated with coal-fired power plants (e.g., As, Se, Hg). Also, our entire group is participating in the analysis of the new NBS coal Standard Reference Materials.

2. Global Air Pollution Studies

For the past several years we have been collecting particles from

SERVICE PROGRAMS

very remote areas of the Earth, especially the South Pole, and analyzing them, primarily by INAA at the NBS reactor, in order to determine the composition of particles that are in global circulation. During the past year, we analyzed a number of samples collected at the South Pole during the period October 1975 to February 1976.

Recently we have begun studies of possible major sources of globally circulating particles, starting with volcanoes. During the past year we performed INAA of samples collected during the eruption of the Mt. Augustine volcano in Alaska in January/February, 1976. Samples were collected using the National Center for Atmospheric Research's Lockheed Electra during periods of different types of volcanic activity. In table 2, concentrations of seven common crustal elements and six volatile elements are listed for volcanic ash (Ag) and four air filters. The first two of these filters were collected on February 1 close to and distant from the volcano vent. The last two filters were collected later on February 18 and 20, respectively, following an eruption characterized by steam instead of by volatile compounds of sulfur, etc. that are usually associated with volcanic eruptions. The higher concentrations in the last two samples for the "crustal" elements indicates a higher ash content in the volcanic plume.

A comparison of the varying composition of the plume samples can be obtained by calculating enrichment factors relative to the ash sample. The calculation is made by using the following equation:

$$EF_{\text{ash}} = \frac{(X/A1)_{\text{filter}}}{(X/A1)_{\text{ash}}}$$

where x refers to the concentration of the trace element of interest and A1 refers to the A1 concentration. An EF_{ash} value near unity indicates that this element is associated with bulk ash. The EF_{ash} values for these samples are given in table 3. The EF values of the non-volatile elements (table 3a) are all quite close to unity and represent ash in the plume. The difference for these elements on the two sample sets represents compositional variations of the ash during the eruptive cycles. The volatile elements (table 3b) show higher

Table 1. Results of elemental resolution of Washington, D. C. aerosols

Element	Contributions from components (ng/m ³)							Total conc. (ng/m ³)		Observed
	Soil	Marine	Coal	Oil	Refuse	Motor Vehicle	Predicted	Observed ^a	Predicted	
Al	1200	<0.001	720	1	14	-	1940	1680+1100	0.87	
Na	63	280	12	27	82	-	460	470+470	1.0	
Fe	750	<0.001	510	6.1	6.5	67	1340	1260+940	0.94	
V	1.6	<0.001	2.2	51	0.031	-	55	54+57	1.0	
Zn	1.7	<0.001	3.6	3.6	120	20	150	150+90	1.0	
Pb	0.23	<0.001	2.9	0.86	81	1300	1380	1400+1660	1.01	
Mn	19	<0.001	2.2	0.22	0.73	-	22	27+16	1.2	
As	0.09	<0.001	4.4	0.061	0.24	-	4.8	5.7+5.0	1.2	
<u>Remaining elements</u>										
K	230	10	94	1.0	-	-	340	510+350	1.5	
Mg	110	37	39	8.6	13	-	210	440+380	2.1	
Ca	97	11	66	18	17	67	280	770+500	2.8	
Ba	10	0.001	6.6	4.2	0.7	17	39	27+24	0.69	
Cl	3.9	510	1.5	27	200	130	870	140+75	0.16 ^b	
Br	0.14	1.8	3.0	0.12	1.6	490	500	190+220	0.38 ^b	
I	0.08	1.6	3.0	-	-	-	4.7	9.3+7.2	2.0 ^b	
Sc	0.22	<0.001	0.25	<0.001	0.001	-	0.47	0.63+0.63	1.3	

Table 1. cont'd. Results of elemental resolution of Washington, D. C. aerosols

Element	Contributions from components (ng/m ³)						Total conc. (ng/m ³)		Observed
	Soil	Marine	Coal	Oil	Refuse	Motor Vehicle	Predicted	Observed ^a	
<u>Remaining elements cont'd.</u>									
Ti	77	0.001	44	0.056	2.0	-	120	120±95	1.0
Cr	1.2	<0.001	1.2	0.13	0.50	-	3.0	11±9	3.7
Co	0.32	<0.001	0.35	0.36	0.007	-	1.0	1.1±1.0	1.1
Ni	0.67	<0.001	1.5	8.6	0.16	-	11	27±28	2.5
Cu	0.34	<0.001	3.0	1.8	1.6	-	6.7	13±12	1.9
Se	0.001	<0.001	1.1	0.076	0.037	-	1.2	3.5±2.7	2.9 ^b
Cd	0.002	<0.001	0.19	0.006	1.5	-	1.7	3.5±2.2	2.1
Sb	0.012	<0.001	0.18	0.015	2.1	-	2.3	9.7±8.5	4.2
La	1.1	<0.001	0.44	0.036	0.004	-	1.6	1.9±1.7	1.2
Ce	1.4	<0.001	0.86	0.030	0.016	-	2.3	3.4±3.1	1.5
Th	0.17	<0.001	0.15	0.004	0.002	-	0.33	0.32±0.24	1.0

^aUncertainty is standard deviation of a single observation

^bVolatile element - not expected to be fitted perfectly.

Table 2. Trace Element Concentrations in Ash and Filter Samples from the Mt. Augustine Volcano.

Element	Ash (ppm unless % indicated)	Filter Samples			
		Feb. 1, 1976	Feb. 18, 1977	Feb. 20, 1976	
		AW-5 0-8 km (ng/m ³)	AW-6 8-30 km (ng/m ³)	AW-13 0-40 km (ng/m ³)	AW-16 0-40 km (ng/m ³)
Al	9.0±3%	675±25	895±20	27,100±800	31,000±1000
Fe	3.36±0.03%	430±15	600±20	13,000±200	12,000±200
Co	11.4±0.2	0.18±0.04	0.24±0.04	0.42±0.10	3.7±0.1
V	147±6	1.6±0.3	2.5±0.3	34±4	41±2
Ti	0.34±0.02%	60±25	70±15	1000±200	1200±100
Sc	15.4±0.1	0.17±0.01	0.24±0.01	4.6±0.6	4.4±0.1
Mn	770±20	7±2	11±1	265±10	270±10
Zn	<1.3%	3±1	3.5±1.0	160±10	130±5
Cl	0.14±0.01%	11,000±400	7,200±200	17,600±500	1200±100
Br	-	54±3	23±1	21±9	11±5
As	1.11±0.01	9.3±0.3	7.7±0.2	2.5±0.2	15±2
Sb	0.061±0.006	0.89±0.04	0.89±0.04	4.3±0.1	3.4±0.1
Se	<0.2	1.4±0.1	3.4±0.2	5.7±0.2	3.7±0.1

SERVICE PROGRAMS

Table 3. Enrichment Factors Relative to Ash for Elements on Suspended Particles.

Element	AW-5	AW-6	AW-13	AW-16
a. <u>Non-volatile Elements</u>				
Fe	1.7	1.8	1.3	1.0
Co	2.1	2.1	1.2	0.9
V	1.4	1.7	0.8	0.8
Ti	2.3	2.1	1.0	1.0
Sc	1.5	1.6	1.0	0.8
Mn	1.2	1.4	1.2	1.0
b. <u>Volatile Elements</u>				
An	>290	>260	>390	>280
Cl	1070	520	42	2.3 ^a
Br	>360	>120	>3.4 ^a	>1.6 ^a
As	1100	700	7.5	38
Sb	2000	1500	240	160
Se	>90	>1700	>90	>50

^aSea salt is primary source.

enrichments on the first samples relative to the later sample, again pointing to chemical variation between the two periods of the eruption. It appears that the volatile elements are lost early in the eruption as the primary magma chamber is initially vented, and their concentration decreases throughout the period of volcanic activity.

3. Radioactive Decay Studies

In our studies of the decay of radioactive nuclides, we have published the results of our discovery of a new isomer, 47-min Eu-154m and presented preliminary results from our studies of the decay of 100-min Pm-149 and the decay of 12-min Nd-151 to levels of Pm-151. As Pm-151 is clearly a deformed nucleus and Pm-149 shows shell model characteristics in its ground state, these studies are useful in characterizing the transition from spherical to deformed nuclear shapes. We have also measured the half life of the 376.6-keV level in Ag-111 populated in the beta decay of Pd-111 isomers. The value of $16\frac{1}{2}$ nsec suggests that this level has a 1-particle-2-hole configuration and a deformed shape.

NEUTRON TRANSMUTATION DOPING OF SILICON

J. W. Cleland, R. D. Westbrook, R. F. Wood and R. T. Young
(Oak Ridge National Laboratory, Oak Ridge, TN)

Normal isotopic silicon contains 3.05% of Si-30 which transmutes to P-31 after thermal neutron absorption, with a half-life of 2.6 hrs. This reaction can be used to introduce extremely uniform concentrations of P, a standard n-type dopant in Si, thus eliminating the areal and spatial inhomogeneities characteristic of conventional melt-growth doping techniques. It has been demonstrated¹ that the performance and yield of high power Si rectifiers and thyristors can be significantly improved by the use of neutron transmutation doped (NTD) Si, and the rate of introduction of P in NTD Si is such that doping concentrations of interest to the semiconductor industry are readily attainable in many reactors.²

Significant improvements in the performance of many types of Si electronic devices may be attainable through the use of NTD Si but many applications are still in the research stage. One interesting use is in solar cell development,³ and another is that of obtaining a uniform dopant distribution in polycrystalline Si regardless of the sample or polycrystalline grain size.⁴ It has been demonstrated that there is no aggregation of P at the grain boundaries in NTD polysil as a consequence of annealing to remove lattice damage, and macroscopic and microscopic spreading resistance measurements on NTD Si epitaxial layers indicate that any fluctuations in dopant distribution are virtually nonexistent.⁵

The program of basic research on Photophysical Processes of Solar Energy Conversion in the Solid State Division at ORNL has been established with the objective of finding methods for increasing the efficiency of conversion of solar energy into forms suitable for terrestrial applications. The program thus far has been concentrated on the study of NTD Si, and particular attention is being given to studies of the characterization and annealing of lattice damage introduced in both single crystal and

SERVICE PROGRAMS

polycrystalline Si. The vertical G-2 facility in the NBSR has been used to introduce $\sim 10^{15}$ to 6×10^{16} P cm⁻³ in 1.25-in. diam x 8-10 in. long single or polysil ingots or ingot sections as a consequence of 1, 11, 7, 21, and 42 day irradiations, and the new vertical G-4 facility has been used to introduce 10^{16} to 10^{17} P cm⁻³ in 3-in. diam x 8-10 in. long single or polysil ingots or ingot sections as a consequence of 7, 21, and 42 day irradiations. This program has benefited from the capable assistance provided by the NBSR personnel.

1. W. E. Haas and M. S. Schnöller, J. Electron. Mater. 5, 57 (1976).
2. See the first four articles in IEEE Trans. Electron Devices, Vol. ED-23, No. 8 (1976).
3. R. F. Wood, R. D. Westbrook, R. T. Young and J. W. Cleland, *Proceedings, High Efficiency Radiation Damage Silicon Solar Cell Meeting*, NASA Lewis Research Center, April 1977 (in press).
4. R. T. Young, J. W. Cleland, and R. F. Wood, *Proceedings of the 12th IEEE Photovoltaic Specialists Conference - 1976*, (IEEE, New York, 1976), 76CH1142-9 ED, p. 65.
5. R. F. Wood, J. W. Cleland, P. H. Fleming, T. L. Polgreen, R. D. Westbrook, and R. T. Young, *Solid State Division Annu. Prog. Rep. for Period ending April 30, 1977*, ORNL-5328 (in press).

POSITRON ANNIHILATION STUDIES

A. C. Ehrlich

(Naval Research Laboratory, Washington, DC)

The Metals Physics Branch of the Naval Research Laboratory has an ongoing program in the electronic structure of metals and alloys. One of the very few methods available for direct study of the electronic structure of alloys is the angular correlation of positron annihilation radiation. This provides a direct measurement of the momentum spectrum of the electrons in the material. From this one can deduce detailed information regarding the electronic structure.

The goal of this work is twofold; first, by determining the evolution of the electronic structure of a simple method like pure Cu as it is alloyed with Zn it is hoped to deduce general information regarding the electronic structure of alloys. Second, delineation of the CuZn system should provide a basis for understanding one of the Hume-Rothery rules, i.e.; the well known phase transition that occurs in a very large number of Cu, Ag and Au based alloys at a conduction electron concentration of approximately 1.35 electrons/atom. In the CuZn alloy system this occurs at 35 atomic percent Zn.

Due to the proximity and unique facilities of the NBS Nuclear Reactor Facility to NRL, it has been possible to design a unique positron annihilation apparatus which takes advantage of the fact that Cu can be rendered strongly positron emitting by exposure to a flux of slow neutrons. Thus the sample under study and the source of positrons are one and the same and the effective positron source strength is much greater than could be obtained using external positron sources. This in turn permits the resolution of the γ -ray momenta in two directions (rather than the usual resolution in only one direction) while still retaining a sufficiently high count rate to obtain the necessary statistical precision.

During the past year measurements have been carried out on single crystals of Cu, $\text{Cu}_{85}\text{Zn}_{15}$ and $\text{Cu}_{77}\text{Zn}_{23}$ in various crystallographic orientations. From these measurements it has been possible to deduce the maximum conduction electron momentum in the crystallographic directions studies. This is closely related to the dimensions of the so called Fermi surface. What is found is that as Zn is added to Cu the Fermi surface growth in the [100] direction is less than that in the [110] direction in contrast to what has been generally assumed. Further, the growth in both directions is greater than expected on the basis of the rigid band model of electron structure. In contrast, the growth of the well known "necks" in the [111] direction is slower than predicted by the rigid band model.

SERVICE PROGRAMS

It has been suggested that possible contact of the [100] Fermi radium and the Brillouin Zone boundary at 1.35 electrons/atom might be responsible for the phase transformation undergone by many noble metal alloys. Extrapolation of our data indicates that no contact will take place at this electron concentration. Thus, future research will examine other aspects of the conduction electron structure as well as possible anisotropies in the more tightly bound 3d electrons in Cu.

NEUTRON ACTIVATION ANALYSIS OF LUNAR SAMPLES AND METEORITES

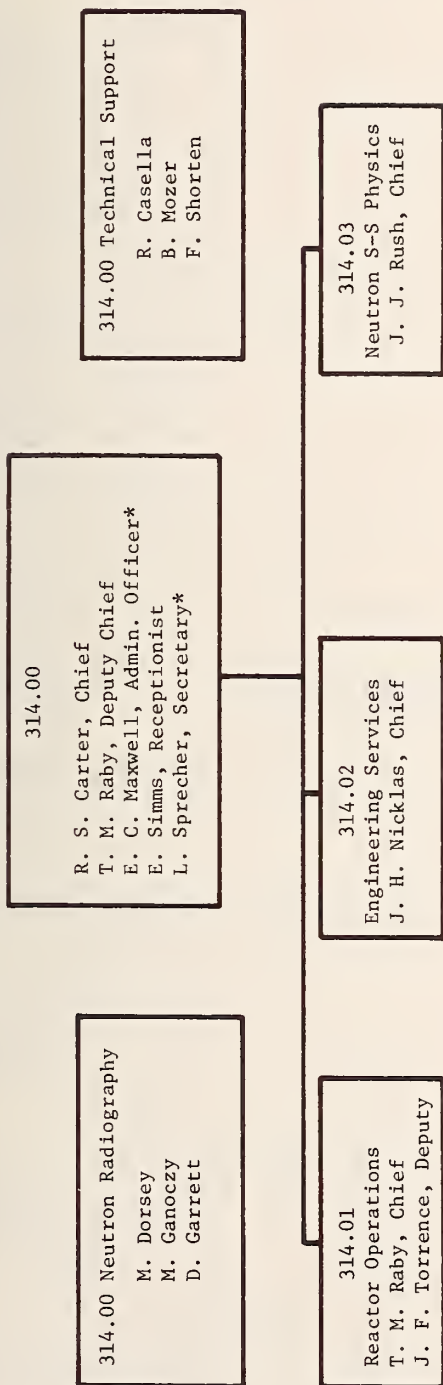
Jan Hertogen, Marie-Josée Janssens, Herbert Palme,
Hiroshi Takahashi, Edward Anders
(Enrico Fermi Institute, University of Chicago, Chicago, IL)

We have continued our analysis of breccias from the lunar highlands, in order to identify meteoritic material from the intense bombardment four billion years ago. The elements analyzed are: Ag, Au, Bi, Br, Cd, Cs, Ge, In, Ir, Ni, Os, Pd, Rb, Re, Sb, Se, Te, Tl, U. and Zn. Nine discrete meteorite types have been recognized, each apparently derived from an impacting body in the 10-100 km size range. Several of these bodies have compositions complementary to that of the Moon, and may comprise left-over planetesimals from the Earth's neighborhood.

F. STAFF ROSTER

Division 314

REACTOR RADIATION



314.00 Neutron Radiography
M. Dorsey
M. Ganoczy
D. Garrett

314.01
Reactor Operations
T. M. Raby, Chief
J. F. Torrence, Deputy

314.02
Engineering Services
J. H. Nicklas, Chief

314.03
Neutron S-S Physics
J. J. Rush, Chief

P. Lewis, Secy.

D. Davitt, Secy.*

C. O'Connor, Secy.

Reactor Operations

- R. Beasley
- M. Bell
- N. Bickford
- H. Brake
- J. Browning
- D. Cea
- A. Chapman
- H. Dilks
- W. Mueller
- D. Nelson
- J. Ring
- R. Stiber
- D. Wilkinson
- B. Young

Mechanical Design

- E. Guglielmo
 - J. Sturrock
- Electronics
- R. Conway
 - J. Darr
 - R. Hayes

Crystallography

- E. Prince
 - A. Santoro
 - C. Choi (GW)
 - A. Tudgay (1/2)
- Metal Hydrides and
Molecular Materials
- J. Rowe
 - A. Cinquepalma
 - W. Rymes (1/2)
 - G. Fish (PD)
 - C. Glinka (GW)

Magnetic Materials

- J. Rhyne
- H. Alperin (GW)
- N. Koon (GW)
- R. Williams (GW)
- J. Lynn

Metastable Materials

- H. Prask (GW)
- S. Trevino (GW)
- W. Rymes (1/2)
- N. Chesser (GW)

Biological Materials

- A. Wlodawer
- A. Tudgay (1/2)

* Part-time
PD - Postdoctoral
GW - Guest Worker

STAFF ROSTER

NON-RRD NBS STAFF LOCATED AT REACTOR

Division 240.01

P. R. Cassidy
K. Eggert
T. Hobbs
F. Moore
J. J. Shubiak

Division 240.05

M. Baier
R. A. Dallatore
C. Eisenhauer
D. Gilliam
J. A. Grundl
E. McGarry
I. G. Schroder
R. Schwartz
V. Spiegel

Division 310.08

D. Anderson
J. Bailey
J. Blackman
B. Carpenter
R. Fleming
M. Gallorini
T. Gills
C. Grabnegger
S. Harrison
G. Hyde
R. Lindstrom
G. Lutz
J. Maples
L. Pilione
H. Rook
N. Sato

GUEST WORKERS AND COLLABORATORS

Division 232.06

R. D. Deslattes
E. G. Kessler
W. C. Sauder
J. Snyder

Division 240.05

C. Bowman
K. Duvall
H. Heaton
G. Tamaze

Division 300.00

H. Berger
L. McClendon

Division 310.00

P. LaFleur

Division 310.01

D. Sweger

Division 311.03

C. Han

Division 311.05

R. Bowen
M. Mathew
L. Schroeder

Division 312.02

J. Early
R. Reno

Division 313.03

D. B. Monor
R. S. Roth

Division 313.04

G. J. Rosasco

STAFF ROSTER

Division 313.06

A. B. Mighell
W. Thurber

Division 461.02

P. Brown

Argonne National Laboratory

R. Armani
H. Flotow
A. Rahman
K. Skold
S. Susman

Battelle, N. W.

W. Nicholson

Bell Laboratory

D. Moncton

Brookhaven National Laboratory

L. Passell
W. Thomlinson

Federal Bureau of Investigation

D. B. Davies
J. Haverkost
J. W. Kilty
E. Mitchell
J. P. Riley

Food and Drug Administration

D. Daly
M. Friedman
J. T. Tanner

Harry Diamond Laboratory

C. Heimbach

NASA-Langley Research Center

R. Buckingham

National Institutes of Health

D. Davies
R. Frank
W. Hagins
W. Robinson

Naval Air Defense Command

M. Stellabotte
W. Williams

Naval Air Rework Facility

R. Chavez

Naval Research Laboratory

P. D'Antonio
B. Das
A. Ehrlich
J. Karle
N. Koon
F. Leppe

Naval Surface Weapons Center
(White Oak Laboratory)

H. Alperin
D. Polansky
R. Williams

Oak Ridge National Laboratory

J. Cleland
M. Mostollor
H. Smith
R. Westbrook
R. Wood
R. Young

Picatinny Arsenal

N. Chesser
C. S. Choi
H. J. Prask
S. Trevino

STAFF ROSTER

Smithsonian Institution

M. Blackman
T. Chase
J. Mishara
S. O'Dell
L. Zacherman

U. S. Geological Survey

P. Baedeker
J. Morgan
J. J. Rowe

U. S. Treasury Department

J. M. Hoffman
W. Kinard
L. Reid

American University

R. Abbundi
R. A. Segnan

Colorado State University

C. E. Patton

Georgetown University

K. Barkigia
C. Quicksall

Harvard University

D. O'Brien
R. Wilson

Howard University

G. A. Ferguson

Reed College

W. Parker

Royal Canadian Military Academy

L. Bennett

University of California
(Lawrence Livermore Laboratories)

J. Browne
S. Hankins

University of Connecticut

J. Budnick

University of Chicago

E. Anders
J. Hertogen
M. Janssens
H. Palme
H. Takanashi

University of Maryland

D. Anderson
C. Choquette
W. Cunningham
M. Failey
P. Gallagher
M. Germani
B. Glagola
M. Glascock
D. Glotfelty
G. Gordon
G. Kowalczyk
E. Lepel
J. Levkoff
J. Lynn
J. Muhlbaier
D. Reamer
E. Schneider
M. Small
P. Solomon
E. Sombrito
K. Steffansson
W. Walters
M. Yiu
W. Zoller

U. S. Naval Academy

C. S. Schneider

STAFF ROSTER

University of Paris

B. Le Neindre

University of Pittsburgh

S. Sankar

W. Wallace

University of Rhode Island

S. J. Pickart

University of Saärlande

(West Germany)

K. Michel

J. Naudts

University of Salford (U.K.)

D. Martin

University of Wisconsin

J. Hinkley

H. Yu

Allied Chemical Corporation

G. Liebowitz

A. Maeland

R. O'Handy

Caterpillar Tractor Company

W. P. Evans

General Electric Company

F. Lubursky

Monsanto Research Corporation

W. Brotherton

Oldelft Corporation

D. Bracher

Zerox Corporation

E. Stein

G. PUBLICATIONS

COLLABORATIVE PROGRAMS

- ALPERIN, H. A., CULLEN, J. R., CLARK, A. E. and CALLEN, E., "Amorphous Magnetism in Bulk Samples of Terbium Iron Alloys," *Physica*, 86-88B, 767 (1977).
- CHOI, C. S. and PRINCE, E., "Refinement of α -Lead Azide by Neutron Diffraction," (to be published).
- CHOI, C. S., PRASK, H. J., PRINCE, E. "Ammonium Perchlorate: Reinvestigation of the Crystal Structure at 298K," *Acta Cryst.* 1332, 2919 (1976).
- GLINKA, C. J., ROWE, J. M., RUSH, J. J., RAHMAN, SINKAR, and FLOTOW, H., "Inelastic Neutron Scattering Lineshapes in PdD_{0.63}," (to be published).
- GLINKA, C. J., MINKIEWICZ, V. J., and PASSELL, L., "Small-Angle Critical Neutron Scattering," (to be published).
- GLINKA, C. J., ROWE, J. M., RUSH, J. J., LIBOWITZ, G. G., and MAELAND, A., "The Lattice Vibrations of CeD_{2.12}," *Solid State Communications*, 22, pp. 541-544 (1977).
- MARTIN D. J., and RHYNE, J. J., "Re-analysis of Dysprosium Magnetostriction," (to be published).
- MASSA, N. E., MITRA, S. S., PRASK, H., SINGH, R. S., and TREVINO, S. F., "Infrared-Active Lattice Vibrations in Alkali Azides," *J. of Chem. Phys.*, 67, 1, 173-179 (1977).
- PICKART, S. J., ALPERIN, H. A., RHYNE, J. J., "Small Angle Magnetic Scattering from a Dilute Amorphous Fe(Tb) Alloy," (to be published).
- PICKART, S. J., "Small Angle Magnetic Scattering in Amorphous TbFe₂." *Proc. of Conf. on Magnetic Scattering*, Troy, NY (1977).
- RHYNE, J. J., "Magnetic Materials," Encyclopedia of Physics, edited by R. G. Lerner and G. L. Trigg, Dowden, Hutchinson and Ross, Inc. (to be published).
- RHYNE, J. J., "Amorphous Magnetic Rare Earth Alloys," Chapter 16, *Handbook on the Physics and Chemistry of Rare Earth*, edited by K. A. Gschneidner and L. Eyring, (1977).

PUBLICATIONS

- ROWE, J. M. and RUSH, J. J., "The Dynamics of Hydrogen in Metals,"
IAEA Conf. on Neutron Inelastic Scattering, Vienna, Austria, (1977).
- ROWE, J. M., RUSH, J. J. and PRINCE, E., "Neutron Diffraction Study of
the Structure and Phase Transitions of Alkali Cyanide Crystals,"
J. Chem. Phys., 61, 11, 5147-49 (1977).
- SANTORO, A., ROTH, R. S. and MINOR, D., "Neutron Powders Diffraction
Study of $M\text{-LiTa}_3\text{O}_8$, *Acta. Cryst.*, (to be published).
- SCHROEDER, L. W., PRINCE, E., "Hydrogen-Bonded Dimers in Tin (II) Hydrogen
Phosphate," *Acta. Cryst.*, B32, 3309, (1976).
- SHORTEN, F. J., "NBS Reactor: Summary of Activities, July 1975 to
June 1976," *NBS Technical Note*, 939, (1977).
- TREVINO, S. F., FARR, M. K., GIGUERE, P. A., ARNAU, J. L., "The Lattice
Dynamics of the Deuterium Peroxide Crystals," (to be published).
- WLODAWER, A., SANTORO, A., "Flat Cone Diffractometer Utilizing a Linear
Position Sensitive Detector," (to be published).
- WLODAWER, A., ROBERTS, J. and HOLCENBERG, J. S., "Characterization of
Crystals of L-Glutaminase-Asparaginase from *Acinetobacter Glutamin-*
asificans and *Pseudomonas 7A*," *J. Mol. Biol.* 112, 515-519 (1977).

INDEPENDENT PROGRAMS

- BARNES, I. L., ROOK, H. L., MURPHY, T. J., "The NBS Program for Standards for Trace Inorganic Analysis in the Marine Environment," *Proc. Tech. Review of Interagency Marine Res. Prog. Associated with Energy Development* (1977).
- BOWEN, R. L., MCCLENDON, L. T. and GILLS, T. E., "Adhesive Bonding of Various Materials to Hard Tooth Tissues XV: Sorption of Mordant Ions Evaluated by Neutron Activation Analysis," (to be published).
- BOYER, K. W., TANNER, J. T. and GAJAN, R., "Multiement Analysis Techniques at the Food and Drug Administration," *American Laboratory* (to be published).
- CAPAR, S., TANNER, J. T., FRIEDMAN, M. H. and BOYER, K. W., "Multiement Analysis of Animal Waste Material," *Environmental Science and Technology*, (to be published).
- CARPENTER, B. S. and REIMER, G. M., "Uranium Analysis of Natural Waters by Fission Tracks," *ANS Transactions*, 26, (1977).
- CARPENTER, B. S., "Mapping and Detecting Selective Elements by Nuclear Track Technique," *Proc. of the Nuclear Methods in Environmental and Energy Conf.* (1977).
- CARPENTER, B. S. and REIMER, G. M., "Homogeneity Considerations in Trace Analysis Using the Nuclear Track Technique," *Proc. of the Seventh Materials Research Symposium*, NBS (1976).
- CARPENTER, B. S., SAMUEL, D., WASSERMAN, I., and YUWILER, A., "A Study of Lithium Uptake and Location in the Brain Using the Nuclear Track Technique," *Proc. of the 1976 Modern Trends in Activation Analysis Conference*, Munich, Germany (1976).
- CARPENTER, B. S. and MYKLEBUST, R. L., "Comparative Analysis for Boron in Steel by Ion Microprobe Mass Analyzer and the Nuclear Track Technique," *Analytica Chimica Acta*. Vol. 91, p. 409-411 (1976).
- DOWTY, E., KEIL, K., PRINZ, M., GRAY, J., and TAKAHASHI, H., "Meteorite-free Apollo 15 KREEP," *Proc. 7th Lunar Sci. Conf. Geochim. Acta, Suppl. 7*, 1833-1844 (1976).
- EISENHAUER, C. M., GRUNDL, J. A. and FABRY, A., "Neutron Transport Calculations for the Intermediate-Energy Standard Neutron Field (ISNF) at the National Bureau of Standards," *Proc. of International Specialists Symposium on Neutron Standards and Applications*, (to be published).

- FARBER, T. M., RITTER, D. L., WEINBERGER, M. A., BIERBOWER, G., TANNER, J. T., FRIEDMAN, M. H., CARTER, C. J., EARL, F. L., and VANLOON, E. J., "The Toxicity of Brominated Sesame Oil and Brominated Soybean Oil in Minature Swine," *Toxicology* 5, 319-336 (1976).
- FILBY, R. H. and CARPENTER, B. S., "Application of Nuclear Techniques to the Characterization of Trace Elements in Petroleum and Coal Conversion Products," *ANS Transactions* 26, (1977).
- FRIEDMAN, M. H. and TANNER, J. T., "A Computer Language for Reducing Neutron Activation Analysis Data and Its Application to the Problems of the Food and Drug Administration," *Journal of Radioanalytical Chemistry*, (to be published).
- GILLS, T. E. and MCCLENDON, L. T., "Role of Neutron Activation Analysis in the Evaluation of Sampling, Storage and Analysis Methodology on Samples for the National Environmental Banking System," *Proc. of the 1976 Modern Trends in Activation Analysis*, (1976).
- GILLS, T. E., ROOK, H. L. and LAFLEUR, P. D., "Assessment of Gunshot Residue Detection Using Neutron Activation Analysis, *Report to the Law Enforcement Standards Program*, LESP Report (1976).
- GILLS, T. E., "Selective Radiochemical Separation for the Activation Analysis of NBS Botanical Standard Reference Materials," (to be published).
- GILLS, T. E., GALLORINI, M. and GREENBERG, R. R., "The Measurement of Selected Toxic Elements in Biological Matrices Using Radiochemical Activation Analysis, *Proc. of the Third International Conf. on Nuclear Methods in Environmental and Energy Research*, (1977).
- GILLIAM, D. M., "Integral Measurement Results in Standard Fields," *Proc. of International Specialists Symposium on Neutron Standards and Applications*, pp. 209-303 (1977).
- GLADNEY, E. S., SMALL, J. A., GORDON, G. E. and ZOLLER, W. H., "Compositions and Size Distribution of In-Stack Particulate Material at a Coal-Fired Power Plant," *Atmos. Environ.* 10, 1071-1077 (1976).
- GORDON, G. E., ANDERSON, D., FAILEY, M., WALTER, W., ZOLLER, W. H. and LINDSTROM, R. M., "Prompt Gamma-Ray Neutron Activation Analysis," *Proc. of 3rd International Conf. Nuclear Methods and Environmental Energy Research*, (to be published).

PUBLICATIONS

- GREENBERG, R. R., ZOLLER, W. H. and GORDON, G. E., "The Contribution of Refuse Incineration to Urban Aerosols," *Proc. of the Fourth Joint Conf. on Sensing of Environmental Pollutants*, (to be published).
- GREENBERG, R. R., ZOLLER, W. H. and GORDON, G. E., "Composition and Size Distributions of Particles Released in Refuse Incineration," (to be published).
- GROS, J., TAKAHASHI, H., HERTOGEN, J., MORTAN, J., ANDERO, E., "Composition of the Projectiles That Bombarded the Lunar Highlands," *Geochim Cosmochim. Acta, Suppl.* 7, 2402-2425 (1976).
- GRUNDL, J. and EISENHAEUER, C., "Fission Reaction Rate Standards and Applications," *Proc. of International Specialists Symposium on Neutron Standards and Applications*, pp. 156-164 (1976).
- GRUNDL, J. A., SPIEGEL, V., EISENHAEUER, C. M., HEATON II, H. T. and GILLIAM, D. M., "A Californium-252 Fission Spectrum Irradiation Facility for Neutron Reaction Rate Measurements," *Nucl. Tech.* Vol. 32, pp. 315-319 (1977),
- HARRISON, S. H. and BLANCHARD, D., "Fine Paper Identification by Trace Elements Profiles of Clay Fillers," (to be published).
- HARRISON, S. H., "Determination of Vanadium and Manganese in NBS-SRM Tissues, Sediments, and Waters by Neutron Activation Analysis," *NBS SPEC. PUBL.* 260(1977).
- HARRISON, S. H., LAFLEUR, P. D. and ZOLLER, W., "Sampling and Sample Handling for Activation Analysis of River Water," *Proc. of the Seventh Materials Research Symposium*, NBS (1976).
- HERTOGEN, J., JANSSENS, M., TAKAHASHI, H., PALME, H. and ANDERS, E., "Lunar Basins and Craters: Evidence for Systematic Compositional Changes of Bombarding Populations," (to be published).
- HERTOGEN, J., JANSSENS, M., "Is Osmium Chemically Fractionated on the Moon?" (to be published).
- HOPKE, P. K., GLADNEY, E. S., GORDON, G. E., ZOLLER, W. H., and JONES, A. G., "The Use of Multivariate Analyses to Identify Sources of Selected Elements in the Boston Urban Aerosol," *Atoms. Environ.* 10, 1015-1025 (1976).
- HUGHES, J. E., ROOK, H. L., DEARDORFF, E. R., MARGESON, J. H. and FUERST, R. G., "Operational Characteristics of Nitrogen Dioxide Permeation Devices," (to be published).

- ROOK, H. L., MOODY, J. R., PAULSEN, P. J. and RAINS, T. C., "Stability of Elemental Components in a Multi-trace Element Water Standard," *Proc. of the Mineral Cycling Symposium*, Savannah River Laboratory (1977).
- ROOK, H. L., "The Determination of Iodine in Biological and Environmental Standard Reference Materials," *J. of Radioanal. Chem.*, 39, 1-2, p. 351-358 (1977).
- ROOK, H. L. and WOLF, W., "The Quantitative Determination of Volatile Trace Elements in NBS Biological SRM 1569, Brewers Yeast," *Proc. of 11th Annual Conf. on Trace Substances in Environmental Health*, Columbia, MO (1977).
- ROOK, H. L., "Environmental Water Standards Applied to Health Effects Studies," *Proc. of the 1976 Modern Trends in Activation Analysis*, (1976).
- SCHNEIDER, E. W., GLASCOCK, M. D., GALLAGHER, P. W., WALTERS, W. B. and MEYER, R. A., "Identification of Low-Lying 0^+ State in ^{128}Xe Populated in the Decay of ^{128}Cs ," *Bull. Am. Phys. Soc.* 22, 596 (1977).
- SCHWARTZ, R. B., "Calibration and Use of Filtered Beams," *Proc. Int. Specialists Symp. on Neutron Standards and Applications*, NBS, (to be published).
- SEGEBADE, C., LUTZ, G. J. and REIMERS, P., "Photon Activation Analysis of Coins and Objects of Art," *1976 Modern Trends* p. 1171 (to be published).
- SEGEBADE, C., LUTZ, G. J. and WEISS, P., "Quantitative Evaluation of Interference Reactions in Photon Activation Analysis," *1976 Modern Trends* (to be published).
- TANNER, J. T. and FRIEDMAN, M. H., "Neutron Activation Analysis for Trace Elements in Foods," *Proc. of Conf. Modern Trends in Activation Analysis*, Munich, Germany (1976).
- TANNER, J. T. and FRIEDMAN, M. H., "Neutron Activation Analysis for Trace Elements in Foods," *Journal of Radioanalytical Chemistry* 37, 529-38 (1977).
- THURBER, W. R. and CARPENTER, B. S., "Determination of Boron in Silicon by the Nuclear Track Technique and Correlations with Resistivity and Capacitance-Voltage Measurements," (to be published).
- WAGNER, G. A. and CARPENTER, B. S., "Liquid Nitrogen Enhancement of Partially Annealed Fission Tracks in Glass," *Nature*, 267, p. 182 (1977).

PUBLICATIONS

- KOWALCZYK, G. S., CHOQUETTE, C. E. and GORDON, G. E., "Chemical Element Balances and Identification of Air Pollution Sources in Washington, DC, *Atoms. Environ.* (to be published).
- LINDSTROM, R. M., "Radial Efficiency Gradients in Ge(Li) Gamma Detectors," *Proc. of the 1976 Modern Trends in Activation Analysis* (1976).
- LINDSTROM, R. M. and FLEMING, R., "Optimized Determination of Aluminum in High Purity Silicon," (to be published).
- LUTZ, G. J., STEMPLE, J. S. and ROOK, H. L., "Evaluation by Activation Analysis of Elemental Retention in Biological Samples After Low Temperature Ashing," *J. of Radioanal. Chem.*, 39, 1-2, p. 277-283 (1977).
- LUTZ, G. J., "Evaluation of Elemental Retention in Biological and Organic Samples After Low Temperature Ashing by Activation Analysis," *Proc. of the 1976 Modern Trends in Activation Analysis*, (1976).
- MCCLENDON, L. T. and GILLS, T. E., "Trace Element Characterization of Automobile Headlamp Glass Using Neutron Activation Analysis," (to be published).
- MCGARRY, E. D. and GILLIAM, D. M., "Standardization of Fast Pulse Reactor Dosimetry," *Proc. of International Specialists Symposium on Neutron Standards and Applications*, pp. 335-341, (1977).
- MOODY, J. R. and LINDSTROM, R. M., "The Selection and Cleaning of Containers for Trace Element Samples," (to be published).
- MOODY, J. R., PAULSER, P. J., RAINS, R. C. and ROOK, H. L., "The Preparation and Certification of Trace Mercury in Water Standard Reference Materials," *Proc. of the Seventh Materials Research Symposium*, NBS (1976).
- MORGAN, J., HIGUCHI, H., TAKAHASHI, H. and HERTOGEN, J., "A Chondritic Euclite Parent Body: Interface From Trace Elements," (to be published).
- MORGAN, J., GROS, J., TAKAHASHI, H., and Hertogen, J., "Lunar Braccia 732 is: Siderophile and Volatile Elements," *Proc. 7th Lunar Sci. Conf. Geochim. Cosmochim. Acta., Suppl. 7* 2189-2199 (1976).
- ROOK, H. L. and GOLDSTEIN, G., "Environmental Specimen Bank Workshop," *NBS Spec. Publ.* (to be published).

PUBLICATIONS

YULE, H. P. and ROOK, H. L., "A Comparison of Photopeak Area Computation Methodologies," *J. of Radioanal. Chem.*, 39 (1977).

ZOLLER, W. H., WALTERS, W. B., GALLAGHER, P. W. and MEYER, R. A.
"Radioactive Decay of 47-min $^{154}\text{Eu}^{\text{m}}$," *Phys. Rev. C*13, 2024-2032 (1976).

U.S. DEPT. OF COMM. BIBLIOGRAPHIC DATA SHEET	1. PUBLICATION OR REPORT NO. NBS TN-969	2. Gov't Accession No.	3. Recipient's Accession No.
4. TITLE AND SUBTITLE NBS REACTOR: Summary of Activities July 1976 to June 1977		5. Publication Date April 1978	6. Performing Organization Code
7. AUTHOR(S) Frederick J. Shorten		8. Performing Organ. Report No.	
9. PERFORMING ORGANIZATION NAME AND ADDRESS NATIONAL BUREAU OF STANDARDS DEPARTMENT OF COMMERCE WASHINGTON, D.C. 20234		10. Project/Task/Work Unit No.	11. Contract/Grant No.
12. Sponsoring Organization Name and Complete Address (Street, City, State, ZIP) Same as item 9		13. Type of Report & Period Covered 7/1/76 to 6/30/77	14. Sponsoring Agency Code
15. SUPPLEMENTARY NOTES			
16. ABSTRACT (A 200-word or less factual summary of most significant information. If document includes a significant bibliography or literature survey, mention it here.) This report summarizes all those programs which depend on the NBS reactor. It covers the period from July 1976 through June 1977. The programs range from the use of neutron beams to study the structure and dynamics of materials through nuclear physics and neutron standards to sample irradiations for activation analysis, isotope production, radiation effects studies, neutron radiography and nondestructive evaluations.			
17. KEY WORDS (six to twelve entries; alphabetical order; capitalize only the first letter of the first key word unless a proper name; separated by semicolons) Activation analysis; crystal structure; diffraction; isotopes; molecular dynamics; neutron; neutron radiography; nondestructive evaluation; nuclear reactor; radiation			
18. AVAILABILITY <input checked="" type="checkbox"/> Unlimited <input type="checkbox"/> For Official Distribution. Do Not Release to NTIS <input checked="" type="checkbox"/> Order From Sup. of Doc., U.S. Government Printing Office Washington, D.C. 20402, SD Stock No. SN003-003- <input type="checkbox"/> Order From National Technical Information Service (NTIS) Springfield, Virginia 22151		19. SECURITY CLASS (THIS REPORT) UNCLASSIFIED	21. NO. OF PAGES 188
		20. SECURITY CLASS (THIS PAGE) UNCLASSIFIED	22. Price \$3.50

NBS TECHNICAL PUBLICATIONS

PERIODICALS

JOURNAL OF RESEARCH—The Journal of Research of the National Bureau of Standards reports NBS research and development in those disciplines of the physical and engineering sciences in which the Bureau is active. These include physics, chemistry, engineering, mathematics, and computer sciences. Papers cover a broad range of subjects, with major emphasis on measurement methodology, and the basic technology underlying standardization. Also included from time to time are survey articles on topics closely related to the Bureau's technical and scientific programs. As a special service to subscribers each issue contains complete citations to all recent NBS publications in NBS and non-NBS media. Issued six times a year. Annual subscription: domestic \$17.00; foreign \$21.25. Single copy, \$3.00 domestic; \$3.75 foreign.

Note: The Journal was formerly published in two sections: Section A "Physics and Chemistry" and Section B "Mathematical Sciences."

DIMENSIONS/NBS

This monthly magazine is published to inform scientists, engineers, businessmen, industry, teachers, students, and consumers of the latest advances in science and technology, with primary emphasis on the work at NBS. The magazine highlights and reviews such issues as energy research, fire protection, building technology, metric conversion, pollution abatement, health and safety, and consumer product performance. In addition, it reports the results of Bureau programs in measurement standards and techniques, properties of matter and materials, engineering standards and services, instrumentation, and automatic data processing.

Annual subscription: Domestic, \$12.50; Foreign \$15.65.

NONPERIODICALS

Monographs—Major contributions to the technical literature on various subjects related to the Bureau's scientific and technical activities.

Handbooks—Recommended codes of engineering and industrial practice (including safety codes) developed in cooperation with interested industries, professional organizations, and regulatory bodies.

Special Publications—Include proceedings of conferences sponsored by NBS, NBS annual reports, and other special publications appropriate to this grouping such as wall charts, pocket cards, and bibliographies.

Applied Mathematics Series—Mathematical tables, manuals, and studies of special interest to physicists, engineers, chemists, biologists, mathematicians, computer programmers, and others engaged in scientific and technical work.

National Standard Reference Data Series—Provides quantitative data on the physical and chemical properties of materials, compiled from the world's literature and critically evaluated. Developed under a world-wide program coordinated by NBS. Program under authority of National Standard Data Act (Public Law 90-396).

NOTE: At present the principal publication outlet for these data is the Journal of Physical and Chemical Reference Data (JPCRD) published quarterly for NBS by the American Chemical Society (ACS) and the American Institute of Physics (AIP). Subscriptions, reprints, and supplements available from ACS, 1155 Sixteenth St. N.W., Wash., D.C. 20056.

Building Science Series—Disseminates technical information developed at the Bureau on building materials, components, systems, and whole structures. The series presents research results, test methods, and performance criteria related to the structural and environmental functions and the durability and safety characteristics of building elements and systems.

Technical Notes—Studies or reports which are complete in themselves but restrictive in their treatment of a subject. Analogous to monographs but not so comprehensive in scope or definitive in treatment of the subject area. Often serve as a vehicle for final reports of work performed at NBS under the sponsorship of other government agencies.

Voluntary Product Standards—Developed under procedures published by the Department of Commerce in Part 10, Title 15, of the Code of Federal Regulations. The purpose of the standards is to establish nationally recognized requirements for products, and to provide all concerned interests with a basis for common understanding of the characteristics of the products. NBS administers this program as a supplement to the activities of the private sector standardizing organizations.

Consumer Information Series—Practical information, based on NBS research and experience, covering areas of interest to the consumer. Easily understandable language and illustrations provide useful background knowledge for shopping in today's technological marketplace.

Order above NBS publications from: Superintendent of Documents, Government Printing Office, Washington, D.C. 20402.

Order following NBS publications—NBSIR's and FIPS from the National Technical Information Services, Springfield, Va. 22161.

Federal Information Processing Standards Publications (FIPS PUB)—Publications in this series collectively constitute the Federal Information Processing Standards Register. Register serves as the official source of information in the Federal Government regarding standards issued by NBS pursuant to the Federal Property and Administrative Services Act of 1949 as amended, Public Law 89-306 (79 Stat. 1127), and as implemented by Executive Order 11717 (38 FR 12315, dated May 11, 1973) and Part 6 of Title 15 CFR (Code of Federal Regulations).

NBS Interagency Reports (NBSIR)—A special series of interim or final reports on work performed by NBS for outside sponsors (both government and non-government). In general, initial distribution is handled by the sponsor; public distribution is by the National Technical Information Services (Springfield, Va. 22161) in paper copy or microfiche form.

BIBLIOGRAPHIC SUBSCRIPTION SERVICES

The following current-awareness and literature-survey bibliographies are issued periodically by the Bureau:

Cryogenic Data Center Current Awareness Service. A literature survey issued biweekly. Annual subscription: Domestic, \$25.00; Foreign, \$30.00.

Liquified Natural Gas. A literature survey issued quarterly. Annual subscription: \$20.00.

Superconducting Devices and Materials. A literature survey issued quarterly. Annual subscription: \$30.00. Send subscription orders and remittances for the preceding bibliographic services to National Bureau of Standards, Cryogenic Data Center (275.02) Boulder, Colorado 80302.

U.S. DEPARTMENT OF COMMERCE
National Bureau of Standards
Washington, D.C. 20234

OFFICIAL BUSINESS

Penalty for Private Use, \$300

POSTAGE AND FEES PAID
U.S. DEPARTMENT OF COMMERCE
COM-215



SPECIAL FOURTH-CLASS RATE
BOOK
